# MIMO Structures for Multicarrier CDMA Systems

*by*
*Bijan Golkar*

A thesis submitted to the Faculty of Graduate
Studies and Research in partial fulfillment to
the requirements for the degree of

Master of Applied Science

Ottawa-Carleton Institute for Electrical and Computer Engineering
Department of Systems & Computer Engineering
Carleton University
Ottawa, Ontario, Canada

June 2007

*Your file Votre référence*
*ISBN: 978-0-494-33649-6*
*Our file Notre référence*
*ISBN: 978-0-494-33649-6*

# Abstract

This thesis focuses on a particular multi-carrier system, known as Multi-Carrier Code Division Multiple Access (MC-CDMA), which simultaneously accommodates several users on the same frequency range. This technique, being a combination of Direct-Sequence CDMA (DS-CDMA) and Orthogonal Frequency Division Multiplexing (OFDM), takes advantage of the frequency diversity gains provided by DS-CDMA systems and the simple FFT architecture of transmit/receive structures in OFDM systems. In addition, it is widely known that Multi-Input Multi-Output (MIMO) structures have the potential to increase the capacity of communication systems. Furthermore, the potential of such structures to provide diversity without exhausting any further time or frequency resources and hence to increase the reliability of the communication has made MIMO structures a very popular area of research.

In this thesis, MIMO structures for MC-CDMA systems in frequency selective channels are investigated. Several known architectures are analyzed and an architecture, which combines spatial multiplexing with space-time coding in order to achieve higher data rates with high quality of service, is proposed. The bit error rate (BER) performance of the proposed system is evaluated and compared with other MIMO systems and it is shown that the proposed system, achieves better performance, is very robust to channel estimation errors and performs well in most of spatially correlated MIMO channels. In addition, a study on the complexity of the proposed system and the other MIMO architectures is carried out and the results show that our system is considerably less complex. A frequency multiplexing scheme is introduced which under certain conditions can significantly decrease the complexity of the system for a required bit error rate.

A thorough BER analysis of MC-CDMA systems in a frequency selective channel

is performed and BER expressions for MC-CDMA multiuser system and space-time coded structure are derived, which perfectly match the simulation results. Furthermore, the impact of the variations of the delay spread of the channel on the bit error performance of MC-CDMA system is studied.

## Acknowledgments

I would like to express my most sincere gratitude to my supervisor, Dr. Florence Danilo-Lemoine, for her continuing support and inspiring supervision throughout the course of my research. She, with her patience, insightful comments and extensive knowledge of the field guided me in all steps of my thesis and I am greatly indebted to her.

I would also like to thank Prof. Claude D'Amours, Prof. Ian Marsland and Prof. Halim Yanikomeroglu, the committee members of my thesis defence, for their helpful and constructive comments and suggestions.

I wish to express my deepest thanks to my family, my parents, my aunt and my brother for their continuous love and support.

# Contents

# List of Figures

# List of Tables

# List of Abbreviations

| | |
|---|---|
| BER | Bit Error Rate |
| BLAST | Bell Laboratories Layered Space-Time |
| CDMA | Code Division Multiple Access |
| DS-CDMA | Direct Sequence Code Division Multiple Access |
| CLT | Central Limit Theorem |
| MC-CDMA | Multi-Carrier Code Division Multiple Access |
| MC-DS-CDMA | Multi-Carrier Direct Sequence Code Division Multiple Access |
| MT-CDMA | Multi-Tone Code Division Multiple Access |
| CSI | Channel State Information |
| CSIR | Channel State Information at the Receiver |
| DBLAST | Diagonal BLAST |
| EGC | Equal Gain Combining |
| FDM | Frequency Devision Multiplexing |
| GLST | Generalized Layered Space-Time |
| ISI | Inter Symbol Interference |
| LLN | Law of Large Numbers |
| LOS | Line Of Sight |
| LPI | Low Probability of Intercept |
| MAI | Multiple Access Interference |
| MIMO | Multiple-Input Multiple-Output |

| | |
|---|---|
| MLD | Maximum Likelihood Detection |
| MMSE | Minimum Mean Square Error |
| MRC | Maximal Ratio Combining |
| MUI | Multi-User Interference |
| OFDM | Orthogonal Frequency Division Multiplexing |
| PDF | Probability Density Function |
| PSD | Power Spectral Density |
| QoS | Quality of Service |
| SIC | Serial Interference Cancellation |
| SI | Self Interference |
| SISO | Single-Input Single-Output |
| S/P | Serial to parallel conversion |
| STBC | Space-time Block Code |
| STTrC | Space-Time Trellis Code |
| STTuC | Space-Time Turbo Code |
| VBLAST | Vertical Bell Laboratories Layered Space-Time |
| ZF | Zero Forcing |

# List of Symbols

| Symbol | Explanation | page where symbol is defined |
|---|---|---|
| $*$ | Complex conjugation of a matrix or vector | |
| $^T$ | Transpose of a matrix or vector | |
| $\|.\|$ | Euclidean norm of a vector | |
| $\otimes$ | Kronecker product | |
| $\Re\{.\}$ | Real part of the argument | |
| $\alpha_u(i)$ | Amplitude of channel coefficient over $u^{th}$ subcarrier in the $i^{th}$ OFDM symbol interval | 20 |
| $\alpha_{ku}$ | Amplitude of channel coefficient of $k^{th}$ user over $u^{th}$ subcarrier in one OFDM symbol interval | 21 |
| $\langle a, b \rangle$ | Computes the correlation between $a$ and $b$ | 43 |
| $BW$ | Bandwidth of transmitted signal | 9 |
| $BW_c$ | Coherence bandwidth of channel | 17 |
| $BW_i$ | Bandwidth of narrowband information signal | 10 |
| $C$ | Capacity of the system | 9 |
| $\mathbf{c}_k$ | Normalized spreading code of $k^{th}$ user | 48 |
| $c_{ku}$ | $u^{th}$ chip of $k^{th}$ user's spreading code | 13 |

| | | |
|---|---|---|
| $\mathbf{H}^m$ | $m^{th}$ column of $\mathbf{H}$ corresponding to the $m^{th}$ substream ($s^m_{\mathrm{SM}}$) | 41 |
| $H^u_{nm}$ | Channel coefficient on the $u^{th}$ subcarrier between the $m^{th}$ transmitter and $n^{th}$ receiver | 49 |
| $\mathbf{h}_{nm}$ | $= [H^0_{nm}, \cdots, H^{U-1}_{nm}]^T$ | 51 |
| $h(\tau; t)$ | Lowpass channel impulse response at time $t$ and delay $\tau$ | 17 |
| $\mathbf{H}_u$ | $N \times M$ channel matrix of $u^{th}$ subcarrier | 48 |
| $\mathbf{H}^u_g$ | Channel matrix corresponding to the $g^{th}$ transmit antenna group | 56 |
| $i$ | $i^{th}$ OFDM symbol interval | 13 |
| $\mathbf{I}_A$ | $A \times A$ identity matrix | 37 |
| $k$ | $k^{th}$ user | 13 |
| $l$ | $l^{th}$ time sample of OFDM symbol | 15 |
| $\lambda_u$ | $u^{th}$ eigenvalue of the frequency domain covariance matrix of the channel | 68 |
| $M$ | Number of transmit antennas | 34 |
| $m$ | $m^{th}$ transmit antenna | 49 |
| $m_g$ | Number of antenna elements in $g^{th}$ group | 52 |
| $\mathbf{n}$ | $NU \times 1$ noise vector | 51 |
| $N$ | Number of receive antennas | 34 |
| $n$ | $n^{th}$ receive antenna | 49 |
| $\mathbf{N}^u_g$ | Null space matrix for the $g^{th}$ group | 57 |
| $\mathbf{n}_u$ | $N \times 1$ Noise vector on $u^{th}$ subcarrier | 49 |
| $\mathbf{n}^u$ | $N \times T$ noise matrix over the $u^{th}$ subcarrier over $T$ OFDM symbol intervals | 56 |
| $p(\gamma)$ | PDF of the channel SNR | 69 |
| $\bar{P}$ | Average of total received power | 24 |
| $\bar{P}_u$ | Average received power over $u^{th}$ subcarrier | 24 |

| | | |
|---|---|---|
| $P_{e\|\alpha_u}$ | Probability of error conditioned on the channel coefficients | 71 |
| $\psi_\gamma(j\nu)$ | Characteristic function of $\gamma$ | 68 |
| $q$ | Time index of the multipath delay | 17, 18 |
| $\mathbf{r}$ | $N \times 1$ receive vector | 39 |
| $\tilde{r}(t)$ | Time domain complex envelope representation of the received signal | 19 |
| $R_q(t)$ | Zero mean complex Gaussian fading random process with $\mathrm{E}[\mid R_q \mid^2] = 1$ | 17 |
| $\mathbf{r}_{\mathrm{Al}}$ | Alamouti scheme $N \times 2$ receive signal matrix | 36 |
| $\bar{\mathbf{r}}_{\mathrm{Al}}$ | Rearranged Alamouti scheme $2N \times 1$ receive signal matrix | 37 |
| $\mathbf{r}_s$ | Received signal at stage $s$ when the contribution of the $(s-1)$ previously detected subtreams is removed from the received signal | 41 |
| $\mathbf{r}^u$ | $N \times T$ received signal matrix over the $u^{th}$ subcarrier over $T$ OFDM symbol intervals | 56 |
| $\mathbf{r}_u$ | $N \times 1$ received signal vector on the $u^{th}$ subcarrier | 48 |
| $\mathbf{r}^u_{g+1}$ | $\mathbf{r}^u_g$ is the received signal of $u^{th}$ subcarrier, when the contribution of $g^{th}$ and previous groups is canceled | 56 |
| $\mathbf{R}_{\mathrm{BS}}$ | Correlation matrix of antenna elements at the base station | 44 |
| $\mathbf{R}_f$ | Frequency domain covariance matrix of the channel | 67 |
| $\mathbf{R}_{\mathrm{MIMO}}$ | Correlation matrix in a MIMO channel | 44 |
| $\mathbf{R}_{\mathrm{MS}}$ | Correlation matrix of antenna elements at the mobile station | 44 |
| $s$ | $s^{th}$ stage of interference cancellation | 41 |
| $s^{(k)}_{\mathrm{MC}}(t)$ | Time domain representation of $k^{th}$ user transmitted signal for MC-CDMA | 13 |
| $\tilde{s}^{(k)}_{MC}(t)$ | Complex envelope representation of transmitted signal of $k^{th}$ user | 13 |
| $s_{ki}$ | $k^{th}$ user data in $i^{th}$ symbol interval | 13 |
| $s^u_{ki}$ | Transmitted signal of $k^{th}$ user over $u^{th}$ subcarrier in $i^{th}$ OFDM symbol interval | 15 |

| | | |
|---|---|---|
| $s_i^u$ | $= \sum_{k=1}^{K} s_{ki} c_{ku}$ | 48 |
| $\tilde{s}_i^u$ | Soft decision estimate of $s_i^u$ | 58 |
| $\tilde{s}_{ki}$ | Soft decision estimate of $s_{ki}$ | 58 |
| $\tilde{s}_{\mathrm{SM}}^s$ | Estimate of the $s^{th}$ substream | 42 |
| $\mathbf{s}_{ki}$ | Low-pass frequency domain representation of transmitted signal of $k^{th}$ user in $i^{th}$ OFDM symbol interval | 15 |
| $\mathbf{s}_i$ | Transmitted signal in one OFDM symbol interval before space-time processing | 54 |
| $\mathbf{s}_{\mathrm{SM}}$ | $M \times 1$ transmit signal vector in a spatial multiplexing system | 39 |
| $\mathbf{s}_m^{\mathrm{Tx}}$ | Transmitted signal in one OFDM symbol from a spatial multiplexing transmitter structure | 48 |
| $\tilde{\mathbf{s}}_k$ | $M \times 1$ estimated data of user $k$ | 49 |
| $\mathbf{S}$ | Alamouti scheme transmit signal matrix | 36 |
| $\mathbf{S}_g^u$ | Space time matrix of $g^{th}$ antenna group | 55 |
| $\tilde{\mathbf{S}}_g^u$ | Estimate of $\mathbf{S}_g^u$ | 56 |
| $\sigma_{n\|\alpha_u}^2$ | Noise variance conditioned on the channel coefficients | 71 |
| $T$ | Number of time intervals involved in each space-time block code | 56 |
| $\tau$ | Multipath delay | 17 |
| $T_c$ | Coherence time of the channel | 17 |
| $T_g$ | Guard interval | 16 |
| $\theta_u(i)$ | Phase of channel coefficient over $u^{th}$ subcarrier in the $i^{th}$ OFDM symbol interval | 20 |
| $\theta_{ku}$ | Phase of channel coefficient of $k^{th}$ user over $u^{th}$ subcarrier in one OFDM symbol interval | 21 |
| $T_{\max}$ | Channel length | 16 |
| $T_s$ | Duration of one OFDM symbol interval | 15 |
| $T_{\mathrm{samp}}$ | Sampling time | 15 |

| | | |
|---|---|---|
| $u$ | $u^{th}$ subcarrier | 13 |
| $U$ | Number of subcarriers | 15 |
| $\mathbf{W}_u^{\text{MMSE}}$ | MMSE weight matrix in a spatial multiplexing MIMO system | 49 |
| $\mathbf{W}_s$ | Weight vector of the $s^{th}$ stage | 42 |
| $\mathbf{Y}$ | $= [\mathbf{y}_0, \mathbf{y}_1, \cdots, \mathbf{y}_{U-1}]$ | 49 |
| $\mathbf{y}_u$ | Estimate of the transmitted signal over the $u^{th}$ subcarrier | 49 |

# Chapter 1

# Introduction

## 1.1 Thesis Objective

As different multimedia services emerge and the demand for higher data rate communication increases, communication systems are urged to accommodate more and more users each day, and to operate with the highest spectral efficiency possible while maintaining Quality of Service (QoS). Over the past few decades, several techniques have emerged to increase the capacity and improve the performance of wireless communication systems. However, harsh degradation of performance due to fading effects of communication channels, have made reliable transmission at high data rates quite challenging.

A system is considered to have a narrowband structure, when the bandwidth of the transmitted signal is considerably smaller than the coherence bandwidth of the channel ($BW \ll BW_c$). The channel is then said to be flat. In this case, when the channel characteristics at the corresponding frequency band is poor, the entire transmitted signal will be in deep fade and the data will be lost for a certain period of time. In spread spectrum systems since the bandwidth is taken considerably larger

than the coherence bandwidth of the channel this problem is solved. Direct-Sequence Code Division Multiple Access (DS-CDMA) is a multiuser spread spectrum technique which accommodates multiple users in the same frequency band simultaneously. In order to combat the flat fading effects, the signal is spread on a bandwidth significantly larger than the coherence bandwidth of the channel. Henceforth, when the channel condition in a frequency band is poor, only the part of the signal transmitted on that specific frequency band will be corrupted and the rest of the signal remains intact. However, increasing the bandwidth of a system in turn increases the time resolution substantially, which requires high resolution complex receiver (RAKE) structures for signal detection. The channel seen by a wideband signal, becomes frequency selective, characterized by the presence of several paths. Due to this multipath phenomenon, the received signal might be subject to Inter Symbol Interference (ISI) for high data rate scenarios, which might degrade the performance significantly.

In Orthogonal Frequency Division Multiplexing (OFDM) systems, the large bandwidth is exploited in a quite different fashion. In this scheme, independent streams of data are transmitted over different subcarriers at the same time and the symbol interval is proportionately increased, hence the system becomes intrinsically less susceptible to ISI. Furthermore, by extending the OFDM symbol with a cyclic extension larger than the maximum delay spread of the channel, ISI between symbols is efficiently mitigated. In addition, the simple IFFT/FFT structure of the transmitter and receiver has considerably reduced the complexity of the system. However, unlike DS-CDMA systems no frequency diversity is achieved [1].

The combination of OFDM and DS-CDMA systems has formed a powerful transmission technique called Multi-carrier Code Division Multiple Access (MC-CDMA) which benefits from both the frequency diversity provided by DS-CDMA and ISI mitigation capabilities and simple IFFT/FFT structure of OFDM systems [2]. Although

the MC-CDMA signal structure resembles that of OFDM, the way the subcarriers are used, is completely different. In MC-CDMA, the users' data are transmitted over the same subcarriers at the same time, and different users are distinguished by their unique spreading codes, whereas in OFDM independent streams of data (of different users) are transmitted over different subcarriers [3].

Over the past few years, Multiple-Input Multiple-Output (MIMO) structures have drawn a lot of attention, and have become one of the most important research areas in the field of wireless communications. Telatar in [4] and Foschini in [5] have independently shown that in a rich scattering environment, the information theoretic capacity of a MIMO system increases linearly with the lesser of the number of transmit and receive antennas. Different techniques have been proposed to exploit the potential of these structures. In [6], Alamouti proposed a simple transmit diversity technique, where Maximum Likelihood Detection (MLD) is performed with simple linear processing at the receiver. Later Tarokh *et al* extended his work and proposed the concept of Space-Time Block Coding (STBC) [7]. Other space-time coding architectures such as Space-Time Trellis Coding (STTrC) [8] and Space-Time Turbo Coding (STTuC) [9] were devised based on convolutional code trellises and turbo codes respectively.

The techniques presented in [6]-[9] provide spatial diversity by transmitting signals carrying the same data over the transmit antenna elements and hence providing the receiver with different (ideally independent) replicas of the transmitted data. Whenever one of the branches (i.e. spatial subchannels) has undesirable channel characteristics, it is very unlikely that other branches are also in deep fade which increases the system reliability and significantly improves the Bit Error Rate (BER) performance. MIMO structures can be exploited in another fashion as well. By transmitting independent streams of data over different antenna elements, the spectral efficiency increases significantly and the high capacities promised for MIMO structures can be achieved.

In the wireless communication terminology, this concept is known as *spatial multiplexing*, which was first introduced by Foschini [10]: In this scheme, the independent substreams (also known as layers) are first independently coded and then space-time multiplexed diagonally over the transmit antenna elements, such that all the layers cyclically benefit from all the branches and no layer is stuck with one particular branch which might suffer from poor channel conditions (see Fig. 1.1-(a)). This technique is known as the Diagonal Bell Laboratories Layered Space-Time (DBLAST) architecture. However, due to the complexity of the decoder, the high probability of error propagations and the waste of resources at the beginning and the end of transmission, a simpler multiplexing approach, where the antenna assignment for the substreams is fixed (see Fig. 1.1-(b)) has been proposed [11]. Furthermore, this technique, known as Vertical BLAST, is shown to be capable of achieving similar bit error rates compared to the diagonal technique. In this technique, the substreams transmitted from each transmit antenna element can be viewed as the data of a virtual user in a DS-CDMA system (with the total number of users equal to the total number of transmit antenna elements), hence most of the detection techniques of DS-CDMA systems can be applied to VBLAST architectures. In addition, it should be noted that the optimum detection of independent substreams transmitted through different transmit antennas, like maximum likelihood detection of a multiuser CDMA system, is very complex and the complexity increases exponentially with the number of transmit antennas. Thus, different suboptimal receiver structures have been proposed (e.g. VBLAST detection scheme, which is based on Serial Interference Cancellation (SIC) multiuser detection technique in DS-CDMA). In [12], DBLAST, VBLAST and a spatial multiplexing technique with a single outer code in various conditions (i.e. with/without knowledge of channel at the transmitter, frequency selectivity of the channel and additive interference) have been investigated. In the end, it should be noted that, all of the mentioned

spatial multiplexing structures increase the data rate at the expense of significantly decreasing the spatial diversity, which can severely degrade the overall performance.

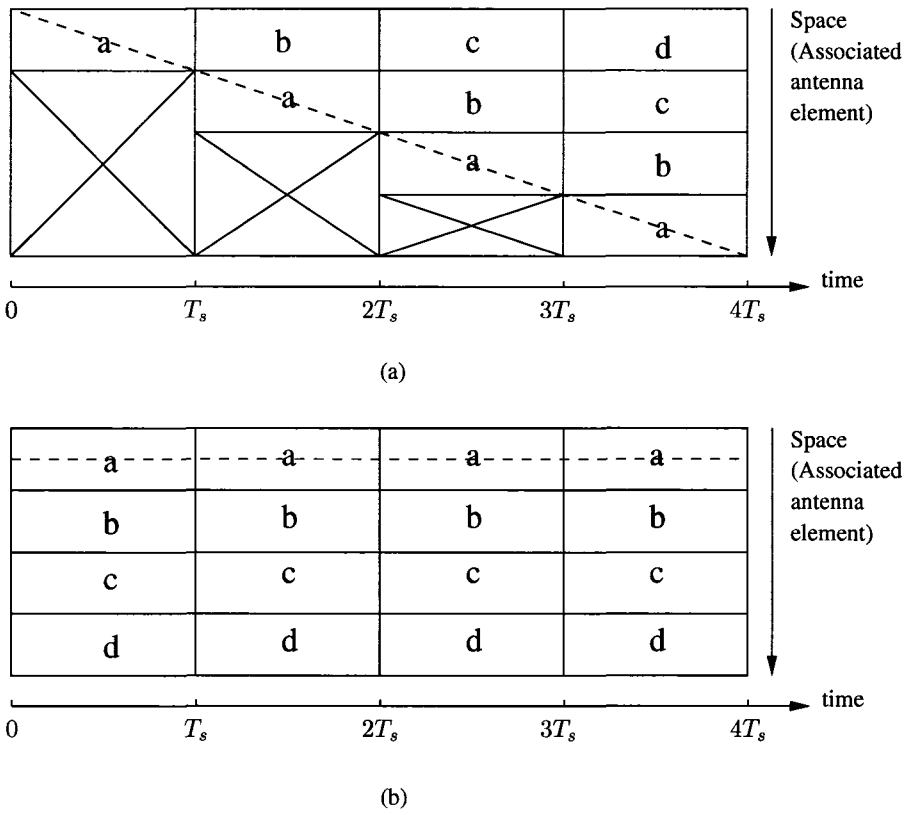


**Fig. 1.1** Input symbol multiplexing pattern for DBLAST (a) and VBLAST (b) in a MIMO structure with 4 transmitters (The 4 layers are labeled as $a, b, c$ and $d$).

In a rich scattering environment, where the correlation between the transmit-receive antenna pairs is low, the combination of spatial multiplexing and space-time coding is believed to improve throughput and performance simultaneously. These structures are often referred to as Generalized Layered Space-Time (GLST) architectures. Essentially, in GLST architectures the concept of spatial multiplexing is applied to groups of antenna elements which have been independently space-time

coded. Hence, the antennas in each group provide spatial diversity gain and the antenna groups increase the spectral efficiency. In [13], it has been shown that there exists a fundamental tradeoff between diversity and spatial multiplexing gains in multiple-antenna channels. In [14], this tradeoff is further investigated and the throughput-reliability tradeoff formulation is proposed. Different GLST structures, as a combination of BLAST and space-time coding architectures are studied in [15].

In this thesis, MIMO structures for MC-CDMA systems are investigated. Spatial multiplexing and space-time coding structures are first studied and then a structure for combining spatial multiplexing and spectral efficiency for MC-CDMA systems is proposed. The complexity of the proposed structure together with its BER performance in uncorrelated and spatially correlated channels are evaluated and compared with the more conventional MIMO structures. Furthermore, the effect of channel estimation error on the performance of the system is also studied. In the second part of the thesis, a thorough BER analysis of MC-CDMA systems is carried out and the BER of the multi-user SISO MC-CDMA and Alamouti space-time coded MC-CDMA system in a correlated frequency selective Rayleigh fading channel are derived.

## 1.2 Original Contributions

The main contributions of this thesis are

- Design of a MIMO-MC-CDMA structure that benefits from both diversity and spatial multiplexing gains simultaneously (section 3.2).
- Assessment of the complexity of the proposed system together with three other MIMO structures and comparison (section 3.3).
- Study of tradeoff between the frequency diversity gain and the constellation

order of the system is carried out. In this regard a frequency multiplexing technique has been proposed and it is shown that in certain conditions considerable improvements in performance can be achieved (section 3.2.2).

- BER performance evaluation of the proposed structure in spatially uncorrelated/correlated channels and perfect/imperfect channel estimation at the receiver with different number of active users and comparisons with other MIMO structures (section 5.3.3).

- Derivation of analytical BER expressions for multi-user MC-CDMA and space-time coded MC-CDMA systems in a correlated Rayleigh frequency selective fading channel with exponential power delay profile and validation of the expressions by computer simulations (sections 4.3 and 4.4).

## 1.3 Thesis Outline

- Chapter 2 studies the MC-CDMA system signal structure and the transmit and receive architectures. Other variations of Multicarrier CDMA systems are briefly presented. An introduction to MIMO structures is provided, Alamouti space-time coding is discussed and different techniques for spatial multiplexing are elaborated. Finally, a model for spatially correlated MIMO channel[1] for simulation purposes is discussed.

- Chapter 3 presents different MIMO MC-CDMA architectures and proposes a new scheme for combining spatial multiplexing and space-time coding in MC-CDMA systems. The trade-off between frequency diversity and constellation order is discussed and a new frequency multiplexing technique is proposed which

[1]Kronecker model

significantly improves the performance under certain conditions. Finally, the complexity comparisons are carried out and it is shown that the proposed scheme is significantly less complex.

- Chapter 4 analyzes the MC-CDMA system in a correlated frequency selective fading channel. An analytical expression for multi-user MC-CDMA and multi-user Alamouti space-time coded systems are derived. Finally, a discussion on the impact of delay spread variations of the channel on the performance of the MC-CDMA system is presented.

- Chapter 5 provides the simulation results of the thesis.

- Chapter 6 concludes the thesis, provides a summary of the work and proposes potential research areas to continue this work.

# Chapter 2

# Literature Review and Background Material

## 2.1 Code Division Multiple Access (CDMA)

Code division multiple access is a Spread Spectrum (SS) technique where multi-user access is achieved by assigning a unique code to each user and all users benefit from the entire resources (i.e. time and frequency) simultaneously. The idea of a spread spectrum system originates from Shannon's famous formula for the capacity of the band-limited Gaussian noise channel [16]:

$$C = \int_0^{BW} \log\left(1 + \frac{P(f)}{N(f)}\right) df \tag{2.1}$$

where $BW$ is the available bandwidth of the channel, $P(f)$ and $N(f)$ are the signal and noise power spectral density at frequency $f$ respectively. Equation (2.1) suggests that the increase in capacity is directly proportional to the increase in the bandwidth of the transmitted signal. In a spread spectrum system, the narrowband input signal is

spread over a very wide frequency range and the ratio of the transmit signal bandwidth to the original information bandwidth is called the processing gain of the system:

$$G_p = \frac{BW}{BW_i}$$

where $BW_i$ denotes the information signal bandwidth.

A multiuser CDMA spread spectrum system has certain properties: Users are assigned unique codes, referred to as spreading codes chosen to be highly uncorrelated to facilitate detection. Moreover, the information of a specific user can only be retrieved provided the spreading code of the user is available, which in turn increases the privacy of the communication. In addition the fact that the transmit signal power is spread over a broad bandwidth contributes to the immunity of the system, this property is often referred to as Low Probability of Intercept (LPI). In other words, the spread spectrum transmitted signal has the same power level as noise in the communication environment, thus detecting the signal with no knowledge of the spreading code is practically impossible [2, 17].

### 2.1.1 Direct Sequence CDMA (DS-CDMA)

As the name of this technique suggests, the information of each user is directly multiplied by its corresponding spreading code. The information is first modulated using an appropriate modulation scheme (e.g. BPSK, QPSK, QAM ...), and then directly multiplied by its corresponding unique code, thus producing the wideband transmit signal. At the receiver, after having despread the incoming signal with a locally generated replica of the spreading code of the user, the receiver recovers the original data using an appropriate demodulator, which could be a matched filter for AWGN or a RAKE receiver for multipath fading channels. Due to the wide bandwidth of

DS-CDMA systems, the received signal over multipath fading channels has several resolved components. Each finger of the RAKE receiver has the capability to lock on one resolvable multipath component captured by the receiver structure. Hence, based on the complexity of the receiver structure only a limited number of paths can be used and thus taking full advantage of the received signal scattered in the time domain is not practically feasible. After detecting the maximum possible number of multipath components, they are combined and the information of the received signal is recovered.

It should be taken into consideration that the code at the receiver should be synchronized to the received signal in a fraction of a chip duration; otherwise, some information may be lost [17]. In the case where all spreading codes are orthogonal and perfect synchronization is achieved, the generated codes need to be merely multiplied with the information signal and the implementation of the system is fairly easy. In addition, since only one carrier frequency is required the frequency synthesizer does not have a complex structure. However, acquiring and maintaining the synchronization is quite a difficult task, which requires a complex structure at the receiver. Moreover, as discussed earlier the synchronization has to be attained within a fraction of a chip duration, which simply would not allow the codes to have chip durations shorter than a certain value and in turn limits the transmitted signal bandwidth.

Another drawback of this technique is a phenomenon known as the near-far effect: The users close to the base station produce high interference for the users farther away. More generally, if the user spreading codes are not perfectly orthogonal, CDMA systems suffer from Multi-User Interference (MUI, also referred to as Multiple Access Interference (MAI)) which degrades the performance. Power control algorithms are applied to combat MUI, which requires further complexity in the receiver structure. Multi-user detection techniques also combat MUI at the expense of additional com-

plexity. Moreover, due to the fact that noise often distorts the auto-correlation function of the transmitted signal, the RAKE receiver might mistakenly combine different components resulting in what is called self interference (SI) and is another source of performance degradation in this system.

## 2.2 Multi-carrier Code Division Multiple Access (MC-CDMA)

Multi-carrier code division multiple access was first proposed by N. Yee, J.P. Linnartz and G. Fettweis for indoor wireless networks [18]. Despite the fact that MC-CDMA and OFDM are both multicarrier systems, the way they utilize the available subcarriers is quite different. OFDM is essentially very similar to Frequency Division Multiplexing (FDM), but for a given number of subcarriers, an OFDM signal occupies a much smaller bandwidth than a FDM signal since OFDM subcarriers overlap. More specifically, in order to reduce the crosstalk between adjacent subcarriers, OFDM subcarriers are chosen to satisfy the minimum spacing for orthogonality. By using several orthogonal subcarriers, a wideband spectrum (subject to multipath fading) is divided into $U$ number of narrowband subchannels (subject usually to flat fading). In addition, when the maximum delay spread is longer than the symbol duration, a cyclic prefix (typically longer than the delay spread of the channel) is appended at the end of each symbol in order to eliminate ISI. A IFFT/FFT structure is exploited, which significantly simplifies the transmit/receive structure [1]. In MC-CDMA, on the other hand, users transmit their data at the same time on the same subcarriers. The data of the users are detected using their distinct spreading codes. Furthermore, since the data of each user is transmitted over multiple subcarriers, frequency diversity is also achieved.

The spreading technique in MC-CDMA structures is quite different from that of the DS-CDMA systems. Unlike DS-CDMA systems where the data is spread in time, MC-CDMA spreads the data in frequency domain: the users' data is replicated to be transmitted over all assigned subcarriers and each copy is multiplied by one chip of the corresponding spreading code (see Fig 2.1-a). This architecture benefits from both the frequency diversity provided by DS-CDMA and ISI mitigation capabilities and simple transmit/receive structure of OFDM.

A downlink MC-CDMA system is presented in more detail in the following. Section 2.2.1 studies the structure of the MC-CDMA transmit signal. Section 2.2.2 discusses the channel characteristics in a MC-CDMA system, a typical example of a MC-CDMA system parameters is provided and an appropriate channel model is developed. In section 2.2.3 the receiver structure is studied and the BER analysis for two main combining methods, namely Equal Gain Combining (EGC) and Maximal Ratio Combining (MRC), is provided and the Minimum Mean Square Error (MMSE) detection technique is presented.

### 2.2.1 MC-CDMA signal structure

The transmitted signal of the $k^{th}$ user can be expressed as:

$$s_{MC}^{(k)}(t) = \Re\{\tilde{s}_{MC}^{(k)}(t)e^{j2\pi(f_c-\frac{U\Delta f}{2})t}\} \tag{2.2}$$

$$\tilde{s}_{MC}^{(k)}(t) = \sum_{i=-\infty}^{+\infty}\sum_{u=0}^{U-1} s_{ki}c_{ku}.p_s(t-iT_s)e^{j2\pi u\Delta f t} \tag{2.3}$$

where, $\tilde{s}_{MC}^{(k)}(t)$ is the complex envelope of the transmitted signal for the $k^{th}$ user with respect to $f_c - \frac{U\Delta f}{2}$, $s_{ki}$ is the $i^{th}$ symbol of user $k$, $c_{ku} \in \{\pm 1\}$ is the $u^{th}$ chip of the spreading code of user $k$, the separation of subcarriers is denoted by $\Delta f = \frac{1}{T_s}$,

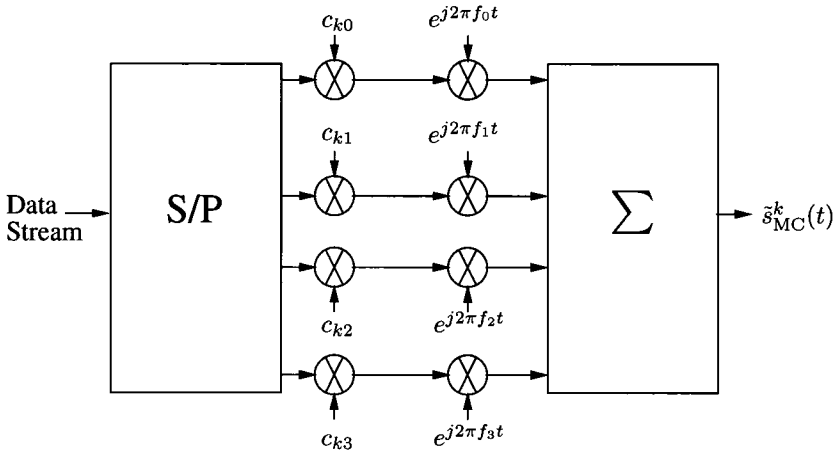


(a) Transmitter Structure

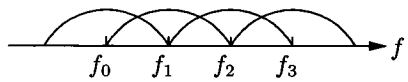


(b) Power spectrum of transmitted signal

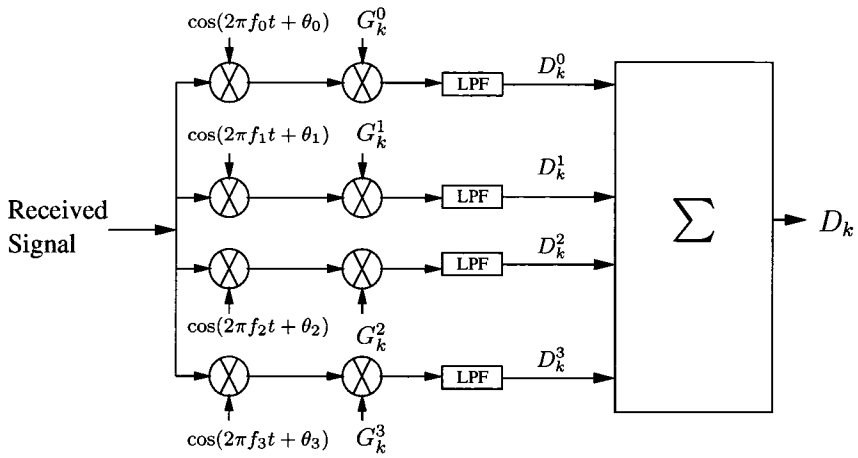


(c) Receiver structure for detection of user $k$ (assuming perfect synchronization)

**Fig. 2.1** MC-CDMA scheme (downlink): (a) transmitter, (b) power spectrum of transmitted signal (c) Receiver structure ($G_{MC} = 4$, $U = 4$)

where $T_s$ is the OFDM symbol interval (not considering the guard intervals), and the pulse waveform for each symbol is:

$$p_s(t) = \begin{cases} 1 & ,0 \leq t \leq T_s \\ 0 & ,\text{Elsewhere} \end{cases}$$

and $U$ is the number of subcarriers. In the frequency domain, $\tilde{s}_{MC}^{(k)}(t)$ in the $i^{th}$ OFDM symbol interval can be described in a vector form as follows:

$$\mathbf{s}_{ki} = \left[s_{ki}^0, s_{ki}^1, \cdots, s_{ki}^{U-1}\right]^T \tag{2.4}$$

where $s_{ki}^u = s_{ki}c_{ku}$ for $u = 0, 1, \cdots, U-1$. By choosing the sampling period of the time-domain signal appropriately ($T_{\text{samp}} = \frac{1}{U\Delta f}$), (2.3) in the $i^{th}$ OFDM symbol interval can be rewritten as:

$$\tilde{s}_{ki}(lT_{\text{samp}}) = \sum_{u=0}^{U-1} s_{ki}c_{ku}e^{\frac{j2\pi lu}{U}} \qquad \text{for} \qquad l = 0, \cdots, U-1 \tag{2.5}$$

where $\tilde{s}_{ki}(lT_{\text{samp}})$ is the $l^{th}$ time-domain sample of the $k^{th}$ user transmit signal in the $i^{th}$ OFDM symbol interval. It is assumed that the number of samples per symbol is equal to the number of subcarriers, which is usually taken as the processing gain of the system. Clearly seen, the time samples in (2.5) can be calculated by simply taking the IFFT of the frequency-domain signal vector in (2.4). Consequently, IFFT/FFT blocks can be employed which significantly simplifies the transmitter/receiver structure. Henceforth, the samples of the signal can be represented in a vector form as follows:

$$\tilde{\mathbf{s}}_{ki} = \mathbf{F}^H(U)\mathbf{s}_{ki}$$

where $\tilde{\mathbf{s}}_{ki} = \left[\tilde{s}_{ki}(0), \tilde{s}_{ki}(T_{\text{samp}}), \cdots, \tilde{s}_{ki}\big((U-1)T_{\text{samp}}\big)\right]^T$ and $\mathbf{F}(U)$ represents the FFT operation matrix:

$$\mathbf{F}(U) = \begin{pmatrix} 1 & 1 & \cdots & 1 \\ 1 & e^{-\frac{j2\pi(1)(1)}{U}} & \ddots & e^{-\frac{j2\pi(1)(U-1)}{U}} \\ \vdots & \ddots & \ddots & \vdots \\ 1 & \cdots & \cdots & e^{-\frac{j2\pi(U-1)(U-1)}{U}} \end{pmatrix}$$

### 2.2.2 Typical system parameters and channel model for MC-CDMA

In this section, the parameters of a typical MC-CDMA system and the channel characteristics in a typical wireless environment are investigated, an example is provided and a proper channel model is developed.

An OFDM symbol interval ($T_s'$) consists of the samples of the transmit signal in (2.5) plus a guard interval in the form of a cyclic prefix longer than the channel length ($T_{\max}$), in order to mitigate the ISI between OFDM symbols.

$$T_s' = \frac{U}{BW} + T_g$$

where $T_g$ represents the guard interval and $T_{\text{samp}} = \frac{1}{BW}$ is the sampling time.

Typical system parameters of a MC-CDMA system are provided in Table 2.1[1]. The OFDM symbol interval is calculated as $T_s' = \frac{512}{1.25\,\text{MHz}} + 12.8\,\mu s = 422.4\,\mu s$ and the guard interval is 16 samples ($\frac{12.8}{0.8} = 16$), which is chosen greater than the channel length (10 samples).

The performance of a MC-CDMA system is not considerably affected by Doppler spread. In other words, for typical values of Doppler spread (hundreds of Hertz),

[1]The parameters correspond to a GSM test channel with a "bad urban area" (BU) power delay profile according to the COST 207 recommendations.

the fading encountered by the system is slow. This matter can be investigated in the example provided in Table 2.1. As can be seen, the subcarrier spacing is 2.44 KHz and a Doppler spread of 277.778 Hz is considered, which is less than 12% of the frequency spacing and does not affect the frequency content of the subcarriers considerably. This matter can be investigated in the time domain as well:
The coherence time of the system can be calculated from the following equation [19]:

$$T_c = \sqrt{\frac{9}{16\pi f_m^2}} \approx \frac{0.423}{f_m}$$

where $f_m$ is the maximum Doppler spread. Hence this system has a coherence time of 1.523 ms which is 3.6 times greater than the symbol duration ($T_s'$), which proves that the system encounters a slow fading channel. Finally, one of the most important characteristics of a MC-CDMA system is that the fading encountered by each subcarrier is considered to be flat. In the example provided in Table 2.1, the bandwidth of each subcarrier is 2.44 KHz which is significantly smaller than the coherence bandwidth of the channel (i.e. 225 KHz) and satisfies $\Delta f \ll BW_c$, where $BW_c$ is the coherence bandwidth of the channel and the RMS delay spread of the channel is $T_{\text{rms}} \approx \frac{1}{BW_c} = 3.92\mu s$.

The low-pass impulse response of a frequency selective Rayleigh fading channel with exponential power delay profile with equi-distant samples in time is described as [20]:

$$h(\tau;t) = \sum_{q=0}^{Q} \sqrt{Ae^{-\frac{\tau}{T_{rms}}}} R_q(t)\delta(\tau - qT_{samp}) \tag{2.6}$$

where $Q = \frac{T_{max}}{T_{samp}}$, $A$ is a normalization constant to satisfy $\sum_{q=0}^{Q} \left| Ae^{-\frac{qT_{samp}}{T_{rms}}} \right| = 1$ and $R_q(t)$ is a zero mean complex Gaussian fading random process with $\mathrm{E}[|R_q(t)|^2] = 1$, where $\mathrm{E}[|R_q(t)|^2]$ is the expected value of $|R_q(t)|^2$.

**Table 2.1** MC-CDMA system parameters and channel model [20]

| | |
|---|---|
| Bandwidth | 1.25 MHz |
| Sampling time ($T_{\text{samp}}$) | 0.8 $\mu$s |
| Number of subcarriers ($U$) | 512 |
| Subcarrier spacing ($\Delta f$) | 2.44 KHz |
| Coherence bandwidth | 225 KHz |
| Carrier frequency ($f_c - \frac{U\Delta f}{2}$) | 1.2 GHz |
| Maximum vehicle speed | 250 Kmph |
| Maximum Doppler spread | 277.778 Hz |
| Guard interval ($T_g$) | 12.8 $\mu$s |
| RMS delay spread ($T_{\text{rms}}$) | 3.921$\mu s$ |
| Channel length | 10 samples |
| Total OFDM symbol duration ($T_s'$) | 422.4 $\mu$s |

Since in a typical MC-CDMA system the coherence time of the channel is considerably greater than the symbol duration of the system and hence the channel is slow fading, a constant channel is assumed over one OFDM symbol interval. Hence the channel impulse response can be rewritten as:

$$h(\tau) = \sum_{q=0}^{Q} \sqrt{Ae^{-\frac{\tau}{T_{rms}}}} R_q \delta(\tau - qT_{samp})$$

and the frequency domain channel impulse response is derived by taking the Fourier transform of $h(\tau)$:

$$\begin{aligned} H(f) &= \int_{-\infty}^{+\infty} h(\tau) e^{-j2\pi f\tau} d\tau \\ &= \sum_{q=0}^{Q} \int_{-\infty}^{+\infty} \sqrt{Ae^{-\frac{\tau}{T_{rms}}}} R_q \delta(\tau - qT_{samp}) e^{-j2\pi f\tau} d\tau \\ &= \sum_{q=0}^{Q} \sqrt{Ae^{-\frac{qT_{samp}}{T_{rms}}}} R_q e^{-j2\pi f qT_{samp}} \end{aligned}$$

Hence the frequency domain channel coefficients are derived by sampling the frequency

domain channel impulse response:

$$H_u = H(f = u\Delta f) = \sum_{q=0}^{Q} \sqrt{Ae^{-\frac{qT_{samp}}{T_{rms}}}} R_q e^{-j2\pi qu\Delta f T_{samp}} \quad , \quad T_{\text{samp}} = \frac{1}{U\Delta f}$$
$$= \sum_{q=0}^{Q} \sqrt{Ae^{-\frac{qT_{samp}}{T_{rms}}}} R_q e^{-\frac{j2\pi qu}{U}} \quad \text{for} \quad u = 0, \cdots, U-1 \tag{2.7}$$

where $H_u$ is the channel coefficient over the $u^{th}$ subcarrier. In addition, assuming $\{R_q\}$ are zero-mean uncorrelated Gaussian random variables with unit variance and $A$ is properly chosen, the frequency domain channel coefficients, following Parseval's theorem [21], satisfy $\text{E}\left[\sum_{u=0}^{U-1} |H_u|^2\right] = U$. In this thesis, $R_q$ is generated independently for each symbol interval. In other words, Doppler spread effects are not considered in this work.

### 2.2.3 MC-CDMA downlink receiver structure

In a downlink system with $K$ active users the complex envelope of the received signal in a channel given in (2.6) during one OFDM symbol interval is [22]:

$$\tilde{r}(t) = \sum_{k=1}^{K} \int_{-\infty}^{+\infty} \tilde{s}_{MC}^{(k)}(t)(t-\tau)h(\tau;t)d\tau + \tilde{n}(t) \tag{2.8}$$

where $\tilde{s}_{MC}^{(k)}(t)$ is the $k^{th}$ user transmit signal in (2.3) and $\tilde{n}(t)$ is an additive zero-mean circularly symmetric complex white Gaussian random process with two-sided power spectral density (PSD) of $\frac{N_0}{2}$.

The received signal is presented as the convolution of the transmitted signal with the channel impulse response in (2.8). Hence, the frequency components of the received signal in one OFDM symbol can be written as the product of the frequency domain channel coefficients in (2.7) and the transmitted signal frequency components

in (2.4). The received signal over the $u^{th}$ subcarrier in the $i^{th}$ OFDM symbol interval can be written as:

$$\begin{aligned} r_{ui} &= \sum_{k=1}^{K} s_{ki} c_{ku} H_u(i) + n_{ui} \\ &= \sum_{k=1}^{K} s_{ki} c_{ku} \alpha_u(i) e^{j\theta_u(i)} + n_{ui} \end{aligned} \tag{2.9}$$

where $H_u(i) = \alpha_u(i) e^{j\theta_u(i)}$ and $n_u$ is the noise over the $u^{th}$ subcarrier.

By taking the IFFT, the complex envelope of the time domain received signal in the $i^{th}$ OFDM symbol interval is derived as:

$$\tilde{r}_i(t) = \sum_{u=0}^{U-1} r_{ui} e^{j2\pi u \Delta f t} = \sum_{u=0}^{U-1} \sum_{k=1}^{K} s_{ki} c_{ku} \alpha_u(i) e^{j(2\pi u \Delta f t + \theta_u(i))} + \tilde{n}_i(t) \tag{2.10}$$

where $\tilde{n}_i(t)$ is the complex envelope representation of the noise signal.

Hence the received signal in the time domain can be written as:

$$\begin{aligned} r(t) &= \sum_{i=-\infty}^{\infty} \Re\left\{ \tilde{r}_i(t) e^{j2\pi (f_c - \frac{U\Delta f}{2})t} \right\} \\ &= \sum_{i=-\infty}^{\infty} \sum_{u=0}^{U-1} \sum_{k=1}^{K} \alpha_u(i) c_{ku} s_{ki} \cos(2\pi (f_c + u\Delta f - U\Delta f/2)t + \theta_u(i)) + n(t) \end{aligned} \tag{2.11}$$

where $\Re\{x\}$ denotes the real part of $x$.

It is of prime significance that the receiver accurately estimates the phase shift introduced by the channel on each frequency component of the received signal, since the spreading codes are incorporated in the transmit signal as 0 or $\pi$ phase shifts. Hence, by a slight error in phase estimation the orthogonality between the codes of different users might be lost which results in severe degradation of performance. In order to combat the performance degradation mentioned above, equalization is

performed at the receiver end. The equalization has the main goal of canceling the interference effects on the desired user's signal, while enhancing the noise component as little as possible. In this section we consider three classical equalization techniques which can be applied whenever diversity either in time, space or frequency is utilized. In these methods the receiver multiplies the received signal (after match filtering for each subcarrier) by a weighting factor on each subcarrier and feeds the result into the detector of the receiver structure, where a decision is made (see Fig 2.1-c). The decision variable for the $k^{th}$ user in the $i^{th}$ OFDM symbol interval is:

$$\begin{aligned} D_{ki} &= \sum_{u=0}^{U-1} D_{ki}^{u} = \frac{2}{T_s} \sum_{u=0}^{U-1} \int_{iT_s}^{(i+1)T_s} r(t) G_k^u \cos(2\pi(f_c + u\Delta f - U\Delta f/2)t + \theta_u) dt \\ &= \sum_{k'=1}^{K} \sum_{u=0}^{U-1} \alpha_u c_{k'u} G_k^u s_{k'i} \frac{2}{T_s} \int_{iT_s}^{(i+1)T_s} \cos^2\big(2\pi(f_c + u\Delta f - U\Delta f/2)t + \theta_u\big) dt + n_k \end{aligned} \tag{2.12}$$

where $G_k^u$ is the weighting factor of $k^{th}$ user over $u^{th}$ subcarrier, and index $i$ has been omitted in the coefficients $\alpha_u$ and $\theta_u$ for clarity. It is assumed that ideal phase synchronization is achieved, and $n_k = \sum_{u=0}^{U-1} n_{ku}$, where $n_{ku} = \frac{2}{T_s} \int_{iT_s}^{(i+1)T_s} n(t) G_k^u \cos(2\pi(f_c + u\Delta f - U\Delta f/2)t + \theta_u) dt$ is the noise component of the $u^{th}$ subcarrier with variance:

$$\begin{aligned} \mathrm{E}[n_{ku} n_{ku}^*] &= \mathrm{E}\Bigg[ \frac{4}{T_s^2} \int_{iT_s}^{(i+1)T_s} G_k^u n(t) \cos(2\pi(f_c + u\Delta f - U\Delta f/2)t + \theta_u) dt \\ &\qquad \cdot \int_{iT_s}^{(i+1)T_s} G_k^{u*} n^*(t') \cos(2\pi(f_c + u\Delta f - U\Delta f/2)t' + \theta_u) dt' \Bigg] \\ &= \frac{4\,|G_k^u|^2}{T_s^2} \int_{iT_s}^{(i+1)T_s} \int_{iT_s}^{(i+1)T_s} \frac{N_0}{2} \delta(t - t') \cos(2\pi(f_c + u\Delta f - U\Delta f/2)t + \theta_u) \\ &\qquad \cdot \cos(2\pi(f_c + u\Delta f - U\Delta f/2)t' + \theta_u) dt\, dt' \end{aligned}$$

$$= \frac{2\left|G_k^u\right|^2 N_0}{T_s^2} \int_{iT_s}^{(i+1)T_s} \cos^2(2\pi(f_c + u\Delta f - U\Delta f/2)t + \theta_u)dt \approx \left|G_k^u\right|^2 \frac{N_0}{T_s} \tag{2.13}$$

In practice the decision variables ($D_{ki}$) are calculated digitally using a IFFT structure. Sampling the received signal $\tilde{r}_i(t)$ at $t = lT_{\text{samp}}$ ($T_{\text{samp}} = \frac{1}{U\Delta f}$), the samples are grouped as:

$$[\tilde{r}_i(0), \cdots, \tilde{r}_i\left((U-1)T_{\text{samp}}\right)]^T = \sum_{k=1}^{K} \mathbf{F}^H(U)\mathbf{r}_{ki}^{\text{sig}} + \tilde{\mathbf{n}}_i' \tag{2.14}$$

where $\mathbf{r}_{ki}^{\text{sig}} = s_{ki}[\alpha_0 e^{j\theta_0} c_{k0}, \alpha_1 e^{j\theta_1} c_{k1}, \cdots, \alpha_{U-1} e^{j\theta_{U-1}} c_{k\,U-1}]^T$ and $\tilde{\mathbf{n}}_i' = [\tilde{n}_i'(0), \tilde{n}_i'(T_{\text{samp}}),$ $\cdots, \tilde{n}_i'((U-1)T_{\text{samp}})]^T$. Hence by taking the FFT of (2.14) we have:

$$\begin{aligned}\mathbf{r} &= \frac{1}{U}\mathbf{F}(U)\left(\sum_{k=1}^{K} \mathbf{F}^H(U)\mathbf{r}_{ki}^{\text{sig}} + \tilde{\mathbf{n}}_i'\right) \\ &= \sum_{k=1}^{K} \mathbf{r}_{ki}^{\text{sig}} + \mathbf{n}\end{aligned}$$

since $\frac{1}{U}\mathbf{F}(U)\mathbf{F}^H(U) = \mathbf{I}_U$. The decision variable for the $k^{th}$ user in the $i^{th}$ OFDM symbol interval is derived as:

$$\begin{aligned}D_{ki} &= \sum_{k'=1}^{K} \mathbf{G}_k \mathbf{r}_{k'i} \\ &= \sum_{k'=1}^{K} \sum_{u=0}^{U-1} \alpha_u c_{k'u} s_{k'i} G_k^u + n_k\end{aligned}$$

where $\mathbf{G}_k = [G_k^0 e^{-j\theta_0}, G_k^1 e^{-j\theta_1}, \cdots, G_k^{U-1} e^{-j\theta_{U-1}}]$. Clearly the decision variable derived in this method (which is implemented in practice) is the same as the one derived in (2.12).

The MC-CDMA receiver can take full advantage of the received signal information scattered in the frequency domain. Nevertheless, in a frequency-selective channel

the frequency components of the system are distorted and the orthogonality of the spreading codes is lost. Thus, the extent of non-selectivity of the channel plays an important role in determining the performance of the system. In addition, it must be noted that by properly choosing the number of subcarriers and the spacing between them, the chance of all the subcarriers being in a deep fade at the same time decreases, and the desired frequency diversity can be achieved. Furthermore, with a proper choice of the symbol duration (in a way that it considerably exceeds the delay spread of the channel), ISI is significantly reduced. The choice of $G_k^u$'s in (2.12) determines the combining technique used for detection. Two principal diversity techniques (i.e. EGC and MRC) will be presented in the downlink scenario. In the end, the MMSE detection method is presented, which takes the power of noise into consideration as well. It should be noted that in a downlink communication, the desired signal and interferers are subject to the same channel, thus by synchronizing the phase of the desired signal, the phase of the interference signals are automatically synchronized.

For simplicity of the discussion, we assume that subcarriers experience independent flat-fading processes[2]:

$$H_u = (H_u)^I + j(H_u)^Q \qquad u = 0, \cdots, U-1 \tag{2.15}$$

where $(H_u)^I$ and $(H_u)^Q$ are assumed to be independent real zero-mean Gaussian random variables with variance $\frac{1}{2}$, representing in-phase and quadrature components of the channel coefficients. Let $\alpha_u$ and $\theta_u$ be the amplitude and phase components of the channel respectively. Then the amplitude of the paths $(\alpha_u)$, are i.i.d Rayleigh

[2]This assumption applies only to this section. In the rest of the thesis the channel model developed in section 2.2.2 is used.

random variables with probability density function:

$$f_{\alpha_u}(\alpha_u) = \frac{\alpha_u}{\sigma^2_{\alpha_u}} \exp\left(-\frac{\alpha_u^2}{2\sigma^2_{\alpha_u}}\right) \tag{2.16}$$

where the first and second moments are calculated as:

$$\mathrm{E}[\alpha_u] = \sqrt{\frac{\pi}{2}}\sigma_{\alpha_u} \quad , \quad \mathrm{E}[\alpha_u^2] = 2\sigma^2_{\alpha_u} \tag{2.17}$$

and the random phase ($\theta_u$) is uniformly distributed over $[0, 2\pi]$ for all subcarriers.

The mean power over the $u^{th}$ subcarrier is:

$$\bar{P}_u = \mathrm{E}\left[\left|\alpha_u \cos\big(2\pi(f_c + u\Delta f - U\Delta f/2)t + \theta_u\big)\right|^2\right] = \frac{1}{2}\mathrm{E}\left[\alpha_u^2\right] \tag{2.18}$$

It is further assumed that the average power received at each of the subcarriers ($\bar{P}_u \triangleq \frac{1}{2}\mathrm{E}[|H_u|^2]$) is the same, thus the total average power received corresponding to each user denoted by $\bar{P}$ is equal to $U\bar{P}_u$.

### a) Equal Gain Combining (EGC)

In this method, the phase of the channel is compensated but the channel amplitude is not taken into consideration. Hence, the weighting factor in (2.12) is given by:

$$G_k^u = c_{ku}$$

The decision variable for the first user in the $i^{th}$ symbol interval can be simplified to:

$$D_{1i} = s_{1i}\sum_{u=0}^{U-1}\alpha_u + \beta_{\text{int}} + n_1 \tag{2.19}$$

In the downlink transmission, as the compound signal in (2.11) is received only through one channel, by compensating for the phase of the desired signal, the phase of the interference signals will be automatically corrected as well, thus the orthogonality of the codes remains intact. In this case, the interference term can be written as:

$$\beta_{\text{int}} = \sum_{k=2}^{K} \sum_{u=0}^{U-1} s_{ki} c_{ku} c_{1u} \alpha_u \tag{2.20}$$

As the codes are still orthogonal, the product $c_{ku}c_{1u}$ has value $+1$ for half of the subcarriers (denoted as $a_j$) and $-1$ for the other half (denoted as $b_j$). Thus the interference term can be rewritten as:

$$\beta_{\text{int}} = \sum_{k=2}^{K} s_{ki} \left( \sum_{j=0}^{\frac{U}{2}-1} \alpha_{a_j} - \sum_{j=0}^{\frac{U}{2}-1} \alpha_{b_j} \right)$$

hence, by applying the Central Limit Theorem (CLT) to each of the sums, the variance can be calculated as:

$$\sigma^2_{\beta_{\text{int}}} = (K-1)U\text{Var}(\alpha_u) = (K-1)U\left(\text{E}[\alpha_u^2] - \text{E}[\alpha_u]^2\right)$$

which considering the statistical characteristics of $\alpha_u$ in (2.17) and (2.18) will equal:

$$\sigma^2_{\beta_{\text{int}}} = (K-1)U\left(2 - \frac{\pi}{2}\right)\sigma^2_{\alpha_u} = 2(K-1)\left(1 - \frac{\pi}{4}\right)\bar{P} \tag{2.21}$$

and from (2.13), the noise variance will be $\sigma^2_{n_1} = U\frac{N_0}{T_s}$.

### b) Maximal Ratio Combining (MRC)

The main idea in this scheme is to maximize the received signal-to-noise ratio [22]. The frequency components are multiplied by their received amplitude and the weighting

factor can be written as:

$$G_k^u = c_{ku}\alpha_u$$

Hence the corresponding decision variable for the first user in downlink will be:

$$D_{1i} = s_{1i}\sum_{u=0}^{U-1}\alpha_u^2 + \sum_{k=2}^{K}\sum_{u=0}^{U-1}\alpha_u^2 s_{ki}c_{1u}c_{ku} + n_1 \tag{2.22}$$

For a large number of subcarriers the interference term can be approximated as a zero mean Gaussian random variable. The variance of the interference and the noise components are:

$$\sigma^2_{\beta_{\text{int}}} = (K-1)U\left(\mathrm{E}[\alpha_u^4] - \mathrm{E}[\alpha_u^2]^2\right) = (K-1)U\left(8\bar{P}_u^2 - 4\bar{P}_u^2\right) = 4\frac{K-1}{U}\bar{P}^2$$
$$\sigma^2_{n_1} = U\frac{N_0}{T_s}\mathrm{E}[\alpha_u^2] = 2\frac{N_0}{T_s}\bar{P} \tag{2.23}$$

### c) Bit error rate comparison

In this section, the downlink bit error rates of EGC and MRC equalization techniques are compared:

- **EGC** The bit error probability for a BPSK modulated system is [22]:

$$P_e = \frac{1}{2}\mathrm{erfc}\left(\sqrt{\frac{\gamma}{2}}\right)$$

where $\gamma$ represents the signal to interference plus noise ratio (SINR).

Using equations (2.19), (2.20) and (2.21) the probability of error in a downlink channel will be:

$$P_e \cong \frac{1}{2}\mathrm{erfc}\left(\sqrt{\frac{\pi}{4}\frac{\bar{P}T_s}{2\frac{K-1}{U}(1-\frac{\pi}{4})\bar{P}T_s + N_0}}\right)$$

where it is assumed that U is sufficiently large to apply the large the Law of Large Numbers (LLN) (i.e. $\sum_{u=0}^{U-1} \alpha_{1u} \approx UE[\alpha_{1u}]$) and the statistical characteristics of a Rayleigh multipath fading channel in (2.16) and (2.17) have been used.

- **MRC** Similarly, the probability of error in a downlink transmission using MRC can be derived from (2.22) and (2.23):

$$P_e \cong \frac{1}{2}\text{erfc}\left(\sqrt{\frac{\bar{P}T_s}{2\frac{K-1}{U}\bar{P}T_s + N_0}}\right)$$

### d) Minimum Mean Square Error (MMSE)

In this combining technique the power of noise is also taken into account and the weighting factor in (2.12) is:

$$G_k^u = \frac{\alpha_u}{\sum_{k=1}^{K} \alpha_u^2 + \frac{N_0}{2}} \cdot c_{ku} = \frac{\alpha_u}{K\alpha_u^2 + \frac{N_0}{2}} \cdot c_{ku}$$

which is derived from the MMSE criterion, stating that the estimated data symbols must be orthogonal to the baseband components of the received subcarriers [23].

## 2.3 Other variations of Multicarrier CDMA systems

As observed in section 2.1.1, DS-CDMA can accommodate a large number of users in a given bandwidth by using codes with satisfactory auto-correlation and cross-correlation properties. However, large and complex RAKE receiver structures are required in order to combat Inter-Symbol Interference (ISI). The multicarrier CDMA system proposed in [18] reduces the aforementioned complexities by transmitting data through different subcarriers and was presented in section 2.2. Other variations of multicarrier CDMA have also been proposed:

Generally speaking, multicarrier CDMA systems are categorized into two main groups: The first group comprises the methods where the original data stream is first spread using a unique spreading code and then each chip is transmitted over a different carrier frequency (as discussed in section 2.2). The second group comprises of techniques where the data stream is first serial to parallel (S/P) converted, each data stream is spread in time (similar to DS-CDMA) and transmitted over a carrier frequency independent of the other data streams. In this section a brief overview of the time spreading multicarrier CDMA structures is provided.

### 2.3.1 Time domain spreading

After Yee, Linnartz and Fettweis devised the MC-CDMA technique for indoor wireless systems [2], other multicarrier CDMA schemes were proposed that instead of frequency employ time domain spreading :

- Multi-carrier DS-CDMA (MC-DS-CDMA) proposed by Dasilva and Sousa in [24] spreads the S/P converted substreams of data in time domain. In this scheme the subcarriers overlap and satisfy the orthogonality criteria. Another MC-DS-CDMA system was proposed by Kondo and Milstein in [25], which suggests a system with no overlap between the subcarriers and exploits the advantages of direct sequence spread spectrum systems (e.g. robustness to multipath fading) together with the narrowband interference suppression effect of multicarrier systems, which mitigates the partial-band interference.

- Multi-Tone CDMA (MT-CDMA) proposed by Vandendorpe in [26].

### Multi-Carrier DS-CDMA (MC-DS-CDMA)[24]

Assume user $k$ transmits a sequence of symbols $\sum_{i=-\infty}^{\infty} s_{ki} p_s(t - T_s)$, then $U$ subsequences $\{a_0^k(i)\}, \cdots, \{a_{U-1}^k(i)\}$ are obtained after S/P conversion, where $a_u^k(i) = s_{k((i-1)U+u+1)}$. The spreading code of user $k$ over the $u^{th}$ subcarrier is defined as:

$$c_u^k(t) = \sum_{m=1}^{G_{MD}} c_{u,m}^k p_c\big(t - (m-1)T_C\big)$$

where $G_{MD}$ is the processing gain of the MC-DS-CDMA system, $c_{u,m}^k$ is the $m^{th}$ chip of the spreading code of $k^{th}$ user over $u^{th}$ subcarrier, and $p_c(t)$ is the chip pulse shaping signal.

The data substreams are multiplied by the spreading sequence, and then are modulated over the available subcarriers. In addition, since U independent substreams are transmitted concurrently, the symbol duration is reduced accordingly and hence chip-level synchronization can be achieved with a much less complex structure (in comparison with DS-CDMA). The transmitted signal in this case can be written as:

$$s_{MD}^k(t) = \sum_{i=-\infty}^{+\infty} \sum_{u=0}^{U-1} \sum_{m=1}^{G_{MD}} a_u^k(i) c_{u,m}^k . p_c\big(t - (m-1)T_C - iT_s'\big) \cos[2\pi(f_c + u\Delta f')t]$$

where $a_u^k(i)$ is the $i^{th}$ symbol of user $k$ over the $u^{th}$ subcarrier, $T_s'$ equals the symbol duration of the original data stream times the number of subcarriers (U), $T_C$ denotes the chip duration for each of the subcarrier streams and $\Delta f'(= \frac{1}{T_C})$ represents the subcarrier separation. It should be noted that the spreading sequence for each user can vary from one subcarrier to the other. Fig. 2.2 depicts a MC-DS-CDMA system with $G_{MD} = U = 4$, where for simplicity the spreading sequence is assumed to be the same for each subcarrier.

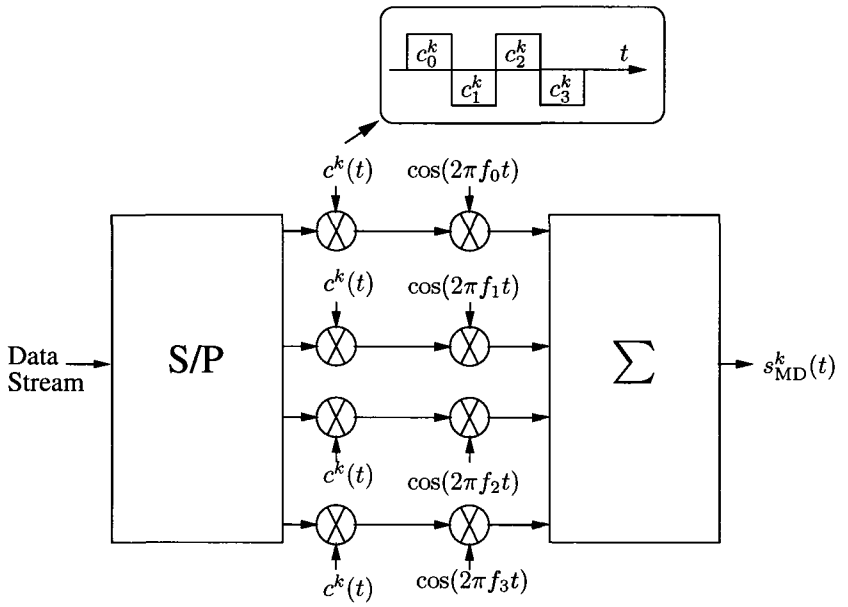


(a) Transmitter Structure (user $k$)

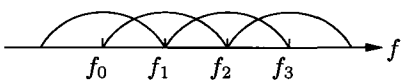


(b) Power spectrum of transmitted signal

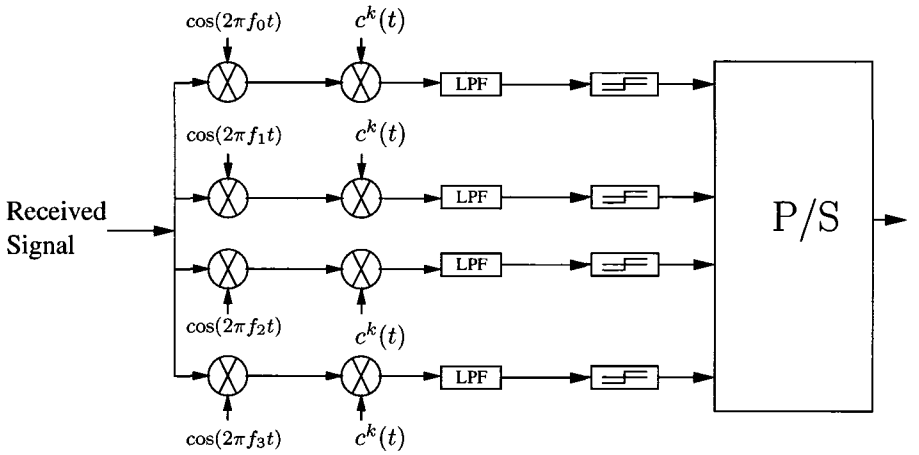


(c) Receiver structure (user $k$)

**Fig. 2.2** MC-DS-CDMA scheme: (a) transmitter, (b) power spectrum of transmitted signal (c) Receiver structure ($G_{MD} = 4$, $U = 4$)

### Multi-Tone CDMA (MT-CDMA)

Multi-tone CDMA is another realization of a time-domain spreading multicarrier CDMA system. The same principle as MC-DS-CDMA is used, however the subcarriers are more densely populated and the code sequences are generally longer. Unlike MC-DS-CDMA where the spread spectrum is achieved by sufficiently separated subcarriers, in this scheme the bandwidth of each subchannel is spread over a wide range of frequencies and the subcarriers are very close to each other (Figure 2.3), thus the spread spectrum of the modulated signals no longer satisfy the orthogonality criterion[3]. The transmitted signal in this case is:

$$s^k_{MT}(t) = \sum_{i=-\infty}^{+\infty} \sum_{u=0}^{U-1} \sum_{m=1}^{G_{MT}} a^k_u(i) c^k_{u,m} . p_c\big(t-(m-1)T_C - iT'_s\big) \cos[2\pi(f_c + u\Delta f'')t]$$

where $\Delta f''$ denotes the separation between the subcarrier frequencies and equals the inverse of the symbol duration, thus the subcarrier frequencies are very close to each other, as opposed to the MC-DS-CDMA technique where the separation of subcarriers determines the extent at which the transmitted signal is spread. Despite the fact that this scheme suffers from inter-subcarrier interference, by using longer codes SI and MUI are canceled effectively. Fig. 2.3 depicts a MT-CDMA transmit/receive structure together with the transmit signal power spectrum of a system with $G_{MT} = 16$ , $U = 4$.

### 2.3.2 Bandwidth comparison

Considering ideal rectangular pulse shapes, the required bandwidth of single carrier DS-CDMA and MT-CDMA is almost the same, but, MC-CDMA and MC-DS-CDMA modulation techniques require half as much bandwidth (see Figures 2.1-b, 2.2-

[3]It should be noted that the subcarriers are chosen such that they satisfy the orthogonality condition with minimum separation prior to spreading.

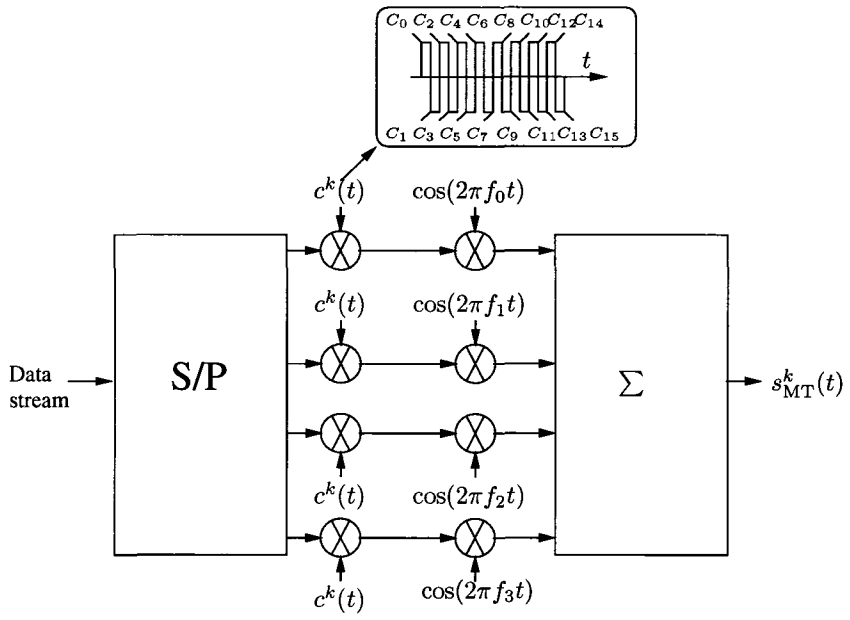


(a) Transmitter Structure (user $k$)

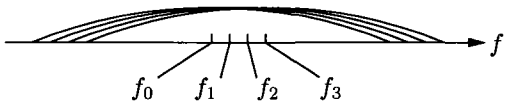


(b) Power spectrum of transmitted signal

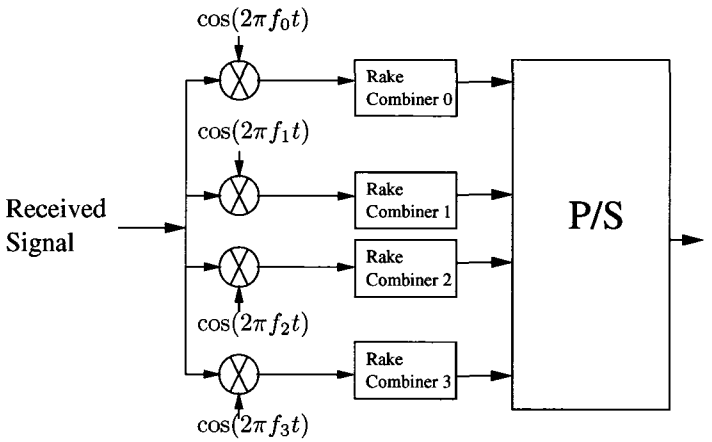


(c) Receiver structure

**Fig. 2.3** MT-CDMA scheme: (a) transmitter, (b) power spectrum of transmitted signal (c) Receiver structure ($G_{\mathrm{MT}} = 16$, $U = 4$)

b and 2.3-b). However, in practical implementations, where Nyquist filtering with a certain roll-off factor is considered, the bandwidth of all the mentioned modulation schemes are in the same order. Table 2.2 provides the system parameters for the discussed CDMA systems [2].

**Table 2.2** System parameters of different CDMA techniques

| CDMA method | DS-CDMA | MC-CDMA | MC-DS-CDMA | MT-CDMA |
|---|---|---|---|---|
| Symbol duration at subcarriers | $T_{DS}$ | $UT_{DS}/G_{MC}(=T_s)$ | $UT_{DS}$ | $UT_{DS}$ |
| Number of subcarriers | 1 | $U$ | $U$ | $U$ |
| Processing gain | $G_{DS}$ | $G_{MC}$ | $G_{MD}$ | $G_{MT}$ |
| Chip duration | $T_{DS}/G_{DS}$ | — | $UT_{DS}/G_{MD}$ | $UT_{DS}/G_{MT}$ |
| Subcarrier separation | — | $G_{MC}/UT_{DS}(=1/T_s)$ | $G_{MD}/(UT_{DS})$ | $1/(UT_{DS})$ |
| Required bandwidth | $\frac{G_{DS}}{T_{DS}}$ | $\frac{U+1}{U} \cdot \frac{G_{MC}}{T_{DS}}$ | $\frac{U+1}{U} \cdot \frac{G_{MD}}{T_{DS}}$ | $\frac{U-1+2G_{MT}}{UT_{DS}}$ |

## 2.4 Multi-Input Multi-Output (MIMO) structures

A MIMO structure takes the input data stream and after applying appropriate modulation and error control coding schemes, generates independent, partially or fully redundant substreams which are transmitted from the antenna elements. The receiver can also be equipped with multiple antennas and depending on the complexity of the transmit structure and a priori knowledge of channel at either end, various detection schemes can be realized.

The main incentive for using multiple antennas at either end of the communication system was originally the capability of MIMO structures to mitigate multipath fading in wireless channels. Smart antennas, one of the first MIMO structures that were developed, pursues this goal through beamforming where multiple antenna elements are employed at either transmit or receive end. In this technique, knowing the required direction of transmission/reception, antenna elements are properly weighted to focus

the transmitted/received energy at a desired direction in order to increase the SNR of the received signal and provides significant improvements when a line of site (LOS) component is available.

Spatial diversity gains can also be achieved using MIMO structures. A system with $M$ transmit antenna elements, sending replicas of the same data over all the antenna elements provides the receiver with $M$ different (ideally independent) versions of the information bearing signal. Hence the reliability of detection is significantly increased. Technically speaking, in this system the BER is proportional to $\frac{1}{\text{SNR}^M}$ as opposed to $\frac{1}{\text{SNR}}$ in a one-transmit antenna system. Hence, by using $M$ transmit antennas the diversity gain[4] is increased by $M$. In the general case, a MIMO structure with $M$ transmit and $N$ receive antennas can achieve a maximum diversity gain of $MN$. Despite the fact that spatial diversity techniques provide better results in Non-LOS (NLOS) environments, they still essentially combat the effects of multipath fading as in the smart antenna architectures.

Foschini and Telatar in two landmark papers have independently shown that in a rich multipath fading environment, the information theoretic capacity of a MIMO system can be increased linearly proportional with the lesser of the transmit and receive antenna elements [5, 4]. In other words, the multipath fading characteristics of the channel, once unfavorable for reliable communication, can now be exploited to increase the overall capacity of the communication system. The MIMO structures pursuing this goal are often known as VBLAST, or more generally as spatial multiplexing, architectures. In these systems independent streams of data are transmitted. The detection is very similar to solving a system of linear equations. The channel can be viewed as a matrix with each element representing the channel between each transmit/receive pair, provided we have single scalar channel coefficients for each

[4] A diversity gain of $d$ is achieved when the average error probability decays as $\frac{1}{\text{SNR}^d}$.

subchannel (i.e. flat fading conditions). Hence, when the channel matrix is full rank, $\min\{M, N\}$ independent data streams can be transmitted over the *eigen modes* of the channel, and properly detected at the receiver. In other words, the rank of the channel matrix determines how many independent substreams can be transmitted, which is clearly lower than $\min\{M, N\}$. Thus, in a VBLAST architecture, where $M$ independent streams of data are transmitted, for proper detection the number of receivers is required to be at least equal to the number of transmitters ($N \geq M$). These architectures significantly increase the spectral efficiency of the system, at the expense of lowering the diversity gain (see section 2.4.2). It should be noted that the transmitted substreams in a spatial multiplexing system can be viewed as virtual users in a multi-user CDMA system, where the signature codes of the users are provided by nature in a close to orthogonal manner (given that the channel matrix is well-conditioned or has a close to maximum rank), without exhausting any frequency resources. Hence, most of the detection techniques for spatial diversity systems are derived from the detection techniques in the multi-user CDMA systems [27, 28].

Based on the above discussion MIMO structures are generally utilized to pursue two main, albeit contradictory, objectives:

- Enhancing the performance (BER) of the system by increasing spatial diversity.

  or

- Increasing the spectral efficiency (bits/s/Hz) of the structure by transmitting independent streams of data over the transmit antenna elements.

In this section an introduction on the MIMO systems providing either diversity gain or higher data rates is provided.

### 2.4.1 Space-time block coding

In this section, the Alamouti simple transmit diversity method for a single carrier system is described [6]. An architecture with two transmit and $N$ receive antennas is assumed. The data is first modulated using a desired constellation, and the modulated data in two consecutive symbol intervals ($s_i$ and $s_{i+1}$) form the transmit signal matrix as follows:

$$\mathbf{S} = \begin{pmatrix} s_i & -s_{i+1}^* \\ s_{i+1} & s_i^* \end{pmatrix} \tag{2.24}$$

where the columns represent two consecutive time intervals and the rows correspond to the first and second transmit antennas. Hence, $s_i$ and $s_{i+1}$ are transmitted from the first and second antennas respectively in the first time interval and in the subsequent symbol interval $-s_{i+1}^*$ and $s_i^*$ are transmitted from the corresponding antenna elements. The received signal can be written as:

$$\mathbf{r}_{\text{Al}} = \begin{pmatrix} r_{11} & r_{12} \\ r_{21} & r_{22} \\ \vdots & \vdots \\ r_{N1} & r_{N2} \end{pmatrix} = \begin{pmatrix} h_{11} & h_{12} \\ h_{21} & h_{22} \\ \vdots & \vdots \\ h_{N1} & h_{N2} \end{pmatrix} \mathbf{S} + \mathbf{n}_{\text{Al}}$$

where $\mathbf{r}_{\text{Al}}$ and $\mathbf{n}_{\text{Al}}$ are $N \times 2$ matrices, with $\mathbf{n}_{\text{Al}}$ being an additive zero-mean circularly symmetric complex white Gaussian random matrix with two-sided PSD of $\frac{N_0}{2}$, $r_{nt}$ is the received signal from the $n^{th}$ receive antenna in the $t^{th}$ time interval, $h_{nm}$ is the channel coefficient between $m^{th}$ transmit and $n^{th}$ receive antenna elements in the time domain. Throughout the thesis, wherever space-time coding is utilized, it is assumed that the channel remains the same for two consecutive symbol intervals.

Fig. 2.4 shows a $2 \times 2$ MIMO structure with the corresponding channel coefficients.

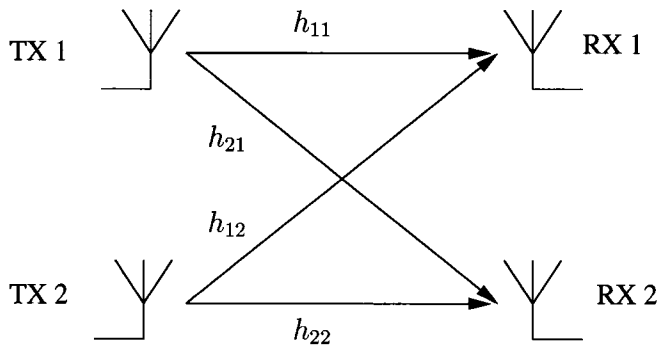


**Fig. 2.4** 2 × 2 MIMO structure - The channel coefficients are assumed to be constant over 2 consecutive symbol intervals.

The received signal can be rewritten in a vector form as:

$$\bar{\mathbf{r}}_{\mathrm{Al}} = \begin{pmatrix} r_{11} \\ r_{12}^* \\ \vdots \\ r_{N1} \\ r_{N2}^* \end{pmatrix} = \overbrace{\begin{pmatrix} h_{11} & h_{12} \\ h_{12}^* & -h_{11}^* \\ \vdots & \vdots \\ h_{N1} & h_{N2} \\ h_{N2}^* & -h_{N1}^* \end{pmatrix}}^{\mathbf{H}_{\mathrm{Al}}} \begin{pmatrix} s_i \\ s_{i+1} \end{pmatrix} + \begin{pmatrix} n_{11} \\ n_{12}^* \\ \vdots \\ n_{N1} \\ n_{N2}^* \end{pmatrix} \tag{2.25}$$

where $r_{nt}$ and $n_{nt}$ are the $nt^{th}$ components of $\mathbf{r}_{\mathrm{Al}}$ and $\mathbf{n}_{\mathrm{Al}}$ respectively.

The encoding scheme is devised in such a way that $\mathbf{H}_{\mathrm{Al}}^H \mathbf{H}_{\mathrm{Al}} = \alpha \mathbf{I}_2$, where $\alpha = \sum_{n=1}^{N} \left( |h_{n1}|^2 + |h_{n2}|^2 \right)$ and $\mathbf{I}_2$ is a $2 \times 2$ identity matrix. Hence by choosing the weighting matrix $\mathbf{G}$ as $\mathbf{H}_{\mathrm{Al}}^H$ the estimate of the transmitted symbols can be calculated:

$$\begin{pmatrix} \tilde{s}_i \\ \tilde{s}_{i+1} \end{pmatrix} = \mathbf{G}\bar{\mathbf{r}}_{\mathrm{Al}} = \mathbf{H}_{\mathrm{Al}}^H \bar{\mathbf{r}}_{\mathrm{Al}} = \alpha \begin{pmatrix} s_i \\ s_{i+1} \end{pmatrix} + \tilde{\mathbf{n}}_{\mathrm{Al}} \tag{2.26}$$

which is essentially a MRC technique. In order to further enhance the performance

of the system, the weighting matrix can be modified to perform MMSE detection and hence incorporate the effect of noise as follows:

$$g_{mn}^{\text{MMSE}} = \frac{g_{mn}^{\text{MRC}}}{\alpha + \frac{N_0}{2}}$$

where $g_{mn}^{\text{MMSE}}$ and $g_{mn}^{\text{MRC}}$ are the elements of $\mathbf{G}$ for MMSE and MRC detection schemes respectively.

### 2.4.2 Spatial multiplexing: ZF, MMSE and VBLAST

The input data stream is first modulated using a desired constellation. Subsequently, it is S/P converted to feed the $M$ transmit antennas, such that the input symbols in $i = lM + 1, ..., lM + M$ (for any arbitrary integer $l$) symbol intervals are transmitted simultaneously from the MIMO structure, hence the spectral efficiency is increased by a factor of $M$, which is achieved at the expense of decreasing the spatial diversity gain, and can severely degrade the overall system performance in undesirable channel conditions. The substreams are cyclically assigned to the available antenna elements such that the symbols in the intervals satisfying $i \mod M = m$ are transmitted over the $m^{th}$ transmit antenna. The receiver, attempts to retrieve the desired data stream by removing the effect of the other interfering substreams. As mentioned on page 35, the independent substreams can be viewed as virtual users in a CDMA system and like the multi-user CDMA system, the optimum Maximum Likelihood detection is computationally very complex. In this section two suboptimum linear (i.e. zero forcing (ZF) and MMSE) and one iterative (i.e. VBLAST) detection schemes for canceling the effect of the interfering signals are presented.

### Linear detection: ZF and MMSE

The received signal can be written as:

$$\mathbf{r} = \mathbf{H}\mathbf{s}_{\text{SM}} + \mathbf{n} \tag{2.27}$$

where $\mathbf{s}_{\text{SM}} = [s_{lM+1}, s_{lM+2}, \cdot\cdot, s_{lM+M}]^T$ for any arbitrary integer $l$ is the signal vector transmitted from the transmitter structure and $\mathbf{H}$ is the $N \times M$ channel matrix defined as:

$$\mathbf{H} = \begin{pmatrix} h_{11} & h_{12} & \cdots & h_{1M} \\ h_{21} & h_{22} & \cdots & h_{2M} \\ \vdots & \ddots & \ddots & \vdots \\ h_{N1} & h_{N2} & \cdots & h_{NM} \end{pmatrix}$$

which satisfies the following[5]:

$$\mathrm{E}\left[h_{nm} h^*_{n'm'}\right] = 0 \quad , \quad m \neq m' \ \vee \ n \neq n'$$

$\mathbf{n}$ is an $N \times 1$ vector with elements being additive zero-mean circularly symmetric complex white Gaussian random variables with two-sided PSD of $\frac{N_0}{2}$.

Assuming that the channel matrix is known at the receiver, by multiplying the received signal in (2.27) by the inverse[6] of the channel matrix the transmitted signal vector can be estimated as:

$$\tilde{\mathbf{s}}_{\text{SM}} = \mathbf{H}^{-1}\mathbf{r} = \mathbf{s}_{\text{SM}} + \overbrace{\mathbf{H}^{-1}\mathbf{n}}^{\mathbf{n}_d}$$

[5]This condition ensures uncorrelated fading for all transmit/receive pairs and holds throughout the thesis unless explicitly mentioned otherwise.

[6]Whenever the number of transmit and receive antennas are not equal Moore-Penrose generalized inverse (Pseudo-inverse) of the channel matrix is used [29].

This method is essentially the same as the zero-forcing equalization technique for removing ISI. Despite the simplicity of this method, it should be noted that the noise variance at the output of detector is $\mathrm{E}[\mathbf{n}_d\mathbf{n}_d^H] = \frac{N_0}{2}\mathbf{H}^+(\mathbf{H}^+)^H$ $(= \frac{N_0}{2}\left(\mathbf{H}^H\mathbf{H}\right)^{-1}$ if $\mathbf{H}^{-1}$ exists), where $\mathbf{H}^+$ is the Pseudo-inverse [29]. Hence according to the conditions of the channel the noise power may be amplified and possibly exceeds the desired signal power which would make correct detection virtually impossible.

In order to avoid noise enhancement and its undesirable consequences, the MMSE linear detection method has been proposed, where an estimate of the transmitted signal is calculated as:

$$\mathbf{y} = \mathbf{W}^{\mathrm{MMSE}}\mathbf{r}$$

where $\mathbf{r}$ is given by (2.27) and the weight matrix $\mathbf{W}^{\mathrm{MMSE}}$ is [30]:

$$\mathbf{W}^{\mathrm{MMSE}} = \left(\mathbf{H}^H\mathbf{H} + \frac{N_0}{2}\mathbf{I}_M\right)^{-1}\mathbf{H}^H$$

It can be seen that when the signal to noise ratio approaches infinity the MMSE detection matrix converges to $\left(\mathbf{H}^H\mathbf{H}\right)^{-1}\mathbf{H}^H$, which is the pseudo-inverse of $\mathbf{H}$ or the detection matrix for the zero forcing technique (assuming that $\left(\mathbf{H}^H\mathbf{H}\right)^{-1}$ exists). Thus, at high SNRs both methods perform almost the same.

### Vertical Bell Laboratory Space Time (VBLAST) architecture

In order to increase the throughput of MIMO systems, Foschini has proposed a scheme, where the data stream is demultiplexed over $M$ transmit antennas (known as *spatial layers*) and at each time interval a $M \times 1$ signal vector $\mathbf{s}_{\mathrm{SM}}$ with independent elements is transmitted over the channel [11].

The received signal is defined in (2.27) and the detection of the substreams is performed in the following 4 steps [30]:

1. *Ordering*: The substreams are sorted based on their channel conditions.

2. *Interference Cancellation*: The contribution of the already detected substreams are subtracted from the received signal.

3. *Interference Nulling*: The undetected substream with the best output SNR is detected using a ZF or MMSE combiner.

4. Steps 2 and 3 are repeated until all substreams are detected.

### Interference Cancellation

Assuming $s^1_{\text{SM}}, s^2_{\text{SM}}, \ldots, s^M_{\text{SM}}$ is the optimal ordering[7] of the substreams (e.g. $\mathbf{s}_{\text{SM}} = [s^1_{\text{SM}}, s^2_{\text{SM}}, \ldots, s^M_{\text{SM}}]^T$ if no ordering was needed), at the $s^{th}$ stage of detection the contribution of the previously detected subtreams is removed from the received signal as follows:

$$\mathbf{r}_s = \mathbf{r} - \sum_{m=1}^{s-1} \mathbf{H}^m s^m_{\text{SM}}$$

where $\mathbf{H}^m$ is the $m^{th}$ column of $\mathbf{H}$ corresponding to the $m^{th}$ substream ($s^m_{\text{SM}}$).

### Interference Nulling

In this step, the contribution of the not yet detected substreams has to be removed from $\mathbf{r}_s$ using ZF or MMSE cancellation techniques. A weight vector corresponding to the $s^{th}$ substream, based on the employed cancellation technique, is generated satisfying the following conditions [30]:

$$\mathbf{W}_s \mathbf{H}^m = 0 \quad \text{for} \quad m = s+1, \ldots, M \tag{2.28}$$

[7]The ordering criteria will be discussed shortly.

and

$$\mathbf{W}_s\mathbf{H}^s = 1$$

It should be noted that in order to be able to calculate the nulling vector for all substreams from (2.28), $N \geq M$ should be satisfied. In other words, VBLAST architecture requires the number of receive antennas to be greater than the number of transmit antennas. Subsequently, the estimate of the $s^{th}$ substream ($\tilde{s}^s_{\text{SM}}$) is calculated as:

$$\tilde{s}^s_{\text{SM}} = \mathbf{W}_s\mathbf{r}_s = s^s_{\text{SM}} + \mathbf{W}_s\mathbf{n}$$

where the noise is enhanced by a factor of $\|\mathbf{W}_s\|^2$. The enhancing factor is used as the criteria to order the signals in Step 1 (i.e. $s^1_{\text{SM}}$ corresponds to the substream having the lowest enhancing factor and so on).

From (2.28), it is clear that at the $s^{th}$ stage, only $M - s$ columns of the channel matrix are used to determine the weight vector $\mathbf{W}_s$. The $N - M + s$ other receive antenna elements provide spatial diversity gain. As the detection progresses, the spatial diversity gain increases and reaches its maximum of $N$ at the last stage. As a result, the substreams which are detected later in the algorithm are less susceptible to multipath fading, which further justifies the SNR ordering criteria utilized in this scheme.

### 2.4.3 Spatially correlated channel model

In [4] and [5], it has been shown that in rich scattering environments significant improvements in capacity are possible. However, this is true provided the channel has a full-rank correlation matrix with distinct eigenvalues, where a maximum number of independent spatial subchannels can be exploited to transmit independent streams of data. In a fully correlated MIMO channel, however, there is only one independent path

and very small gains, if any, can be achieved. In reality, lack of dominant scatterers or insufficient spacing between antenna elements in either transmit or receive structures result in partial correlation of the spatial channels, thus only a fraction of the promised theoretic capacities can be achieved. In order to analyze MIMO structures in such environments a proper modeling of the channel is inevitable. In this section the 'Kronecker model' for simulating correlated MIMO channels is briefly introduced.

Let us define the correlation between the antenna elements at the base station and mobile station as follows:

$$\mathbf{R}_{\mathrm{BS}} = \begin{pmatrix} \rho_{11}^{\mathrm{BS}} & \rho_{12}^{\mathrm{BS}} & \cdots & \rho_{1M}^{\mathrm{BS}} \\ \rho_{21}^{\mathrm{BS}} & \rho_{22}^{\mathrm{BS}} & \cdots & \rho_{2M}^{\mathrm{BS}} \\ \vdots & \vdots & \ddots & \vdots \\ \rho_{M1}^{\mathrm{BS}} & \rho_{M2}^{\mathrm{BS}} & \cdots & \rho_{MM}^{\mathrm{BS}} \end{pmatrix}$$

where $\rho_{m_1 m_2}^{\mathrm{BS}}$ represents the spatial correlation between base station antenna $m_1$ and $m_2$ and is defined as: $\rho_{m_1 m_2}^{\mathrm{BS}} = \langle h_{m_1 n}, h_{m_2 n} \rangle$, where $\langle a, b \rangle$ computes the correlation between $a$ and $b$. It is assumed that the correlation between the antennas at the base station is independent of the antennas at the mobile station. In other words, all mobile station antennas illuminate the same scatterers in the surrounding of the base station.

$$\mathbf{R}_{\mathrm{MS}} = \begin{pmatrix} \rho_{11}^{\mathrm{MS}} & \rho_{12}^{\mathrm{MS}} & \cdots & \rho_{1N}^{\mathrm{MS}} \\ \rho_{21}^{\mathrm{MS}} & \rho_{22}^{\mathrm{MS}} & \cdots & \rho_{2N}^{\mathrm{MS}} \\ \vdots & \vdots & \ddots & \vdots \\ \rho_{N1}^{\mathrm{MS}} & \rho_{N2}^{\mathrm{MS}} & \cdots & \rho_{NN}^{\mathrm{MS}} \end{pmatrix}$$

where $\rho_{n_1 n_2}^{\mathrm{MS}}$ represents the spatial correlation between mobile station antenna $n_1$ and $n_2$ and is defined as: $\rho_{n_1 n_2}^{\mathrm{MS}} = \langle h_{n_1 m}, h_{n_2 m} \rangle$, which is again assumed to be independent of the antenna elements of the base station.

It can be shown that the channel correlation matrix in such environment can be derived as [31]:

$$\mathbf{R}_{\text{MIMO}} = \mathbf{R}_{\text{MS}} \otimes \mathbf{R}_{\text{BS}} \tag{2.29}$$

where $\otimes$ denotes the Kronecker product (or direct product).

### Generation of correlated channel coefficients for simulation purposes

In order to generate a channel realization with a desired correlation matrix, primarily $NM$ complex Gaussian random variables are generated and stacked in a $MN \times 1$ column vector $\mathbf{A} = [\alpha_{11}, \alpha_{21}, \cdots, \alpha_{M1}, \cdots, \alpha_{N1}, \cdots, \alpha_{NM}]^T$. Assuming the correlation of antenna elements at the two ends of the system is known, the correlation matrix of the MIMO system can be calculated from (2.29), which using the Cholesky factorization can be decomposed as $\mathbf{R}_{\text{MIMO}} = \mathbf{B}\mathbf{B}^H$. Henceforth, the channel coefficients of the correlated MIMO channel can be derived as:

$$\mathbf{B}\mathbf{A} = [h_{11}, h_{12}, \cdots, h_{1M}, \cdots, h_{N1}, \cdots, h_{NM}]^T$$

and by rearranging the elements the channel matrix can be generated:

$$\mathbf{H} = \begin{pmatrix} h_{11} & h_{12} & \cdots & h_{1M} \\ h_{21} & h_{22} & \cdots & h_{2M} \\ \vdots & \vdots & \ddots & \vdots \\ h_{N1} & h_{N2} & \cdots & h_{NM} \end{pmatrix}$$

It should be noted that the above discussions hold for a flat-fading channel where the channel characteristics can be represented by a complex coefficient for each transmit/receive antenna pair at each instant.

# Chapter 3

# Multiple Input Multiple Output MC-CDMA structures

In this chapter MIMO structures for downlink MC-CDMA systems are studied. A downlink MIMO system with $M$ transmitters at the base station and $N$ receivers at the mobile station is considered. The well-known MIMO MC-CDMA architectures are studied in section 3.1 and in section 3.2 a new scheme is proposed. The new technique is compared with the other MIMO structures in terms of complexity and in chapter 5 BER performance comparisons are presented.

## 3.1 System model and receiver structures: Well-known architectures

In section 3.1.1 the space-time block coded MC-CDMA system is described. Section 3.1.2 discusses three spatial multiplexing MIMO structures (i.e. MMSE, MMSE-MUD and VBLAST). Subsequently, in section 3.1.3 space-time coding and spatial multiplexing are combined and a structure based on space-time-frequency MMSE

(STF-MMSE) detection technique [32] is presented.

### 3.1.1 Space-time block coding

Based on the discussion on the channel model in section 2.2.2, it is assumed that all subcarriers in the MC-CDMA system experience flat fading. Hence the space-time coded MC-CDMA system is identical to a single-carrier space-time coded system (see section 2.4.1) with the difference that the steps therein have to be carried out for all subcarriers. Once space-time decoding is performed and an estimate of the transmitted signals over all subcarriers is available (e.g. (2.26) for Alamouti space-time coding), the users' data are derived using a simple single user detection technique. Hence for a space-time coded system the despreading of the $k^{th}$ user's data will be:

$$\tilde{s}_{k(i+t-1)} = \sum_{u=0}^{U-1} \tilde{s}^{u}_{i+t-1} c_{ku} \qquad \text{for} \quad t = 1, 2, \cdots, p \tag{3.1}$$

where $\tilde{s}^{u}_{i+t-1}$ is the estimate of the transmitted signal over $u^{th}$ subcarrier in the $i+t-1$ symbol interval, $p$ is the number of independent transmitted signals in each space-time coded block (e.g. $p = 2$ for Alamouti space-time coding) and $\tilde{s}_{k(i+t-1)}$ is the estimate of the $k^{th}$ user data in the given interval.

### 3.1.2 Spatial multiplexing

The input data streams of all $K$ users are first modulated using a desired constellation, the symbol of user $k$ in the $i^{th}$ symbol interval ($s_{ki}$) is multiplied by its corresponding spreading code and spread in the frequency domain. Subsequently, the input is S/P converted to feed the $M$ transmit antennas, such that the input symbols of $i = lM+1, ..., lM+M$ (for any arbitrary integer $l$) OFDM symbol intervals are transmitted simultaneously; hence the spectral efficiency is increased by a factor of $M$. The

substreams are cyclically assigned to the available antenna elements such that the symbols in the OFDM symbol intervals satisfying $i \mod M = m$ are transmitted from the $m^{th}$ transmit antenna, which for one OFDM symbol and all subcarriers can be written in a column vector as:

$$\mathbf{s}_m^{\mathrm{Tx}} = \left[s_{lM+m}^0 \, , \, s_{lM+m}^1 \, , \, \cdots \, , \, s_{lM+m}^{U-1}\right]^T$$

where $s_i^u = \sum_{k=1}^{K} s_{ki} c_{ku}$, $\mathbf{c}_k = [c_{k0}, c_{k1}, \cdots, c_{k\,U-1}]^T$ is defined as the normalized spreading code of the $k^{th}$ user and $|c_{ku}| = \frac{1}{\sqrt{U}}$.

### MMSE

In this receiver structure, Minimum Mean Square criteria is employed to detect the substreams from the transmit antenna elements over each subcarrier. Signals transmitted over different subcarriers are assumed to be completely independent, which is not generally true.

The received signal over the $u^{th}$ subcarrier can be written as:

$$\mathbf{r}_u = \mathbf{H}_u \mathbf{s}_u^{\mathrm{MMSE}} + \mathbf{n}_u \quad \text{for} \quad u = 0, \cdots, U-1 \tag{3.2}$$

where $\mathbf{s}_u^{\mathrm{MMSE}} = [s_{lM+1}^u, s_{lM+2}^u, \cdots, s_{lM+M}^u]^T$ is the signal vector transmitted over the $u^{th}$ subcarrier and $\mathbf{H}_u$ is the $N \times M$ channel matrix over the $u^{th}$ subcarrier defined as:

$$\mathbf{H}_u = \begin{pmatrix} H_{11}^u & H_{12}^u & \cdots & H_{1M}^u \\ H_{21}^u & H_{22}^u & \cdots & H_{2M}^u \\ \vdots & \ddots & \ddots & \vdots \\ H_{N1}^u & H_{N2}^u & \cdots & H_{NM}^u \end{pmatrix}$$

which satisfies the following two constraints:

$$\mathrm{E}\left[\sum_{u=0}^{U-1}|H_{nm}^{u}|^{2}\right]=U \quad , \quad \forall\, n,m \quad \text{(refer to section 2.2.2)} \tag{3.3}$$

$$\mathrm{E}\left[H_{nm}^{u}H_{n'm'}^{u*}\right]=0 \quad , \quad m\neq m'\ ,\ n\neq n'\ ,\forall\, u \tag{3.4}$$

where $H_{nm}^{u}$ is the channel coefficient between the $m^{th}$ transmit and $n^{th}$ receive antenna elements over the $u^{th}$ subcarrier.

The noise term $\mathbf{n}_u$ is an $N\times 1$ vector with elements being additive zero-mean circularly symmetric complex white Gaussian random variables with two-sided PSD of $\frac{N_0}{2}$.

The estimate of the transmitted signal from the transmit antennas over the $u^{th}$ subcarrier will be:

$$\mathbf{y}_u=\mathbf{W}_u^{\mathrm{MMSE}}\mathbf{r}_u \quad \text{for} \quad u=0,\cdots,U-1$$

where $\mathbf{r}_u$ is given by (3.2) and the weight matrix $\mathbf{W}_u^{\mathrm{MMSE}}$ is:

$$\mathbf{W}_u^{\mathrm{MMSE}}=\left(\frac{K}{U}\mathbf{H}_u^H\mathbf{H}_u+\frac{N_0}{2}\mathbf{I}_M\right)^{-1}\mathbf{H}_u^H \tag{3.5}$$

After having estimated the transmitted independent substreams over all subcarriers, a conventional single user detection scheme is employed to detect the users' data. The estimated substreams are first arranged in a matrix $\mathbf{Y}=[\mathbf{y}_0,\mathbf{y}_1,\cdots,\mathbf{y}_{U-1}]$, then the $k^{th}$ user's data vector is estimated as:

$$\tilde{\mathbf{s}}_k=\left[\tilde{s}_{k(lM+1)},\tilde{s}_{k(lM+2)},\cdots,\tilde{s}_{k(lM+M)}\right]^T=\mathbf{Y}\mathbf{c}_k^* \tag{3.6}$$

where $\mathbf{c}_k=[c_{k0},c_{k1},\cdots,c_{kU-1}]^T$.

It should be noted that the CDMA single user detection method employed in this architecture is only optimal when the codes of the users are perfectly orthogonal

and the channel characteristics do not compromise this feature, which is practically impossible.

### VBLAST

The MC-CDMA VBLAST system operates on a per subcarrier basis. In other words, the receiver, employing the single carrier VBLAST technique (see section 2.4.2), retrieves an estimate of the transmitted signals from all the transmitters and over all subcarriers. Subsequently, the user's data are extracted using the single user detection technique in (3.6). Depending on whether ZF or MMSE is used as the interference nulling technique MC-CDMA-(ZF or MMSE)-VBLAST architecture is realized.

### MMSE-MUD

The optimal multi-user detector in a CDMA system is required to thoroughly search through trellises and has a very complex structure which increases exponentially with the number of active users [28]. Hence, other linear detectors have been devised that fill the significant performance gap between optimal detection and the single user detection technique, which was employed in the previous MIMO architectures. In this structure, a linear multi-user detection technique known as MMSE-MUD is implemented. Unlike the MMSE receiver, this structure considers all the spreading codes in the detection process, and all users' data are detected at once. The transmitted signal (before spreading) is written as follows:

$$\mathbf{s} = [s_{1\,lM+1}, \cdots, s_{1\,lM+M}, \cdots, s_{K\,lM+1}, \cdots, s_{K\,lM+M}]^T$$

where $s_{ki}$ is the symbol of user $k$ in the $i^{th}$ symbol interval. The received signal can then be expressed as:

$$\mathbf{r} = \mathbf{H}_{\text{MUD}}\mathbf{s} + \mathbf{n} \tag{3.7}$$

where $\mathbf{n}$ is an $NU \times 1$ additive zero-mean circularly symmetric complex white Gaussian random vector with two-sided PSD of $\frac{N_0}{2}$, and the channel matrix $\mathbf{H}_{\text{MUD}}$ is the concatenation of the $K$ users' channel matrices given by:

$$\mathbf{H}_{\text{MUD}} = [\mathbf{H}^1, \mathbf{H}^2, \cdots, \mathbf{H}^K] \in \mathbb{C}^{NU \times MK}$$

$$\mathbf{H}^k = \begin{pmatrix} \mathbf{H}^k_{11} & \cdots & \mathbf{H}^k_{1M} \\ \vdots & \ddots & \vdots \\ \mathbf{H}^k_{N1} & \cdots & \mathbf{H}^k_{NM} \end{pmatrix}, \ \mathbf{H}^k_{nm} = [\mathbf{C}_k \mathbf{h}_{nm}]_{U \times 1} \tag{3.8}$$

where $\mathbf{C}_k$ is a $U \times U$ diagonal matrix with the spreading code of the $k^{th}$ user on the diagonal and $\mathbf{h}_{nm} = [H^0_{nm}, \cdots, H^{U-1}_{nm}]^T$ is the channel matrix corresponding to the $m^{th}$ transmit and $n^{th}$ receive antennas, satisfying the conditions (3.3) and (3.4).
The estimated data is calculated as:

$$\tilde{\mathbf{s}} = \mathbf{W}_{\text{MMSE-MUD}}\mathbf{r}$$

where $\mathbf{r}$ is given by (3.7) and the MMSE-MUD weight matrix has a similar form as that of MMSE detection in (3.5):

$$\mathbf{W}_{\text{MMSE-MUD}} = \left(\mathbf{H}^H_{\text{MUD}}\mathbf{H}_{\text{MUD}} + \frac{N_0}{2}\mathbf{I}_{MK}\right)^{-1} \mathbf{H}^H_{\text{MUD}} \tag{3.9}$$

where we have assumed $\mathrm{E}\left[s_{klM+r}s_{k'l'M+r'}\right] = \delta_{kk'}\delta_{ll'}\delta_{rr'}$ (normalized uncorrelated data).

This receiver performs significantly better than the MMSE receiver, since the frequency domain and spatial components of the received signal are jointly considered. It should be noted, however, that the spreading codes of all users are required for detection and the overall structure is considerably more complex (see section 3.3).

### 3.1.3 Combined Space-time coding and Spatial multiplexing

The main idea in the architectures combining space-time coding and spatial multiplexing, is to compromise between the spectral efficiency and diversity gains of the system such that a higher data rate communication with a required reliability is achieved. In order to pursue this goal, the transmit antenna elements are divided into groups, which transmit independent data streams (hence increasing the spectral efficiency) and within each group space-time coding is implemented to increase the reliability of the performance. The transmitters are divided into $G$ groups, also known as layers, each containing $m_1, m_2, \cdots, m_G$ antennas, such that $\sum_{g=1}^{G} m_g = M$. The input data stream is demultiplexed into $G$ substreams and each substream is transmitted through the corresponding antenna group. In this section a system based on a multi-user detection scheme presented in [32] is discussed and in section 3.2 our proposed scheme based on successive interference cancellation (SIC) is developed.

#### STF-MMSE-MUD

For simplicity of discussion a base station with $M = 2G$ transmitters and $G$ antenna groups using Alamouti space-time block coding is considered. Grouping all the subcarrier components together with their complex conjugates in one column vector, the received signal can be rewritten as:

$$\mathbf{r} = \left[r_{11}^{0}, \cdots, r_{11}^{U-1}, r_{12}^{0*}, \cdots, r_{12}^{U-1*}, \cdots, r_{N1}^{0}, \cdots, r_{N1}^{U-1}, r_{N2}^{0*}, \cdots, r_{N2}^{U-1*}\right]^{T}$$

where $r_{ni}^{u}$ represents the received signal at the $n^{th}$ receive antenna over the $u^{th}$ sub-carrier in the $i^{th}$ OFDM symbol interval.

$$\mathbf{r} = \mathbf{H}_{\text{STF}}\mathbf{s}_{\text{STF}} + \mathbf{n}$$

$$\mathbf{H}_{\text{STF}} = [\mathbf{H}_1 \ , \ \cdots \ , \ \mathbf{H}_G] \in \mathbb{C}^{2NU \times 2KG}$$

$$\mathbf{H}_g = \left[(\mathbf{H}_{1g}^{A})^T \ , \ \cdots \ , \ (\mathbf{H}_{Ng}^{A})^T\right]^T$$

where $\mathbf{H}_{ng}^{A}$ corresponds to the Alamouti space-time block coding channel matrix of the $g^{th}$ transmit antenna group and $n^{th}$ receive antenna defined as:

$$\mathbf{H}_{ng}^{A} = [\mathbf{H}_{ng}^{A1}, \mathbf{H}_{ng}^{A2}, \cdots, \mathbf{H}_{ng}^{AK}]$$

where,

$$\mathbf{H}_{ng}^{Ak} = \begin{pmatrix} \mathbf{C}_k\mathbf{h}_{n(2g-1)} & \mathbf{C}_k\mathbf{h}_{n(2g)} \\ \mathbf{C}_k\mathbf{h}_{n(2g)}^{*} & -\mathbf{C}_k\mathbf{h}_{n(2g-1)}^{*} \end{pmatrix}$$

and $\mathbf{C}_k$ and $\mathbf{h}_{nm}$ are the same as in (3.8).

The data vector in one OFDM interval is defined as:

$$\mathbf{s}_{\text{STF}} = [\overbrace{s_{1i}, s_{1\,i+1}, \cdots, s_{Ki}, s_{K\,i+1}}^{\text{First group}}, \overbrace{s_{1\,i+2}, \cdots, s_{K\,i+3}}^{\text{Second group}}, \cdots, s_{K\,i+G+1}]^T$$

According to the Wiener solution, the weight vector that minimizes $\mathrm{E}\left[\left\|\mathbf{s}(k) - \mathbf{w}_k^H\mathbf{r}\right\|\right]$ is calculated as $\mathbf{w}_k = \mathbf{R}^{-1}\mathbf{p}^{(k)}$, where:

$$\mathbf{s}(k) = [\overbrace{s_{ki}, s_{k\,i+1}}^{\text{First group}}, \overbrace{s_{k\,i+2}, s_{k\,i+3}}^{\text{Second group}}, \cdots, s_{k\,i+G+1}]^T$$

and $\mathbf{R}, \mathbf{p}^{(k)}$ are defined as:

$$\mathbf{R} = \mathrm{E}\left[\mathbf{r}\mathbf{r}^H\right] = \mathbf{H}_{\mathrm{STF}}\mathbf{H}_{\mathrm{STF}}^H + \frac{N_0}{2}\mathbf{I}_{2NU}$$

$$\mathbf{p}^{(k)} = \mathrm{E}\left[\mathbf{r}\mathbf{s}^H(k)\right] = \begin{pmatrix} \mathbf{H}_{11}^{Ak} & \cdots & \mathbf{H}_{1G}^{Ak} \\ \mathbf{H}_{21}^{Ak} & \cdots & \mathbf{H}_{2G}^{Ak} \\ \vdots & \ddots & \vdots \\ \mathbf{H}_{N1}^{Ak} & \cdots & \mathbf{H}_{NG}^{Ak} \end{pmatrix}_{2NU \times 2G}$$

Ultimately, the signal estimates can be calculated by:

$$\tilde{\mathbf{s}}(k) = \mathbf{w}_k^H \mathbf{r} \quad \text{for} \quad k = 1, \cdots, K$$

## 3.2 Proposed scheme: Multistage SIC (MSIC)

The transmit signal in one OFDM symbol interval before space-time processing can be written as:

$$\mathbf{s}_i = \left[\sum_{k=1}^{K} s_{ki}c_{k0}\ ,\ \sum_{k=1}^{K} s_{ki}c_{k1}\ ,\ \cdots\ ,\ \sum_{k=1}^{K} s_{ki}c_{k\,U-1}\right]^T \tag{3.10}$$

The transmit signal vectors ($\mathbf{s}_i$) are then spatially multiplexed over the $G$ transmit antenna groups and each group is processed in a space-time coding block. Considering a common space-time coding technique with a unit spectral efficiency for all the groups and assuming each space-time block spans $T$ OFDM symbol intervals, the MC-CDMA input stream given in (3.10) is demultiplexed as follows: $\mathbf{s}_i, \cdots, \mathbf{s}_{i+T-1}$ is transmitted through group 1, $\mathbf{s}_{i+T}, \cdots, \mathbf{s}_{i+2T-1}$ through group 2, and $\mathbf{s}_{i+(G-1)T}, \cdots, \mathbf{s}_{i+GT-1}$ is transmitted through the last group (see Fig. 3.1). Hence the $GT$ symbols of all the users are transmitted in $T$ OFDM symbol intervals and a spatial multiplexing of $G$ is

achieved.

The transmit signal can be expressed as:

$$\mathbf{S}^u = [\mathbf{S}_1^u\ ,\ \mathbf{S}_2^u\ ,\ \ldots\ ,\ \mathbf{S}_G^u]^T \tag{3.11}$$

where $\mathbf{S}_g^u$ is the space-time matrix of the $g^{th}$ component code. Due to its simple linear

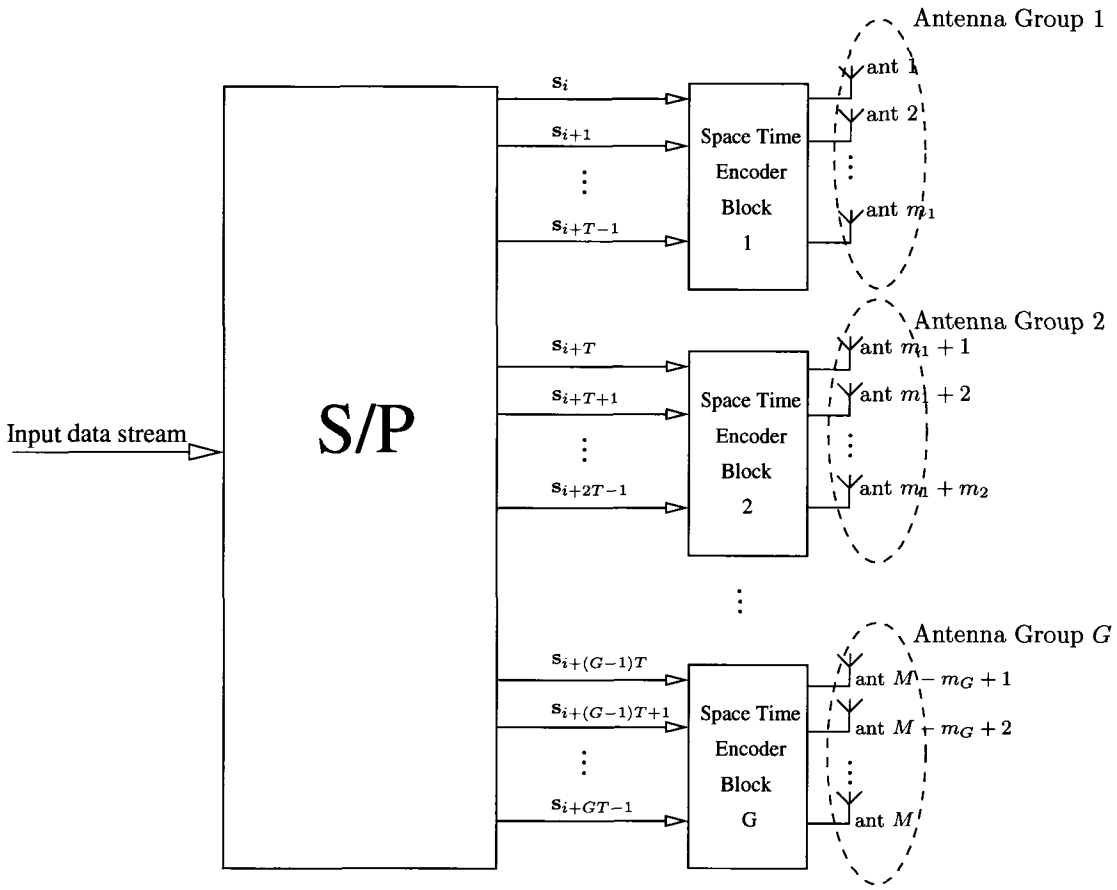


**Fig. 3.1** Transmitter structure - The input substreams are spatially multiplexed over $G$ transmit antenna groups and processed in a space-time coding block.

Maximum Likelihood detection method and full diversity gain without any loss in spectral efficiency, Alamouti space-time coding with two transmitters is chosen as the

component code [6]. In this case the space-time matrix $\mathbf{S}_g^u$ is:

$$\mathbf{S}_g^u = \begin{pmatrix} s^u_{i+2(g-1)} & -s^{u*}_{i+2(g-1)+1} \\ s^u_{i+2(g-1)+1} & s^{u*}_{i+2(g-1)} \end{pmatrix} \tag{3.12}$$

where $s_i^u$ is the $u^{th}$ element of $\mathbf{s}_i$ in (3.10) and $s_i^{u*}$ denotes the complex conjugate of $s_i^u$.

The receiver in this design operates on a per subcarrier basis. The received signal over the $u^{th}$ subcarrier is similar to (3.2) with the difference that the time dimension is also incorporated, yielding the $N \times T$ matrix:

$$\mathbf{r}^u = \mathbf{H}_u.\mathbf{S}^u + \mathbf{n}^u \tag{3.13}$$

where $\mathbf{S}^u$ is given by (3.11) and $\mathbf{n}^u$ is an $N \times T$ matrix with elements being additive zero-mean circularly symmetric complex white Gaussian random variables with two-sided PSD of $\frac{N_0}{2}$ and $T$ is the number of time intervals involved in each space-time coded block.

The data of the groups are detected sequentially. Let us describe the received signal over the $u^{th}$ subcarrier when the contribution of the $g^{th}$ and previous groups is canceled as:

$$\mathbf{r}^u_{g+1} = \mathbf{r}^u_g - \mathbf{H}^u_g.\tilde{\mathbf{S}}^u_g \qquad \text{for} \qquad g = 1, \cdots, G-1 \tag{3.14}$$

where $\mathbf{r}_1^u = \mathbf{r}^u$ is given in (3.13). Clearly, no cancellation for the first group is required. $\mathbf{H}_g^u$ is the $N \times m_g$ channel matrix corresponding to the $g^{th}$ transmit antenna group defined as:

$$\mathbf{H}_g^u = \begin{pmatrix} H^u_{1\left(1+\sum_{i=1}^{g-1} m_i\right)} & \cdots & H^u_{1\left(m_g+\sum_{i=1}^{g-1} m_i\right)} \\ \vdots & \ddots & \vdots \\ H^u_{N\left(1+\sum_{i=1}^{g-1} m_i\right)} & \cdots & H^u_{N\left(m_g+\sum_{i=1}^{g-1} m_i\right)} \end{pmatrix}$$

and $\tilde{\mathbf{S}}_g^u$ is the estimate of $\mathbf{S}_g^u$ in (3.12) obtained as follows:

Starting with the first group ($g = 1$), the null space of the channel matrix corresponding to the other not yet detected groups, is calculated [33]:

$$\mathbf{N}_g^u = \mathcal{N}ull\{\bar{\mathbf{H}}_g^u\} \in \mathbb{C}^{(N-M+\sum_{i=1}^{g} m_i)\times N} \tag{3.15}$$

and

$$\mathbf{N}_g^u.(\mathbf{N}_g^u)^H = \mathbf{I}_{N-M+\sum_{i=1}^{g} m_i} \tag{3.16}$$

where $\mathcal{N}ull\{\mathbf{A}\}$ is an orthonormal basis for the null space of $\mathbf{A}$ that can be obtained from the singular value decomposition of $\mathbf{A}$ (see appendix A). $\bar{\mathbf{H}}_g^u$ is a $N \times (M - \sum_{i=1}^{g} m_i)$ matrix defined as:

$$\bar{\mathbf{H}}_g^u = \begin{pmatrix} H^u_{1(1+\sum_{i=1}^{g} m_i)} & H^u_{1(2+\sum_{i=1}^{g} m_i)} & \cdots & H^u_{1M} \\ \vdots & \vdots & \ddots & \vdots \\ H^u_{N(1+\sum_{i=1}^{g} m_i)} & H^u_{N(2+\sum_{i=1}^{g} m_i)} & \cdots & H^u_{NM} \end{pmatrix} \tag{3.17}$$

Clearly $\bar{\mathbf{H}}_g^u$ corresponds to the channel matrix of the $g+1, g+2 \ldots, G$ groups over the $u^{th}$ subcarrier.

Henceforth, $\mathbf{r}_g^u$ is multiplied by the null-space matrix calculated in (3.15) and an equivalent received signal (after removing the zero components of $\mathbf{N}_g^u\mathbf{r}_g^u$) can be written as:

$$\mathbf{r}_{eq,g}^u = \mathbf{H}_{eq,g}^u.\mathbf{S}_g^u + \mathbf{n}_{eq,g}^u \tag{3.18}$$

where $\mathbf{H}^u_{eq,g}$ is a $N_{eq} \times m_g$ matrix, $N_{eq} = N - M + \sum_{i=1}^{g} m_i$ is the number of equivalent receive antennas and due to (3.16), $\mathbf{n}^u_{eq,g}$ is a noise term with the same statistics as $\mathbf{n}^u$ in (3.13). If Alamouti simple diversity scheme in [6] is used for all component codes, $\mathbf{S}^u_g$ is given by (3.12) and $\mathbf{r}^u_{eq,g}$ is of dimension $N_{eq} \times 2$, hence rearranging $\mathbf{r}^u_{eq,g}$ in a vector

$$\mathbf{r}^u_{g,\mathrm{Al}} = \left[ r^u_{eq,11}, r^{u*}_{eq,12}, r^u_{eq,21}, r^{u*}_{eq,22}, \cdots, r^u_{eq,N_{eq}1}, r^{u*}_{eq,N_{eq}2} \right]^T$$

where $r^u_{eq,nt}$ is the $nt^{th}$ element of $\mathbf{r}^u_{eq,g}$ (for simplicity the index $g$ has been omitted in $r^u_{eq,nt}$), the estimate of $s^u_{i+2(g-1)}$ and $s^u_{i+2(g-1)+1}$ (denoted by $\tilde{s}^u_{i+2(g-1)}$ and $\tilde{s}^u_{i+2(g-1)+1}$ respectively) are obtained by[1]:

$$\begin{pmatrix} \tilde{s}^u_{i+2(g-1)} \\ \tilde{s}^u_{i+2(g-1)+1} \end{pmatrix} = \frac{\begin{pmatrix} H^{u*}_{eq,11} & H^u_{eq,12} & \cdots & H^{u*}_{eq,N_{eq}1} & H^u_{eq,N_{eq}2} \\ H^{u*}_{eq,12} & -H^u_{eq,11} & \cdots & H^{u*}_{eq,N_{eq}2} & -H^u_{eq,N_{eq}1} \end{pmatrix}}{\sum_{n=1}^{N_{eq}} \left( \left| H^u_{eq,n1} \right|^2 + \left| H^u_{eq,n2} \right|^2 \right) + \frac{N_0}{2}} \cdot \mathbf{r}^u_{g,\mathrm{Al}} \tag{3.19}$$

where $H^u_{eq,nt}$ is the $nt^{th}$ element of $\mathbf{H}^u_{eq,g}$. The obtained estimates are grouped into a matrix of a similar form as in (3.12) and used to form the new received vector $\mathbf{r}^u_{g+1}$ in (3.14) for the next cancellation step. The users' data can be extracted by despreading the subcarrier estimates:

$$\tilde{s}_{k(i+2(g-1)+t)} = \sum_{u=0}^{U-1} \tilde{s}^u_{i+2(g-1)+t} c_{ku} \qquad \text{for} \quad t = 0, 1 \tag{3.20}$$

The steps (3.14)-(3.20) for $g = 1, \ldots, G$, represent the MSIC algorithm with no iteration. From (3.18) it is clear that a diversity gain of $m_g \times N_{eq}$ is achieved in

[1]The reader is referred to section 2.4.1.

the $g^{th}$ stage, which increases as the detection progresses such that the last group experiences the maximum diversity gain of $m_G \times N$. MSIC performance can be further improved by iterative detection: the $g^{th}$ group is detected by suppressing all of the other substreams, with the estimates calculated in the previous iteration, hence for subsequent iterations the nulling operation is not required and all groups benefit from the maximum diversity gain of $m_G \times N$.

### 3.2.1 Ordering criterion

The proposed sequential interference canceler is essentially a decision feedback system, hence the initial decisions potentially have a significant impact on the overall performance. In this section a criteria for the order of detection of the groups is proposed and its impact on the performance is discussed in chapter 5.

In a VBLAST system, interference canceling generally results in noise enhancement. And as discussed in section 2.4.2 the amount of noise enhancement is chosen as the criteria for ordering the detection of substreams. In the proposed method, however, the nulling matrix ($\mathbf{N}_g^u$) forms an orthonormal basis of the nulling space and hence the noise variance in the equivalent system remains the same. On the other hand, the SNR of the equivalent system in (3.18) is proportional to the second norm of the equivalent channel matrix ($\mathbf{H}_{eq,g}^u$). Hence, at the $g^{th}$ stage of detection the group satisfying the following condition will be detected:

$$\max_i \sum_{a,b} \left|\mathbf{H}_{eq,g_i}^u\right|_{ab}^2 \quad \forall\, u \quad , \quad i \in \{g, g+1, \cdots, G\} \tag{3.21}$$

where $\left|\mathbf{H}_{eq,g}^u\right|_{ab}$ represents the absolute value of $ab^{th}$ element of $\mathbf{H}_{eq,g}^u$ in (3.15). It should be noted that the ordering process has to be carried out for all subcarriers.

A simpler approach is to average the sum in (3.21) over all subcarriers and decide

on the next group to be detected. Hence, an alternate ordering criteria could be written as:

$$\max_{i} \sum_{u} \sum_{a,b} \left|\mathbf{H}^{u}_{eq,g_i}\right|^2_{ab} \quad , \quad i \in \{g, g+1, \cdots, G\} \tag{3.22}$$

Unlike (3.21), where the ordering criterion is checked for all subcarriers, and the groups are ordered for each subcarrier independently, in the simpler approach the ordering is performed once based on the average results for all the subcarriers which will clearly yield smaller improvement (see Fig. 5.10).

### 3.2.2 Frequency diversity gain and constellation order trade-off

In a purely spatial multiplexing architecture with $M$ transmit antenna elements, the spectral efficiency of the system is $M\eta$, where $\eta$ represents the spectral efficiency of the employed constellation (e.g. BPSK, QPSK, QAM, ...). In the proposed system, however, part of the transmit antenna elements are utilized to provide spatial diversity and the spectral efficiency is reduced to $\frac{M\eta}{G}$. In order to maintain the same spectral efficiency an obvious solution is to use higher order constellations. In a multi-carrier system, the problem can be tackled in another way as well. It is well known that in a frequency selective channel, increasing the processing gain above a certain value (corresponding to the maximum achievable frequency diversity which can be approximated by the normalized delay spread of the channel[2]) results in diminishing returns in terms of frequency diversity gain. Hence, in scenarios where the channel does not allow further increase in the frequency diversity and yet only a fraction of the allo-

[2]The maximum achievable frequency diversity of a channel is defined as [22]:

$$D_f \approx \frac{BW}{BW_c} = \frac{1/BW_c}{1/BW} = \frac{T_{\text{rms}}}{1/BW} = (T_{\text{rms}})_{\text{Normalized}} \tag{3.23}$$

where $T_{\text{rms}}$ and $(T_{\text{rms}})_{\text{Normalized}}$ are the RMS delay spread and normalized RMS delay spread of the system respectively. In order to obtain the real achievable frequency diversity gain for a given channel simulations are performed (see section 5.2).

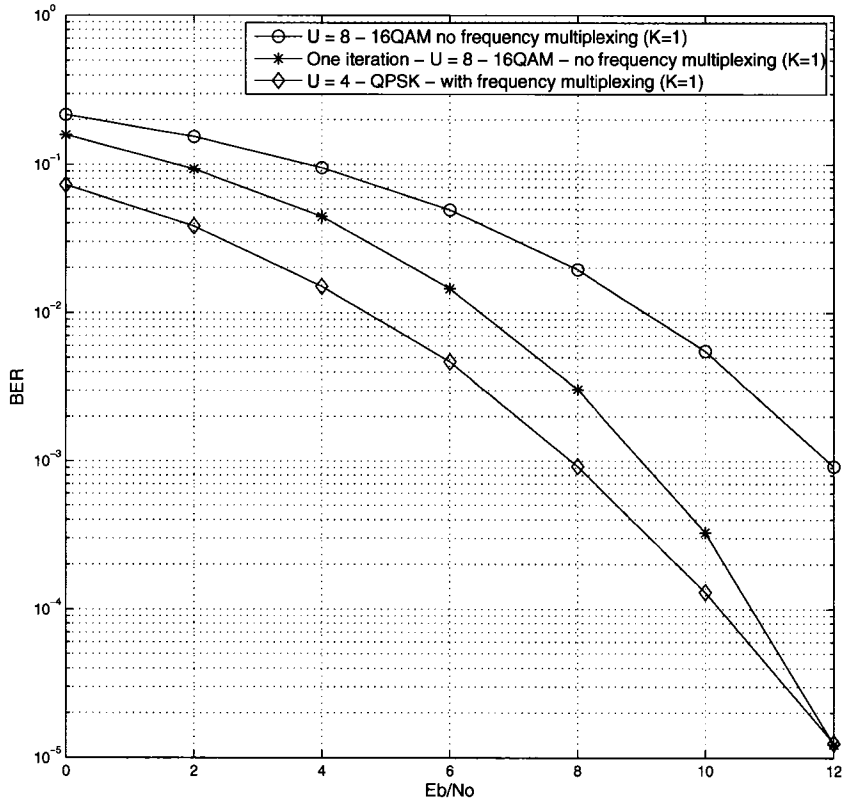


**Fig. 3.2** Comparison of BER performances of MSIC with and without frequency multiplexing in a single user system ($K = 1$).

cated frequency resources have been used, we can adjust (appropriately decrease) the processing gain and benefit from the rest of the bandwidth in order to increase the overall spectral efficiency to a desired amount, without increasing the constellation order (similar to frequency multiplexing in OFDM). In this way, the desired probability of error can be achieved with a significantly lower complexity. Fig. 3.2 depicts the improvement of the BER performance of MSIC with frequency multiplexing. In this system the processing gain has been reduced from 8 to 4 and the constellation size

is reduced from 16QAM to QPSK, hence the same data rate is achieved. It should be noted, however, that the gains achieved are at the expense of reduced capacity (in terms of number of active users). Thus, this method can be advantageous in scenarios where the system is not densely populated and high data rates are required.

## 3.3 Receivers complexity

The level of complexity of the MMSE, MMSE-MUD and STF-MMSE receivers is dominated by the number of matrix inversions and for MSIC the nulling operation is the dominant factor, which has to be carried out for all $G$ groups over all subcarriers. In general, the number of floating point operations (flops[3]) for inverting a $L \times L$ matrix by LU decomposition is approximately $\frac{5}{3}L^3 - \frac{2}{3}L$ and the number of flops required for calculating the null space of a $L \times P$ matrix can be approximated by $4LP^2 + 8L^3$ when the Golub-Reinsch SVD algorithm is used (see appendix A). Table 3.1 summarizes the number of flops required for each method[4]. Details on the complexity analysis of the proposed scheme (MSIC) are provided in appendix B.

As seen in section 3.1, MMSE, MMSE-MUD and STF-MMSE have very similar structures, and their main difference complexity-wise is their channel correlation matrices order (e.g. $M \times M$ for MMSE, $MK \times MK$ for MMSE-MUD and $2NU \times 2NU$ for STF-MMSE). Table 3.1 shows that the complexity of the proposed scheme (MSIC) is significantly lower than the other schemes. The complexity of STF-MMSE is proportional to $U^3$ (cube of total number of subcarriers) which could be very large, whereas in MSIC the complexity is merely proportional to the first power of $U$. As an example, a system with $U = 8$ and $M = N = 4$ is considered. As can be seen in Table 3.2

[3]Following [29], we define a flop as one addition or one multiplication.

[4]It should be noted that MSIC and STF-MMSE detect the symbols of two consecutive intervals simultaneously and the number of flops provided here for these two methods corresponds to the detection of two consecutive intervals.

the complexity of STF-MMSE is approximately 214 times more than MSIC in a full-load system, 165 times more in a half-load and 124 times in the single user scenario. Furthermore, the complexity of MMSE-MUD increases with $K^3$ (cube of the number of users), whereas MSIC complexity involves only the first power of $K$ (83 times less complex for full-load, 19 times less complex for half-load and 1.2 times less complex for single-user).

**Table 3.1** Complexity comparison

| Receiver | Matrix inversion (LU decomposition) | Matrix multiplication |
|---|---|---|
| MMSE | $\frac{5}{3}UM^3 - \frac{2}{3}UM$ | $4UM^2N + 2UMN + 2UKM$ |
| MMSE-MUD | $\frac{5}{3}K^3M^3 - \frac{2}{3}KM$ | $4UK^2M^2N + 2UKMN$ |
| STF-MMSE | $\frac{40}{3}U^3N^3 - \frac{4}{3}UN$ | $16U^2KMN^2 + 6UKMN$ |
| Receiver | Nulling operation | Matrix multiplication |
| MSIC (no iteration) | $UN^2M^2 + \frac{4}{3}UNM^3 - 4UNM^2$ | $2UKM + UMN(2N - M + \frac{19}{2})$ |
| | $-2UN^2M + \frac{8}{3}UNM$ | $-U(4N^2 + \frac{5}{2}M^2) + U(\frac{13}{2}M - 5N)$ |
| Additional computations (per iteration) | — | $UM^2N + \frac{7}{2}UMN + \frac{3}{2}UM$ |

and full-load systems respectively. Finally, MMSE (the simplest well-known MIMO structure considered) is 1.5 times more complex than MSIC for different number of active users, which as will be seen in chapter 5, performs poorly in most scenarios.

**Table 3.2** Complexity comparison example (for two consecutive symbol intervals)

| | Single user | Half-load | Full-load |
|---|---|---|---|
| MMSE | 6400 | 6784 | 7296 |
| MMSE-MUD | 4944 | 81728 | 376448 |
| STF-MMSE | 503168 | 702080 | 967296 |
| MSIC | 4064 | 4256 | 4512 |

# Chapter 4

# Bit Error Rate Analysis

In this chapter, we start with a thorough bit error rate analysis of a single user downlink MC-CDMA system in a correlated frequency selective fading channel. Subsequently, the bit error rate expression for multi-user environments is derived. The BER performance of a space-time coded MC-CDMA system is studied and an expression for the bit error rate is calculated. In the end the effect of frequency selectivity of the channel on the BER performance of the MC-CDMA system is discussed. As an introduction to the chapter, a brief literature review on the bit error rate analysis of MC-CDMA systems is provided.

## 4.1 Literature review

In [18], the BER performance of a MC-CDMA system for uplink and downlink transmission has been investigated. MRC and EGC techniques are considered and the BER expressions for both uplink and downlink are evaluated. Independent flat-fading is considered and assuming the number of the subcarriers is sufficiently large, Central Limit Theorem is employed to obtain the average bit error rate. In [34], the perfor-

mance of an asynchronous MC-CDMA system for an uplink system in a frequency selective fading channel is studied. MRC and EGC detection techniques are considered. An analytical expression for the Probability Density Function (PDF) of the channel coefficients is not simplified, hence the average BER is presented in an integral form and Monte Carlo integration is proposed to evaluate the final result. In [25], a multicarrier signaling technique has been applied to DS-CDMA and the BER performance has been evaluated. Perfect carrier, code and bit synchronization is assumed and the MRC combining BER performance is evaluated in a slowly frequency selective fading channel. Furthermore, the spreading codes of the users are assumed to be independent and random. The conditional probability of error is derived and the average BER expression is given in an integral form for a frequency selective fading channel. In [35], a BER lower bound for a MC-CDMA system (achievable in a single-user system with MRC detection) in a slow-varying frequency selective fading system is provided. All of the above mentioned works consider Gaussian approximation for Multi User Interference. Recently, an exact BER analysis of an uplink synchronous MC-CDMA system operating in a Rayleigh fading channel using the Moment Generating Function (MGF) without any assumptions on the distribution of the interferences has been proposed in [36]. It should be noted, however, that frequency correlation in the channel is not considered, in other words, the fading processes over different subcarriers are considered to be independent from one another.

In [37], the BER analysis of a space-time coded MC-CDMA system is presented. The effect of carrier frequency offset is studied and the bit error rate for EGC and MRC is derived. The subcarriers corresponding to the same data substream are chosen sufficiently apart, hence the frequency domain channel coefficients are assumed independent (In a MC-CDMA system design the subcarriers are chosen as separated as possible, however considering them completely independent is not a very practical

assumption).

## 4.2 Bit Error Rate Analysis of a single-user MC-CDMA system in a frequency selective Rayleigh fading channel

One of the most intriguing characteristics of MC-CDMA systems is that a wideband frequency selective channel can be treated as parallel narrowband flat fading subchannels over the available subcarriers. Despite the fact that one would choose the subcarriers as distant as possible (from one another) they are still correlated. In this section the BER performance of a MRC combiner in a single user MC-CDMA system in a frequency selective channel is investigated.

Defining $\mathbf{r}$ as a vector with components representing the received signal over different subcarriers as $\mathbf{r} = [r_0, r_1, \cdots, r_{U-1}]^T$, the frequency domain covariance matrix of the channel is defined as [35]:

$$\mathbf{R}_f = \frac{1}{2}\mathrm{E}[\mathbf{r}\mathbf{r}^H] = \left\{r_f^{a,b}\right\} \tag{4.1}$$
$$r_f^{a,b} = \Phi_C((a-b)\Delta f)$$

where $\mathbf{R}_f$ is the covariance matrix with elements $r_f^{a,b}$ and $\Phi_C(\Delta f)$ denotes the spaced frequency correlation function defined as the Fourier transform of the power delay profile:

$$\Phi_C(\Delta f) = \int_{-\infty}^{+\infty} \phi_c(\tau) e^{-j2\pi\Delta f\tau} d\tau$$

The nonzero eigenvalues ($\lambda_u$'s) of the covariance matrix ($\mathbf{R}_f$) determine the number of equivalent independent subchannels in the frequency domain. It should be noted that, there lies a very strong analogy between a MC-CDMA system and a narrowband communication system in a Rayleigh flat fading multipath channel, with the

difference that in the MC-CDMA system the multipath components of the received signal reside in the frequency domain whereas in a Rayleigh multipath fading channel they are generated through different paths in space. In our discussion we assume the channel is well-conditioned and the channel covariance matrix has $U$ distinct eigenvalues[1]. Henceforth, an equivalent channel with $U$ independent subchannels, each having a mean square expected value equal to the corresponding eigenvalue ($\mathrm{E}[(\alpha'_u)^2] = \lambda_u$) is considered.

The SNR for each subcarrier can be modeled as a Chi-squared random variable with two degrees of freedom (see MRC detection in section 2.2.3). Hence the characteristic function for each equivalent subchannel can be written as:

$$\psi_{\gamma_{eq,u}}(j\nu) = \frac{1}{1 - j\nu\bar{\gamma}_{eq,u}} \quad , \quad \bar{\gamma}_{eq,u} = \frac{2}{N_0}\lambda_u$$

where $\gamma_{eq,u}$ is the SNR over the $u^{th}$ equivalent subchannel and the channel SNR is defined as $\gamma_{eq} = \sum_{u=0}^{U-1} \gamma_{eq,u}$. The symbol energy is assumed to be normalized and the noise variance is scaled such that the signal to noise ratio in an AWGN channel would be equal to $\frac{2}{N_0}$.

Since the equivalent subchannels are independent, the characteristic function of $\gamma_{eq}$ can be written as the product of the characteristic functions of all subchannels:

$$\psi_{\gamma_{eq}}(j\nu) = \prod_{u=0}^{U-1} \frac{1}{1 - j\nu\bar{\gamma}_{eq,u}}$$

Consequently, the PDF of the channel can be calculated by taking the inverse Fourier

[1]This is a reasonable assumption since although the subcarriers are correlated, the subcarriers are still sufficiently spaced apart.

transform of the characteristic function:

$$p(\gamma_{eq}) = \sum_{u=0}^{U-1} \frac{\pi_u}{\bar{\gamma}_{eq,u}} e^{-\frac{\gamma_{eq}}{\bar{\gamma}_{eq,u}}} \quad , \quad \pi_u = \prod_{u'=0,u'\neq u}^{U-1} \frac{\lambda_u}{\lambda_u - \lambda_{u'}} \tag{4.2}$$

Thus, the BER of the system can be calculated by averaging the conditional probability of error over the channel realizations, which with binary antipodal signaling[2] is calculated as:

$$\begin{aligned} \text{BER} = \int_0^\infty Q\left(\sqrt{\gamma_{eq}}\right) p_{\gamma_{eq}}(\gamma_{eq}) d\gamma_{eq} &= \sum_{u=0}^{U-1} \frac{\pi_u}{\bar{\gamma}_{eq,u}} \int_0^\infty Q\left(\sqrt{\gamma_{eq}}\right) e^{-\frac{\gamma_{eq}}{\bar{\gamma}_{eq,u}}} d\gamma_{eq} \\ &= \frac{1}{2} \sum_{u=0}^{U-1} \pi_u \left[1 - \sqrt{\frac{\bar{\gamma}_{eq,u}}{\bar{\gamma}_{eq,u}+2}}\right] \end{aligned} \tag{4.3}$$

## 4.3 Multi user MC-CDMA Bit Error Rate analysis

### 4.3.1 Analytical BER expression for multiuser MC-CDMA

In a downlink MC-CDMA system with MRC detection the decision variable for the first user in the $i^{th}$ OFDM symbol interval is:

$$D_{1i} = \overbrace{s_{1i} \sum_{u=0}^{U-1} \alpha_u^2}^{D} + \overbrace{\sum_{k=2}^{K} \sum_{u=0}^{U-1} s_{ki} c_{1u} c_{ku} \alpha_u^2}^{\beta_{\text{int}}} + n_1 \qquad \text{(see section 2.2.3)}$$

Hence the average power of the desired user conditioned on the channel coefficients can be written as:

$$P_{D|\alpha_u} = \text{E}\left[D^2 | \{\alpha_u\}_{u=0}^{U-1}\right] = \text{E}\left[s_{1i}^2 \left(\sum_u \alpha_u^2\right)^2 \Big| \{\alpha_u\}_{u=0}^{U-1}\right] = \left(\sum_u \alpha_u^2\right)^2 \tag{4.4}$$

[2]It is well-known that the conditional error probability of a BPSK modulated system is equal to $Q\left(\sqrt{\gamma}\right)$. Throughout this chapter BPSK modulation is considered.

and the conditional variance of the interference is:

$$\mathrm{E}[\beta_{\mathrm{int}}^2 | \{\alpha_u\}_{u=0}^{U-1}, c_{1u}c_{1u'}] = \sum_{k\neq 1}\sum_{k'\neq 1}\sum_{u}\sum_{u'} \mathrm{E}[s_{ki}s_{k'i}\alpha_u^2\alpha_{u'}^2 c_{ku}c_{k'u'}c_{1u}c_{1u'} | \{\alpha_u\}_{u=0}^{U-1}, c_{1u}c_{1u'}]$$
$$= \sum_{k\neq 1}\sum_{u}\sum_{u'} \alpha_u^2\alpha_{u'}^2 c_{1u}c_{1u'}\mathrm{E}[c_{ku}c_{ku'}|c_{1u}c_{1u'}]$$

assuming uncorrelated normalized user data. We consider orthogonal Walsh-Hadamard codes which have the property of (see appendix C)[3]:

$$\mathrm{E}[c_{ku}c_{ku'}|c_{1u}c_{1u'}] = \begin{cases} -\frac{1}{U-1}c_{1u}c_{1u'} & , \quad u \neq u', k \neq 1 \\ 1 & , \quad \text{Otherwise} \end{cases}$$

Hence:

$$\mathrm{E}\left[\beta_{\mathrm{int}}^2 \middle| \{\alpha_u\}_{u=0}^{U-1}, c_{1u}c_{1u'}\right] = (K-1)\sum_u \alpha_u^4 - \frac{1}{U-1}(K-1)\left[\left(\sum_u \alpha_u^2\right)^2 - \sum_u \alpha_u^4\right]$$
$$= \left(1+\frac{1}{U-1}\right)(K-1)\sum_u \alpha_u^4 - \frac{1}{U-1}(K-1)\left(\sum_u \alpha_u^2\right)^2 \tag{4.5}$$

and $n_1$ is a zero mean Gaussian random variable defined as:

$$n_1 = \sum_u n_u c_{1u}\alpha_u$$

[3]One should take into consideration that the spreading codes of the users are chosen at random from the available spreading codes. This is done to average out the effect of each spreading code and to ensure same performance for all active users of the system.

with variance conditioned on the channel coefficients:

$$\begin{aligned}\sigma^2_{n|\alpha_u} &= \mathrm{E}\left[\sum_u n_u c_{1u}\alpha_u \sum_{u'} n^*_{u'} c_{1u'}\alpha_{u'} \middle| \{\alpha_u\}_{u=0}^{U-1}, c_{1u}c_{1u'}\right] \\ &= \mathrm{E}\left[\sum_u n_u n^*_u c^2_{1u}\alpha^2_u \middle| \{\alpha_u\}_{u=0}^{U-1}, c_{1u}c_{1u'}\right] = \frac{N_0}{2}\sum_u \alpha^2_u \end{aligned} \tag{4.6}$$

From (4.4)-(4.6), the signal to interference plus noise ratio is obtained as:

$$\begin{aligned}\gamma_{\mathrm{MU}} &= \frac{\left(\sum_u \alpha^2_u\right)^2}{(K-1)\left[\left(1+\frac{1}{U-1}\right)\sum_u \alpha^4_u - \frac{1}{U-1}\left(\sum_u \alpha^2_u\right)^2\right] + \frac{N_0}{2}\sum_u \alpha^2_u} \\ &= \frac{\sum_u \alpha^2_u}{(K-1)\left[\left(1+\frac{1}{U-1}\right)\frac{\sum_u \alpha^4_u}{\sum_u \alpha^2_u} - \frac{1}{U-1}\sum_u \alpha^2_u\right] + \frac{N_0}{2}}\end{aligned}$$

Hence the conditional probability of error can be written as:

$$\begin{aligned}P_{e|\alpha_u} &= Q\left(\sqrt{\gamma_{\mathrm{MU}}}\right) \\ &= Q\left(\sqrt{\frac{\sum_u \alpha^2_u}{(K-1)\left[\left(1+\frac{1}{U-1}\right)\frac{\sum_u \alpha^4_u}{\sum_u \alpha^2_u} - \frac{1}{U-1}\sum_u \alpha^2_u\right] + \frac{N_0}{2}}}\right) \\ &= Q\left(\sqrt{\frac{\frac{2\sum_u \alpha^2_u}{N_0}}{(K-1)\frac{2\sum_u \alpha^2_u}{N_0}\left[\left(1+\frac{1}{U-1}\right)\frac{\sum_u \alpha^4_u}{\left(\sum_u \alpha^2_u\right)^2} - \frac{1}{U-1}\right] + 1}}\right)\end{aligned} \tag{4.7}$$

which can be simplified to:

$$P_{e|\alpha_u} = Q\left(\sqrt{\frac{\gamma_{\mathrm{SU}}}{\mu(K-1)\gamma_{\mathrm{SU}}+1}}\right)$$

where $\mu = \left[\left(1+\frac{1}{U-1}\right)\frac{\sum_u \alpha^4_u}{\left(\sum_u \alpha^2_u\right)^2} - \frac{1}{U-1}\right]$ and $\gamma_{\mathrm{SU}} = \frac{2\sum_u \alpha^2_u}{N_0}$.

As mentioned in the single-user case, the system is equivalent to one with U independent paths and channel coefficients $\alpha'_u$ such that $\mathrm{E}[(\alpha'_u)^2] = \lambda_u$. Hence, the PDF of the equivalent channel is given in (4.2) and the average BER will be:

$$\mathrm{BER} = \int_0^\infty Q\left(\sqrt{\frac{\gamma_{eq}}{\mu(K-1)\gamma_{eq}+1}}\right) p_\gamma(\gamma_{eq}) d\gamma_{eq} \tag{4.8}$$

where $\gamma_{eq} = \sum_u \gamma_{eq,u}$ and $\gamma_{eq,u} = \frac{2(\alpha'_u)^2}{N_0}$.

To obtain a simplified analytical expression of the BER, $\mu$ is replaced by $\mathrm{E}[\mu]$ in (4.8), which is estimated through computer simulations as follows: Fig. 4.1 depicts the simulation result for $\mathrm{E}\left[\frac{\sum_u \alpha_u^4}{(\sum_u \alpha_u^2)^2}\right]$ and its curve fitted function $(\frac{1.8U-0.8}{U^2})$ versus processing gain. An estimate of $\mathrm{E}[\mu]$ is then obtained as

$$\begin{aligned} E[\mu] &= \left(1+\frac{1}{U-1}\right)\mathrm{E}\left[\frac{\sum_u \alpha_u^4}{(\sum_u \alpha_u^2)^2}\right] - \frac{1}{U-1} \\ &= \left(1+\frac{1}{U-1}\right)\frac{1.8U-0.8}{U^2} - \frac{1}{U-1} = \frac{0.8}{U} \end{aligned}$$

Hence using (4.2) and replacing $\mu$ by $\mathrm{E}[\mu] = \frac{0.8}{U}$ in (4.8), an estimate of the BER expression for the MC-CDMA multiuser system in a frequency selective fading channel is:

$$\mathrm{BER} = \sum_{u=0}^{U-1} \frac{\pi_u}{\bar{\gamma}_{eq,u}} \int_0^\infty Q\left(\sqrt{\frac{\gamma_{eq}}{(K-1)\frac{0.8}{U}\gamma_{eq}+1}}\right) e^{-\frac{\gamma_{eq}}{\bar{\gamma}_{eq,u}}} d\gamma_{eq} \tag{4.9}$$

Note that if $K = 1$ (single-user case), (4.9) reduces to the well-known BER expression single-user MC-CDMA given by (4.3).

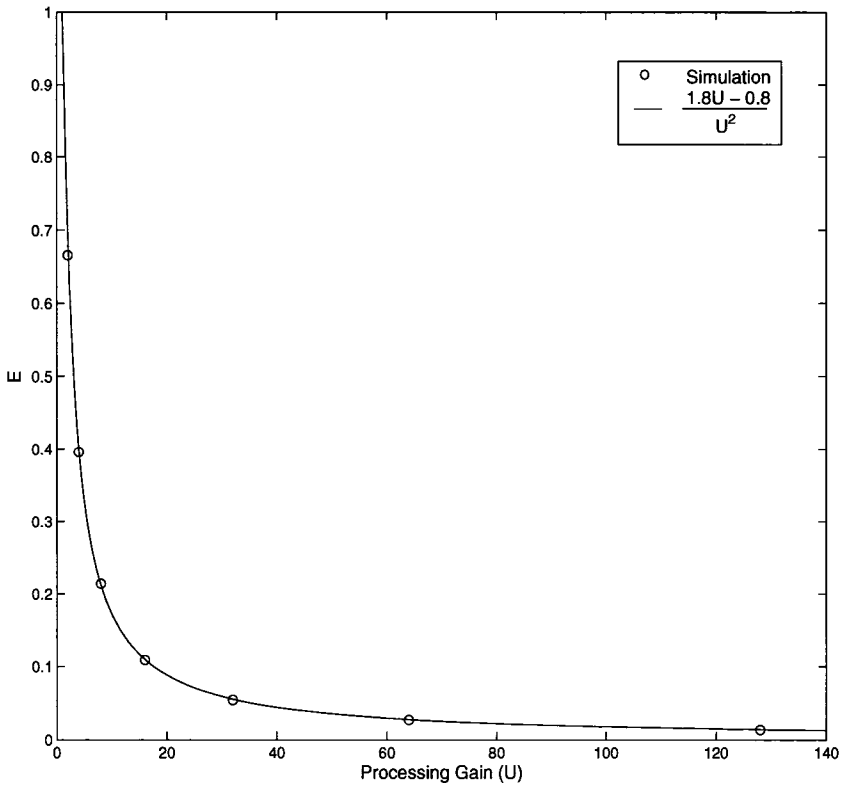


**Fig. 4.1** $\mathrm{E}\left[\frac{\sum_u \alpha_u^4}{(\sum_u \alpha_u^2)^2}\right]$ is derived by curve-fitting the simulation points.

### 4.3.2 BER simulation versus Analysis for multi user MC-CDMA

In this section the accuracy of the BER analysis for MC-CDMA is verified by comparing the simulation results and the derived analytical expression given by (4.9). The simulations are performed in a correlated frequency selective fading channel characterized by its normalized delay spread and normalized maximum delay. The system has a total of 64 available subcarriers and processing gains of 8 and 16 are considered. The number of simulated bits for each simulation are chosen in a way that ensures at

least 10 independent bit errors for each SNR.

Fig. 4.2 depicts the simulation and analysis results for a BPSK-modulated MC-CDMA system with processing gain of 8 and different number of active users assuming a normalized delay spread of 3 and a normalized maximum delay of 10. Fig. 4.3 shows the results for a system with a processing gain of 16 and a normalized delay spread[4] of 20. Fig. 4.2 and Fig.4.3 show that the BER found using the analytical expression given by (4.9) agrees very well with the simulation results.

[4]The maximum delay spread is properly selected in order to ensure that the channel covariance matrix is well-conditioned and thus has distinct eigenvalues.

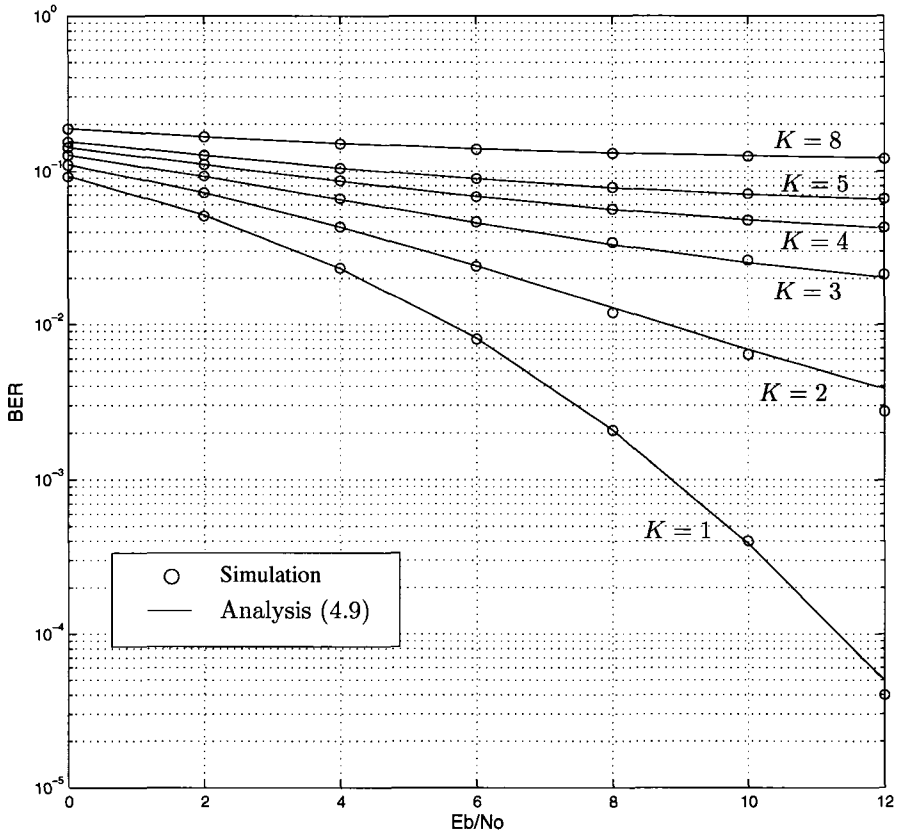


**Fig. 4.2** Simulation and Analysis results for a MC-CDMA system for K=[1,2,3,4,5,8]

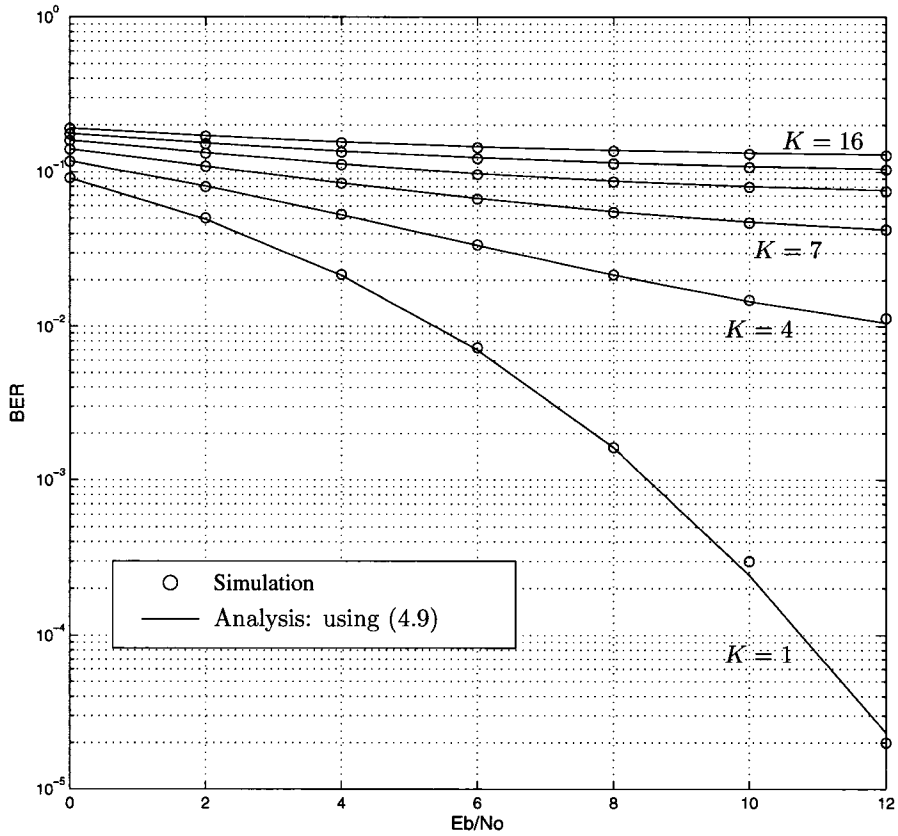


**Fig. 4.3** Simulation and Analysis results for a MC-CDMA system with maximum delay spread of 20 and K=1,4,7,10,13,16

## 4.4 BER analysis of STBC MC-CDMA

### 4.4.1 Analytical BER expression for STBC MC-CDMA

In this section the BER analysis of a downlink space-time coded MC-CDMA deploying Alamouti scheme with two transmit and one receive antennas in a spatially uncorrelated MIMO environment is provided. The received signal for two consecutive symbol intervals after Alamouti spatial detection over the $u^{th}$ subcarrier can be written as (see sections 2.4.1 and 3.1.1):

$$\begin{cases} \tilde{s}_i^u = \overbrace{\left(|H_{11}^u|^2 + |H_{12}^u|^2\right)}^{\alpha_u^{\mathrm{ST}}} s_i^u + \overbrace{H_{11}^{u*} n_i^u + H_{12}^u n_{i+1}^{u*}}^{n_{ui}} & s_{i+t}^u = \dfrac{1}{\sqrt{2}} \sum_{k=1}^{K} s_{k\,i+t} c_{ku} \\ \tilde{s}_{i+1}^u = \overbrace{\left(|H_{11}^u|^2 + |H_{12}^u|^2\right)}^{\alpha_u^{\mathrm{ST}}} s_{i+1}^u + \overbrace{H_{12}^{u*} n_i^u - H_{11}^u n_{i+1}^{u*}}^{n_{u\,i+1}} & t = 0, 1 \end{cases} \tag{4.10}$$

where $\tilde{s}_i^u$ and $\tilde{s}_{i+1}^u$ denote the spatially processed received signals over the $u^{th}$ subcarrier, and correspond to the estimate of signals transmitted in two consecutive symbol intervals and $n_t^u$ is the noise over the $u^{th}$ subcarrier in the $t^{th}$ symbol interval. After spatial processing for all subcarriers, EGC is employed to combine the energy of the users' data in the frequency domain. Hence, the decision variable for user 1 in the $i^{th}$ symbol interval will be:

$$\begin{aligned} D_{1i} &= \sum_{u=0}^{U-1} \tilde{s}_i^u c_{1u} = \sum_{u=0}^{U-1} (\alpha_u^{\mathrm{ST}} s_i^u + n_{ui}) c_{1u} \\ &= \frac{1}{\sqrt{2}} \sum_{u=0}^{U-1} s_{1i} \alpha_u^{\mathrm{ST}} c_{1u}^2 + \frac{1}{\sqrt{2}} \sum_{k=2}^{K} \sum_{u=0}^{U-1} s_{ki} \alpha_u^{\mathrm{ST}} c_{ku} c_{1u} + \sum_{u=0}^{U-1} n_{ui} c_{1u} \end{aligned} \tag{4.11}$$

where the conditional instantaneous signal power is:

$$P = \mathrm{E}\left[\left(\frac{1}{\sqrt{2}}\sum_{u=0}^{U-1} s_{1i}\alpha_u^{\mathrm{ST}} c_{1u}^2\right)^2 \mid \{\alpha_u^{\mathrm{ST}}\}_{u=0}^{U-1}\right] = \frac{1}{2}\left(\sum_{u=0}^{U-1}\alpha_u^{\mathrm{ST}}\right)^2$$

and the variance of the interference term can be written as:

$$\begin{aligned}&\mathrm{E}\left[\beta_{\mathrm{int}}^2 \mid \{\alpha_u^{\mathrm{ST}}\}_{u=0}^{U-1}, c_{1u}c_{1u'}\right]\\ &= \frac{1}{2}\mathrm{E}\left[\sum_{k=2}^{K}\sum_{u} s_{ki}\alpha_u^{\mathrm{ST}} c_{ku}c_{1u}\sum_{k'=2}^{K}\sum_{u'} s_{k'i}\alpha_{u'}^{\mathrm{ST}} c_{k'u'}c_{1u'} \mid \{\alpha_u^{\mathrm{ST}}\}_{u=0}^{U-1}, c_{1u}c_{1u'}\right]\end{aligned}$$

Following the same line of reasoning as in section 4.3 the variance of the interference can be simplified to:

$$\begin{aligned}\mathrm{E}[\beta_{\mathrm{int}}^2 \mid \{\alpha_u^{\mathrm{ST}}\}_{u=0}^{U-1}, c_{1u}c_{1u'}] =& \frac{1}{2}\left(1+\frac{1}{U-1}\right)(K-1)\sum_u (\alpha_u^{\mathrm{ST}})^2\\ &- \frac{1}{2(U-1)}(K-1)\left(\sum_u \alpha_u^{\mathrm{ST}}\right)^2\end{aligned}$$

and the noise variance conditioned on $\alpha_u^{\mathrm{ST}}$ is:

$$\begin{aligned}\sigma^2_{n|\alpha_u^{\mathrm{ST}}} &= \mathrm{E}\left[\sum_u n_{ui}c_{1u}\sum_{u'} n^*_{u'i}c_{1u'}\middle|\{\alpha_u^{\mathrm{ST}}\}_{u=0}^{U-1}, c_{1u}c_{1u'}\right]\\ &= \frac{N_0}{2}\sum_u\left(E\left[|H_{11}^u|^2 + |H_{12}^u|^2\middle|\{\alpha_u^{\mathrm{ST}}\}_{u=0}^{U-1}, c_{1u}c_{1u'}\right]\right) = \frac{N_0}{2}\sum_u \alpha_u^{\mathrm{ST}}\end{aligned}$$

Hence the signal to interference plus noise ratio will be:

$$\gamma_{\mathrm{MU}}^{\mathrm{ST}} = \frac{\frac{1}{2}\sum_{u=0}^{U-1}\alpha_u^{\mathrm{ST}}}{\frac{1}{2}(K-1)\left[\left(1+\frac{1}{U-1}\right)\frac{\sum_u(\alpha_u^{\mathrm{ST}})^2}{\sum_u \alpha_u^{\mathrm{ST}}} - \frac{1}{U-1}\sum_u \alpha_u^{\mathrm{ST}}\right] + \frac{N_0}{2}}$$

and the conditional probability of error can be written as:

$$P_{e|\alpha_u^{\mathrm{ST}}} = Q\left(\sqrt{\gamma_{\mathrm{MU}}^{\mathrm{ST}}}\right) = Q\left(\sqrt{\frac{\gamma_{\mathrm{SU}}^{\mathrm{ST}}}{(K-1)\mu_{\mathrm{ST}}\gamma_{\mathrm{SU}}^{\mathrm{ST}}+2}}\right)$$

where $\gamma_{\mathrm{SU}}^{\mathrm{ST}} = \frac{2}{N_0}\sum_u \alpha_u^{\mathrm{ST}}$ and $\mu_{\mathrm{ST}} = \left(1+\frac{1}{U-1}\right)\frac{\sum_u \left(\alpha_u^{\mathrm{ST}}\right)^2}{\left(\sum_u \alpha_u^{\mathrm{ST}}\right)^2} - \frac{1}{U-1}$.

The PDF of $\gamma_{\mathrm{SU}}^{\mathrm{ST}}$ has a form similar to (4.2), with the difference that for each frequency there exists two independent paths corresponding to the spatial components with same eigenvalues ($2U$ independent paths).

$$p(\gamma_l) = \frac{1}{\bar{\gamma}_l} e^{-\frac{\gamma_l}{\bar{\gamma}_l}} \quad , \quad l = 0, \cdots, 2U-1$$
$$\bar{\gamma}_l = \frac{2}{N_0}\mathrm{E}[(\alpha_l')^2] \quad , \quad \mathrm{E}[(\alpha_l')^2] = \lambda_u \quad (u = l \bmod 2)$$

**Probability Distribution Function:** In a MC-CDMA system without space-time coding the PDF of the channel coefficients is derived by taking the IFFT of its characteristic function:

$$\psi_{\gamma_{eq}}(j\nu) = \prod_{u=0}^{U-1} \frac{1}{1-j\nu\bar{\gamma}_{eq,u}} \quad \xrightarrow{\text{IFFT}} \quad p(\gamma_{eq}) = \sum_{u=0}^{U-1} \frac{\pi_u}{\bar{\gamma}_{eq,u}} e^{-\frac{\gamma_b}{\bar{\gamma}_{eq,u}}}$$

where $\bar{\gamma}_{eq,u} = \frac{2}{N_0}\lambda_u$ and $\pi_u = \prod_{u'=0,u'\neq u}^{U-1} \frac{\lambda_u}{\lambda_u - \lambda_{u'}}$.

In the space-time coded system, however, there are two spatial independent paths for each subcarrier with the same average power. The characteristic function can be written as:

$$\psi_{\gamma_{eq}^{\mathrm{ST}}}(j\nu) = \prod_{u=0}^{U-1} \left(\frac{1}{1-j\nu\bar{\gamma}_{eq,u}}\right)^2 \quad \xrightarrow{\text{IFFT}} \quad ? \quad , \quad \bar{\gamma}_{eq,u} = \frac{2}{N_0}\lambda_u \qquad (4.12)$$

And the PDF is calculated by taking the IFFT of the characteristic function which

can be simplified as:

$$\begin{aligned}\psi_{\gamma_{eq}^{\mathrm{ST}}}(s) &= \prod_u \left(\frac{1}{1+s\bar{\gamma}_{eq,u}}\right)^2 = \left(\frac{\pi_0}{1+s\bar{\gamma}_{eq,0}} + \cdots + \frac{\pi_{U-1}}{1+s\bar{\gamma}_{eq,U-1}}\right)^2 \\ &= \sum_u \left(\frac{\pi_u}{1+s\bar{\gamma}_{eq,u}}\right)^2 + \sum_{u_i \neq u_j} \frac{\pi_{u_i}\pi_{u_j}}{(1+s\bar{\gamma}_{eq,u_i})(1+s\bar{\gamma}_{eq,u_j})} \\ &= \sum_u \left(\frac{\pi_u}{1+s\bar{\gamma}_{eq,u}}\right)^2 + \sum_{u_i \neq u_j} \pi_{u_i}\pi_{u_j} \left(\frac{\frac{\bar{\gamma}_{eq,u_i}}{\bar{\gamma}_{eq,u_i}-\bar{\gamma}_{eq,u_j}}}{1+s\bar{\gamma}_{eq,u_i}} + \frac{\frac{\bar{\gamma}_{eq,u_j}}{\bar{\gamma}_{eq,u_j}-\bar{\gamma}_{eq,u_i}}}{1+s\bar{\gamma}_{eq,u_j}}\right)\end{aligned}$$

Given the two identities:

$$\frac{1}{as+1} \xrightarrow{\mathcal{L}^{-1}} \frac{1}{a}e^{-\frac{t}{a}} \quad , \quad \left(\frac{1}{1+sa}\right)^2 \xrightarrow{\mathcal{L}^{-1}} \frac{t}{a^2}e^{-\frac{t}{a}}$$

where $\mathcal{L}^{-1}$ denotes the inverse Laplace transform, the PDF is calculated as:

$$p(\gamma_{eq}^{\mathrm{ST}}) = \sum_u \frac{\pi_u^2}{\bar{\gamma}_{eq,u}^2}\gamma_{eq}^{\mathrm{ST}} e^{-\frac{\gamma_{eq}^{\mathrm{ST}}}{\bar{\gamma}_{eq,u}}} + \sum_{u_i \neq u_j} \frac{\pi_{u_i}\pi_{u_j}}{\bar{\gamma}_{eq,u_i}-\bar{\gamma}_{eq,u_j}} \left(e^{-\frac{\gamma_{eq}^{\mathrm{ST}}}{\bar{\gamma}_{eq,u_i}}} - e^{-\frac{\gamma_{eq}^{\mathrm{ST}}}{\bar{\gamma}_{eq,u_j}}}\right)$$

And the average bit error probability will be:

$$\begin{aligned}\mathrm{BER} = &\sum_u \frac{\pi_u^2}{\bar{\gamma}_{eq,u}^2} \int_0^\infty Q\left(\sqrt{\frac{\gamma_{eq}^{\mathrm{ST}}}{(K-1)\mu_{\mathrm{ST}}\gamma_{eq}^{\mathrm{ST}}+2}}\right) \gamma_{eq}^{\mathrm{ST}} e^{-\frac{\gamma_{eq}^{\mathrm{ST}}}{\bar{\gamma}_{eq,u}}} d\gamma_{eq}^{\mathrm{ST}} \\ &+ \sum_{u_i \neq u_j} \frac{\pi_{u_i}\pi_{u_j}}{\bar{\gamma}_{eq,u_i}-\bar{\gamma}_{eq,u_j}} \int_0^\infty Q\left(\sqrt{\frac{\gamma_{eq}^{\mathrm{ST}}}{(K-1)\mu_{\mathrm{ST}}\gamma_{eq}^{\mathrm{ST}}+2}}\right) \left(e^{-\frac{\gamma_{eq}^{\mathrm{ST}}}{\bar{\gamma}_{eq,u_i}}} - e^{-\frac{\gamma_{eq}^{\mathrm{ST}}}{\bar{\gamma}_{eq,u_j}}}\right) d\gamma_{eq}^{\mathrm{ST}}\end{aligned} \tag{4.13}$$

Similar to section 4.3, $\mu_{\mathrm{ST}}$ is replaced by $\mathrm{E}[\mu_{\mathrm{ST}}]$, which through computer simulations is shown to be $\frac{0.4}{U}$. Fig. 4.4 depicts the simulation result for $\mathrm{E}\left[\frac{\sum_u (\alpha_u^{\mathrm{ST}})^2}{(\sum_u \alpha_u^{\mathrm{ST}})^2}\right]$ and its curve fitted function $(\frac{1.4U-0.4}{U^2})$ versus processing gain.

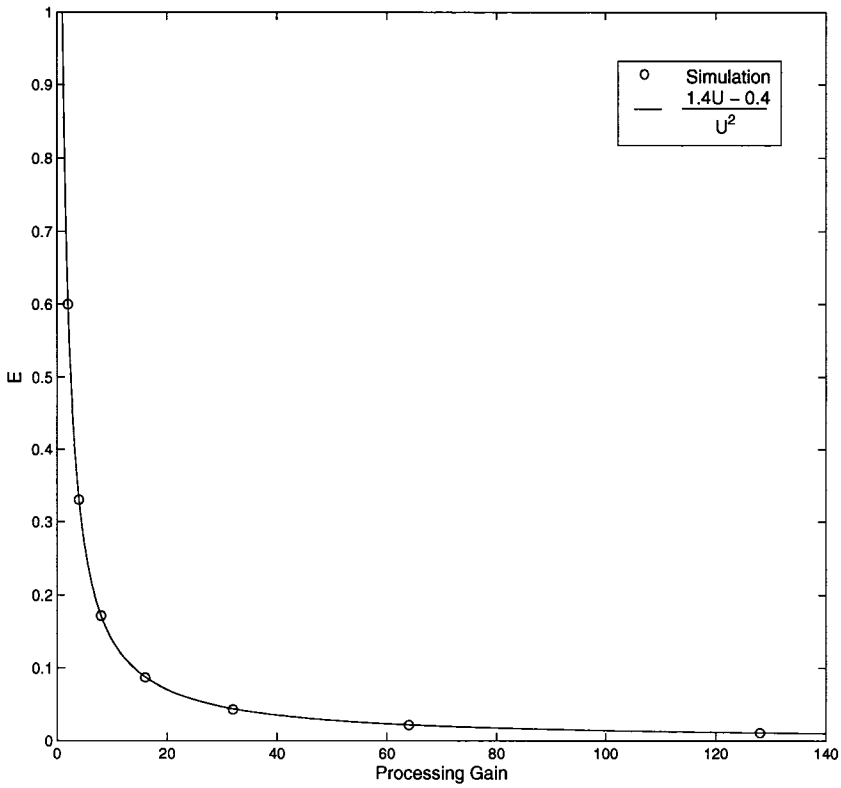


**Fig. 4.4** $\mathrm{E}\left[\frac{\sum_u (\alpha_u^{\mathrm{ST}})^2}{(\sum_u \alpha_u^{\mathrm{ST}})^2}\right]$ is derived by curve-fitting the simulation points.

### 4.4.2 BER Simulation versus Analysis for STBC MC-CDMA

In this section the accuracy of the BER analysis for STBC MC-CDMA is verified by comparing the simulation results in a correlated frequency selective fading channel and the derived analytical expression given by (4.13). Similar to section 4.3.2, the system has a total of 64 available subcarriers and processing gains of 8 and 16 are considered. The number of simulated bits for each simulation are chosen in a way that ensures at least 10 independent bit errors for each SNR. Fig. 4.5 depicts the

simulation results and the analytic BER curves for a BPSK modulated Alamouti space-time coded system with two transmit and one receive antenna elements with a processing gain of 8 and shows a good agreement between simulation and analysis.

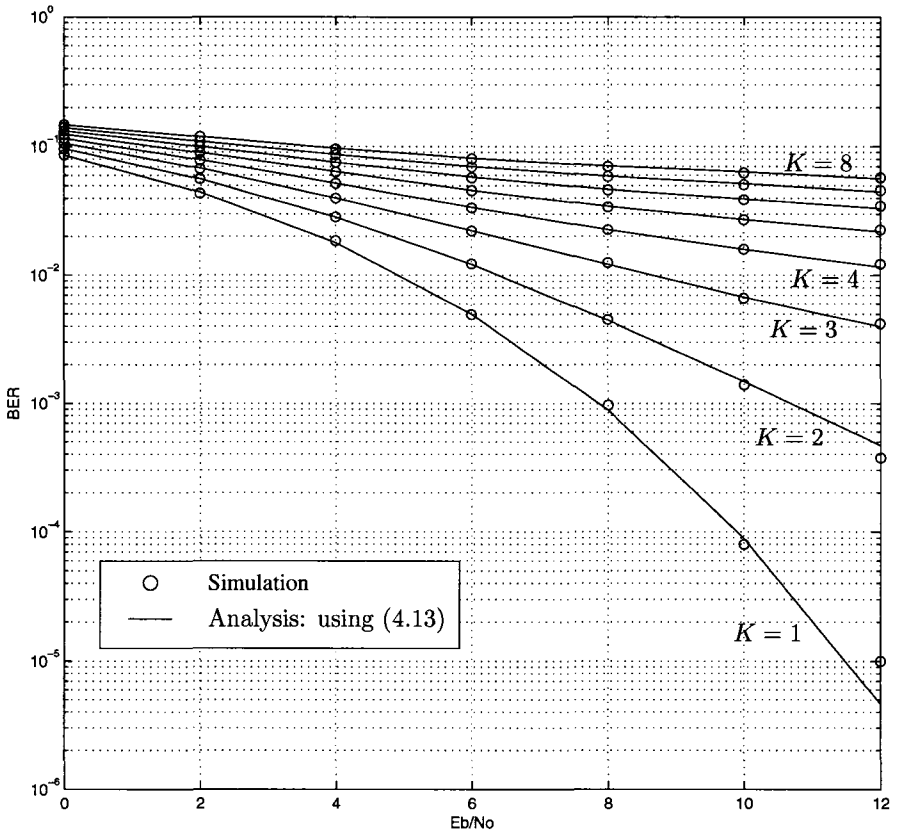


**Fig. 4.5** Simulation and Analysis results for a Alamouti space-time coded MC-CDMA system for K=[1,2,3,4,5,6,7,8] with processing gain of 8.

## 4.5 Effect of frequency selectivity on the performance of MC-CDMA system

The bit error expressions derived for multiuser MC-CDMA and space-time coded MC-CDMA systems in (4.9) and (4.13) respectively, show that the performance of the system is only dependent on the eigenvalues of the frequency correlation matrix of the channel in (4.1). It will be shown in this section that as the RMS delay spread of the channel increases[5], the eigenvalues converge to a constant value. Thus, provided that the cyclic prefix of the system is adjusted such that ISI between OFDM symbols is avoided, it can be concluded that the variations of the delay spread of the channel do not have a significant impact on the performance of the system in fairly high frequency selective channels.

The degradation or improvement of the performance due to frequency selectivity of the channel depends on the number of active users: In a multiuser system, where MRC detection is employed it is known that the orthogonality of the codes will be lost. Hence, as the channel becomes more frequency selective the received signal components received over different subcarriers become less correlated and cause further degradation in performance. Based on the fact that the eigenvalues converge, however, it can be concluded that the degradation of performance due to the correlation of frequency components of the received signal is limited. In a single user system, on the other hand, the orthogonality of the codes is not an issue. In this case, as the channel becomes more frequency selective, the frequency diversity of the system increases and hence the performance improves (This discussion should not be confused

[5]Higher RMS delay spread of a channel translates into lower coherence bandwidth and hence higher frequency selectivity, which in turn means lower correlation between subcarriers, thus loss of orthogonality of the spreading codes in a multiuser system (It is assumed that the level of frequency selectivity affects the correlation between the channels of the available subcarriers, and all subcarriers experience flat fading).

with the scenario where the processing gain is increased in a given channel. In which case, by increasing the processing gain the frequency diversity is increased and since the transmit bandwidth is fixed the subcarrier spacing is decreased and according to the coherence bandwidth of the channel a maximum frequency diversity can be achieved (see (3.23))).

Fig. 4.6 shows the eigenvalues of a frequency selective channel with a maximum normalized delay spread of 10 and a varying $T_{\text{rms}}$. As can be seen large variations of the eigenvalues can no more be observed for $T_{\text{rms}}$ values of greater than 3 and for delay spreads higher than 6 the eigenvalues have almost the same values. Fig. 4.7 shows the BER performance curves of a single user MC-CDMA system with MRC detection. The results provided in Fig. 4.7 agree well with the predictions based on the discussions in the previous paragraph. As can be seen the improvement of the BER performance from a normalized delay spread of 6 to a normalized delay spread of 9 is very small, which can be explained by the minimal change in the eigenvalues of the channel in that range.

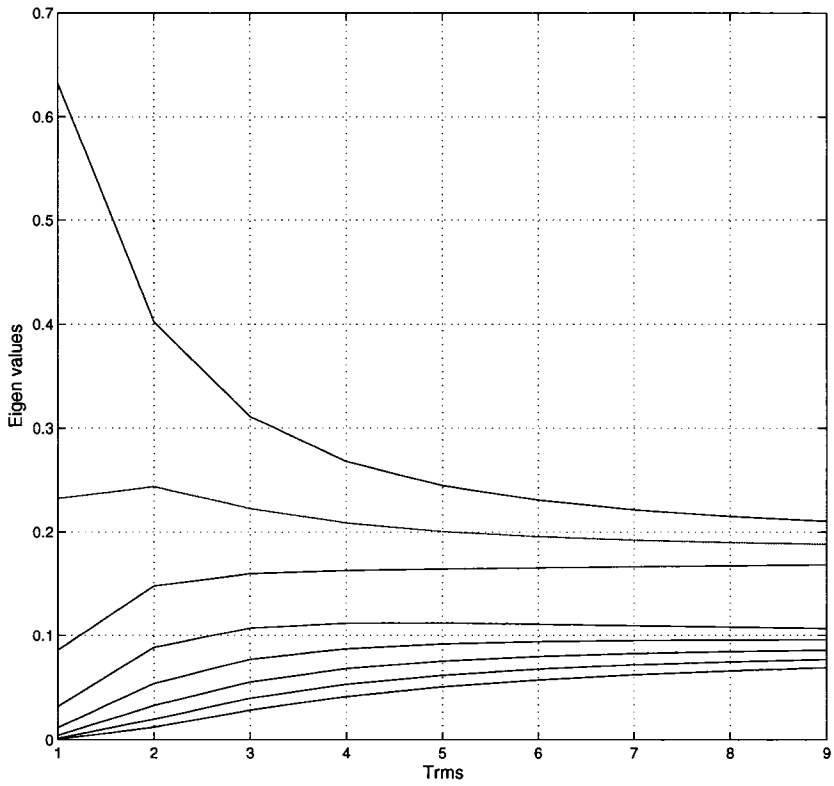


**Fig. 4.6** Eigenvalues of a frequency selective channel with varying $T_{\text{rms}}$ and normalized maximum delay spread of 10.

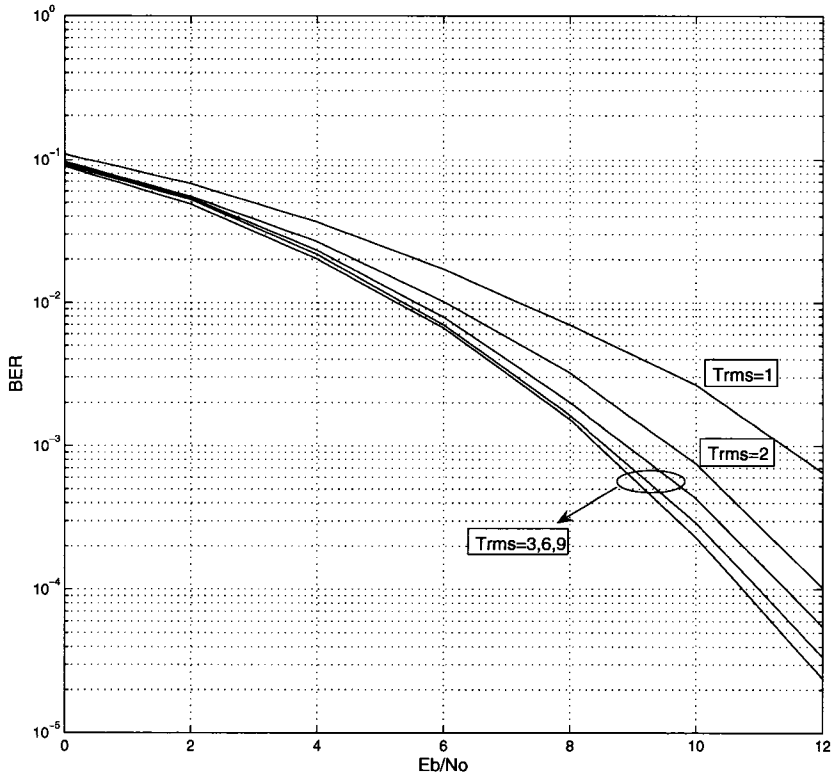


**Fig. 4.7** BER performance of a single user MC-CDMA system with MRC detection. The performance improves as the delay spread of the system increases but the improvement is limited.

# Chapter 5

# Simulation Results

## 5.1 Simulation parameters

Unless specified otherwise, the system parameters used in simulations are provided in Table 5.1. A frequency selective channel based on an exponential power delay profile with equi-distant taps is used (see (2.6)). Throughout the simulations, it has been assumed that the delay spread of the channel is not larger than the cyclic prefix resulting in an ISI-free communication.

**Table 5.1** Common simulation Parameters

| | |
|---|---|
| Modulation scheme | BPSK, QPSK or 16QAM |
| Spreading codes | Walsh-Hadamard |
| Processing gain ($U = G_{MC}$) | 8 |
| Normalized RMS delay spread | 3 |
| Normalized maximum delay spread | 10 |
| Number of available subcarriers | 64 |

In all simulations, for bit error rates greater than $10^{-4}$, 100000 symbols have been simulated and for lower bit error rates, the number of simulated bits was adjusted to ensure the occurrence of at least 10 independent bit errors. The confidence intervals are derived based on appendix D. Fig. 5.1 shows the performance of a BPSK modu-

lated single user MC-CDMA system with MRC detection and the corresponding error bars. For clarity of the simulation results the error bars have been removed from the rest of the BER performance figures.

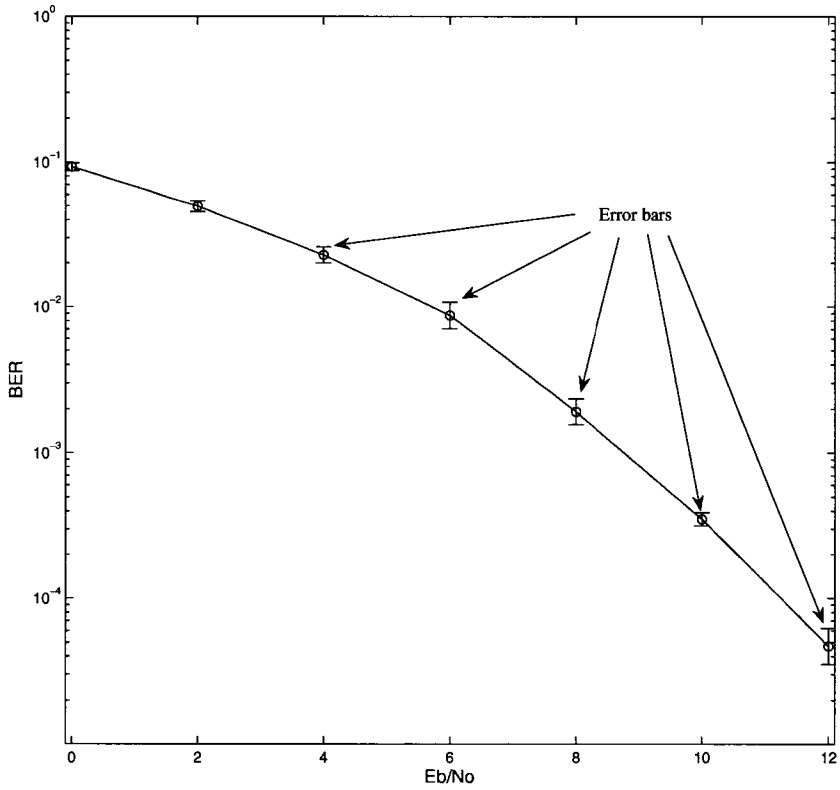


**Fig. 5.1** BER performance of a BPSK modulated single user MC-CDMA with MRC detection and the corresponding error bars.

## 5.2 Different detection techniques for MC-CDMA

In this section, the performance of the BPSK modulated MC-CDMA system using three combining methods (i.e. EGC, MRC and MMSE) is provided.

Figs 5.2, 5.3 and 5.4 depict the performance of the three combining techniques in single user, half-load and full-load scenarios respectively. Fig. 5.2 clearly shows that the MRC detection technique achieves minimum BER in a single user environment as expected, since MRC is the optimal detection method in single user systems [22]. It is worth observing that as the number of users increases, the performance of MRC degrades severely, which is due to the loss of orthogonality of the codes. EGC is a simple combining method which does not attempt to compensate for the channel distortion of the received signal in anyway, however, it performs better than MRC in multiuser scenarios. MMSE is a more complex structure and requires the number of active users and the noise level for detection, however it performs very well independently of the number of users.

The effect of increasing the processing gain in a single user MC-CDMA system is depicted in Fig. 5.5. As can be seen from Fig. 5.5, the performance improves very slightly as the processing gain is increased beyond 8. Hence it can be deduced that for this channel the achievable frequency diversity gain is approximately (close to) 8.

## 5.3 Multicarrier CDMA MIMO architectures

A MIMO structure with $M = 4$ transmit and $N = 4$ receive antennas is considered. In section 5.3.1, Alamouti space-time coding is simulated, and the reason for choosing MMSE detection in the proposed method is demonstrated. Section 5.3.2 presents the performance of the VBLAST structures and shows the inefficiency of such structures for MC-CDMA systems. Subsequently, the performance of the proposed scheme together with three other MIMO structures discussed in chapter 3 for different number of users with perfect/imperfect channel knowledge of the receiver and correlated MIMO

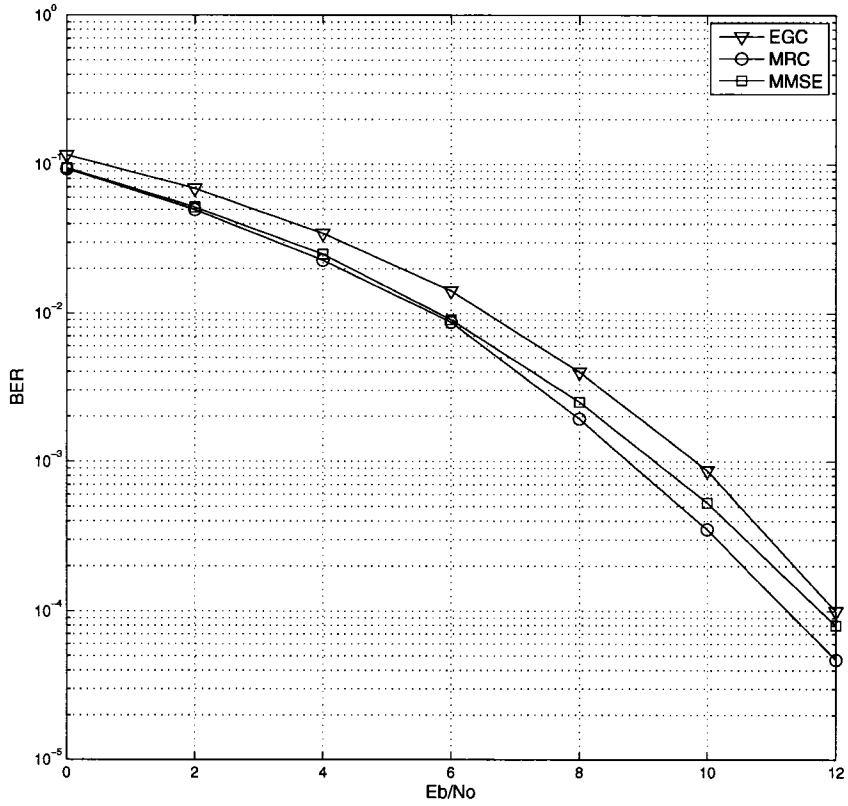


**Fig. 5.2** BER performance of MC-CDMA with MRC, EGC and MMSE detection in a single user environment ($K = 1$)

channels are presented and compared. In order to gain the same spectral efficiency for all structures the constellation order is modified accordingly: For spatial multiplexing systems QPSK modulation is employed and for combined spatial multiplexing and space-time coding architectures 16QAM constellation is used.

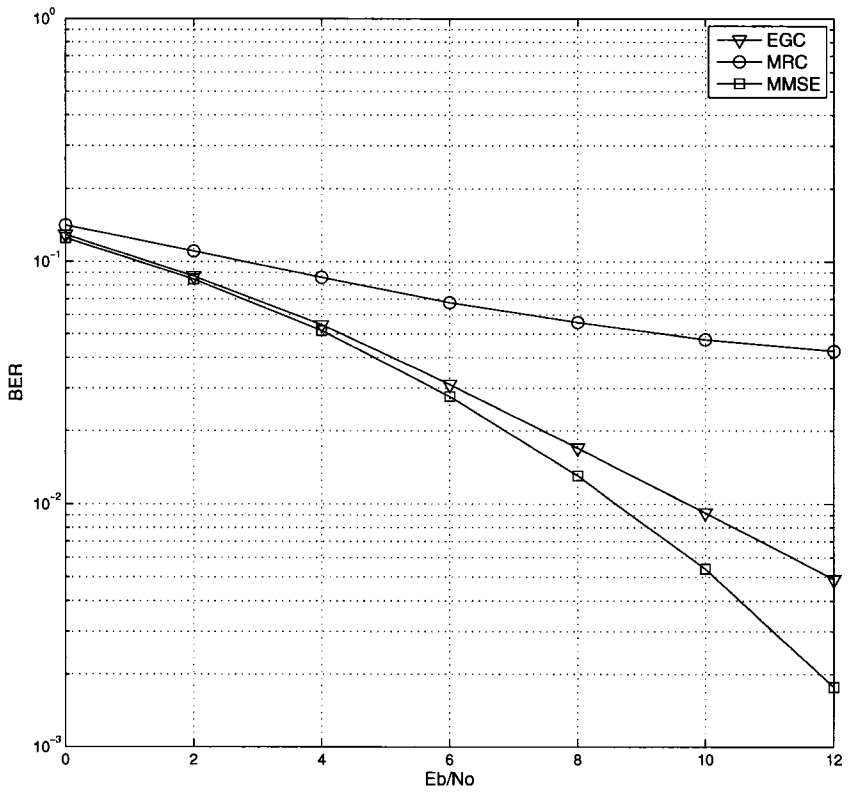


**Fig. 5.3** BER performance of MC-CDMA with MRC, EGC and MMSE detection in a half-load system ($K = 4$)

### 5.3.1 Space-time coding

Fig. 5.6 shows the BER performance of a BPSK-modulated Alamouti space-time coded MC-CDMA system with one antenna at the receiver, with different number of users using MRC detection. It is evident that the performance of MRC detection degrades significantly as the number of users increases, which is due to the loss of orthogonality of the users' spreading codes. On the other hand, the degradation due to Multi User Interference for the MMSE detector is considerably less (see Fig. 5.7).

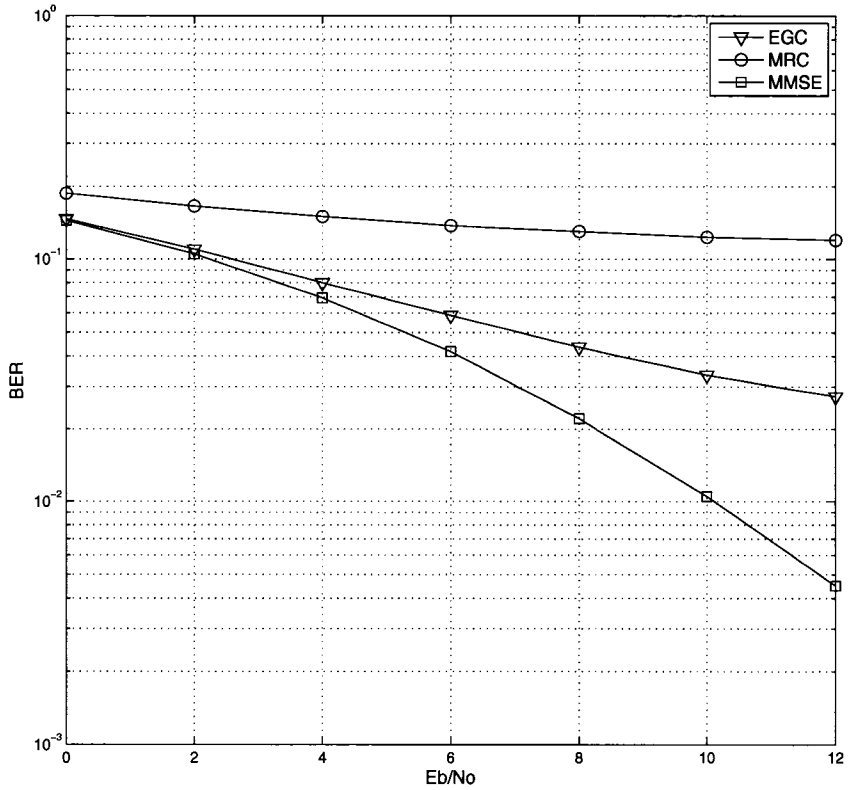


**Fig. 5.4** BER performance of MC-CDMA with MRC, EGC and MMSE detection in a full-load system ($K = 8$)

### 5.3.2 MC-CDMA VBLAST

The performance of MC-CDMA VBLAST architectures in a single user environment is provided in Fig. 5.8. As can be seen, the BLAST algorithm significantly improves the performance of the zero-forcing detector, whereas, MMSE-VBLAST degrades the performance in comparison with simple MMSE, which can be explained as follows: VBLAST spatially processes the received signal and makes decisions on each subcarrier prior to combining the frequency components, which causes error propagation to

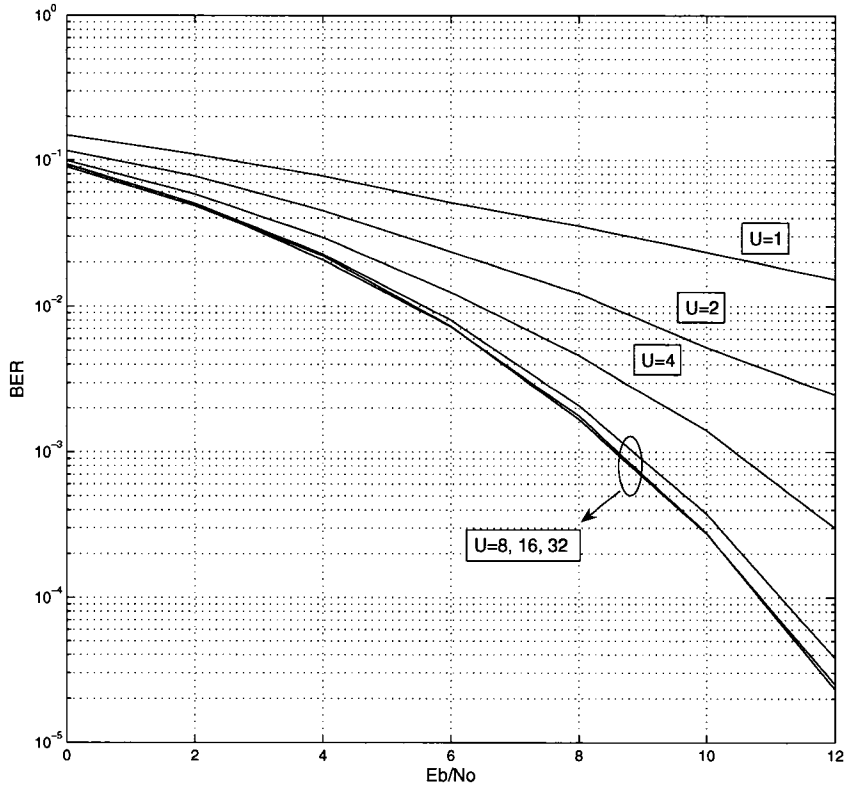


**Fig. 5.5** Effect of increasing the processing gain in a single user MC-CDMA system ($K = 1$).

the despreading block of the receiver (essentially the orthogonality of the spreading codes will be jeopardized) and degrades the performance. In Fig. 5.8 the performance of the VBLAST receivers with one iteration is also provided. It is seen that despite the fact that iterative detection provides further improvement, MMSE-VBLAST with one iteration still performs worse than simple MMSE.

Fig. 5.9 depicts the performance of the ZF, MMSE and their VBLAST counterparts for a MC-CDMA system in a half-load system. Fig. 5.9 further illustrates the

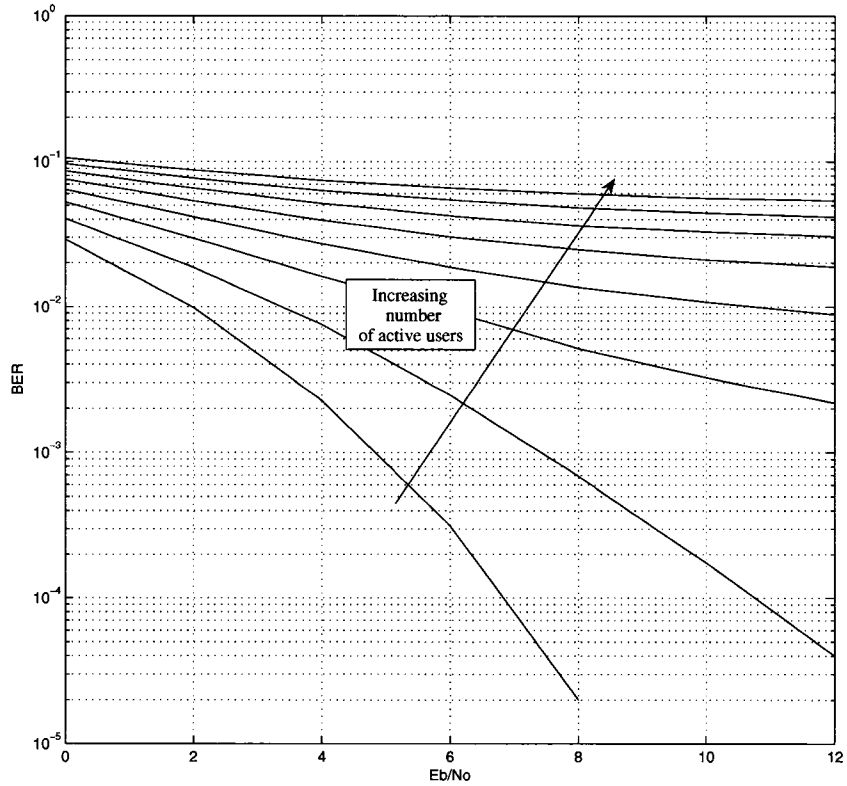


**Fig. 5.6** BER performance of Alamouti space-time coded MC-CDMA system with MRC detection (K=1,2,3,4,5,6,7,8)

error propagation problem in the VBLAST architectures for MC-CDMA systems. As can be seen in Fig. 5.9 both the ZF- and MMSE- VBLAST detectors with or without iteration have error floors. Hence, it is concluded that the direct use of VBLAST for MC-CDMA systems is not beneficial.

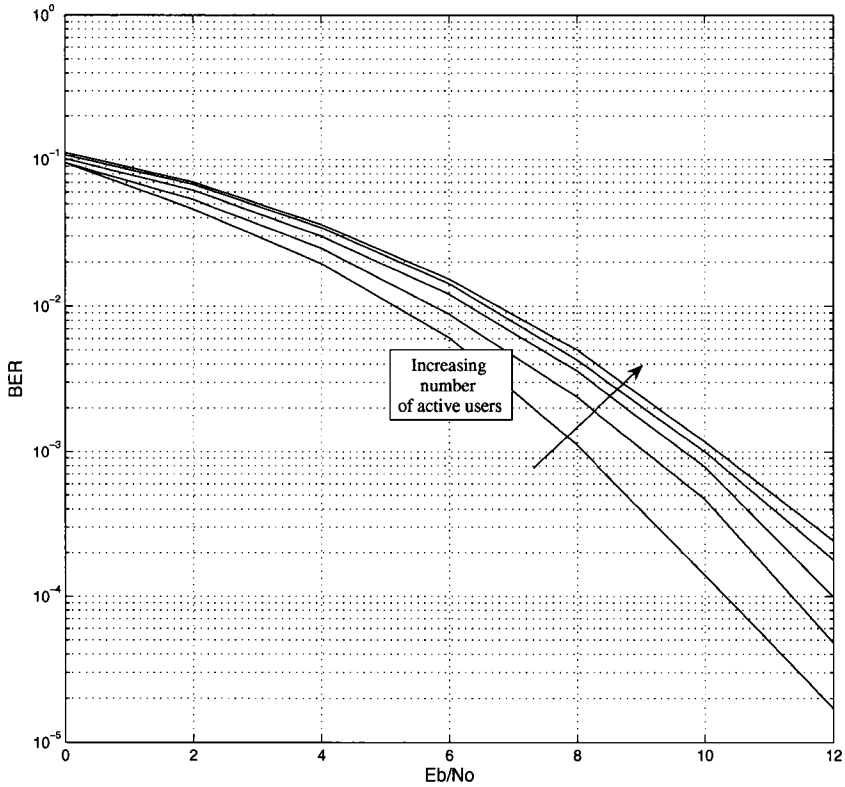


**Fig. 5.7** BER performance of Alamouti space-time coded MC-CDMA system with MMSE detection (K=[1,3,5,7,8])

### 5.3.3 Proposed scheme and comparisons

### 5.3.3 a) Proposed scheme and comparisons (perfect CSIR)

The simulations are performed in a frequency selective Rayleigh fading channel with parameters given in Table 5.1. In MSIC and STF-MMSE, the transmit antennas are divided into two groups and each group is space-time coded based on the Alamouti transmit diversity method.

Fig. 5.10 presents the BER performance of the proposed structure in a single

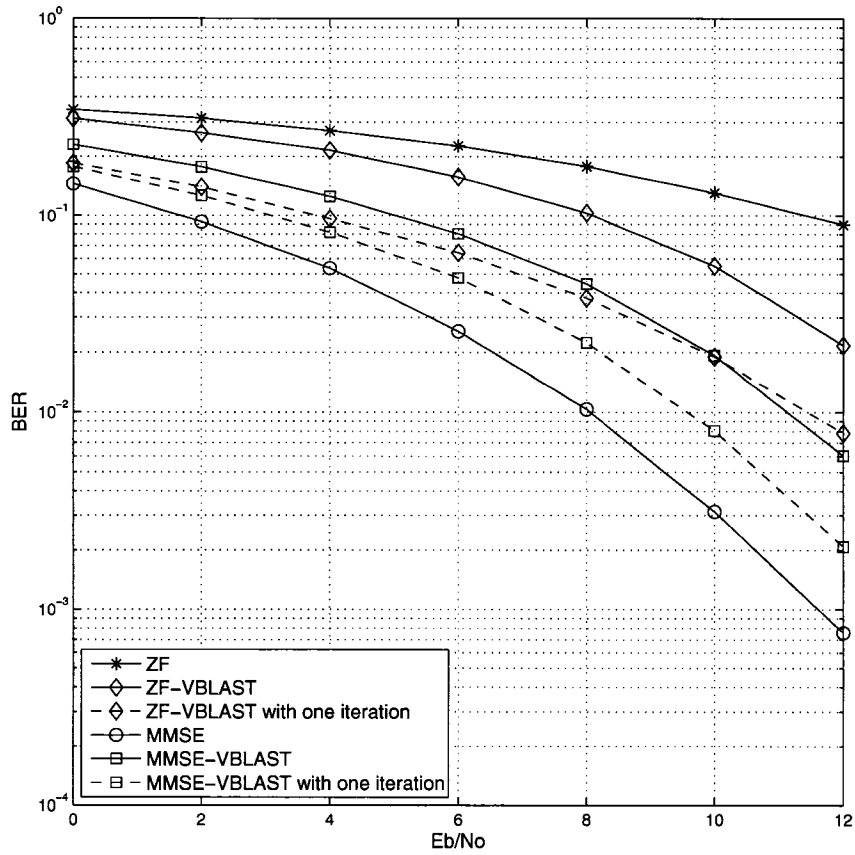


**Fig. 5.8** BER performance of MC-CDMA ZF and MMSE BLAST for K=1

user system with and without ordering (see section 3.2.1). As expected the ordering improves the performance: at a BER of $10^{-2}$, average ordering yields 0.3dB gain and per subcarrier ordering improves the performance by 0.6dB. It should be noted that the ordering gains observed here, were not achieved when iterative detection was performed. In other words, the ordering of the groups does not affect the performance of MSIC with iteration. This is due to the large diversity gain (over 2dB at a BER of $10^{-3}$) provided by the second iteration which overshadows the small ordering gains

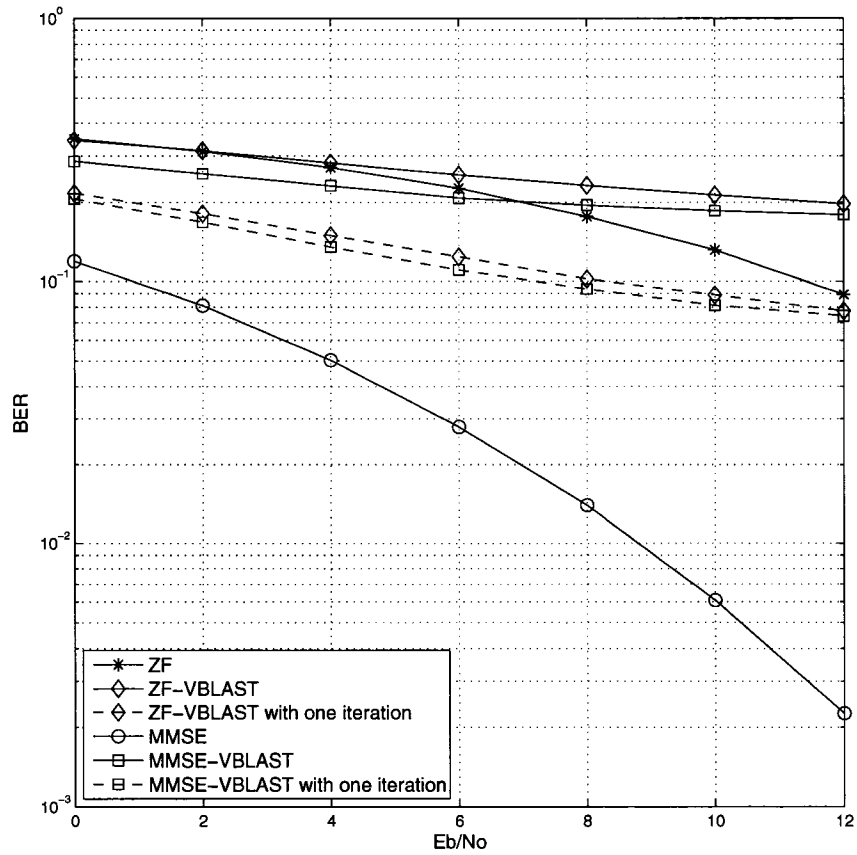


**Fig. 5.9** BER performance of MC-CDMA ZF and MMSE BLAST for K=4

provided in the first iteration. Furthermore, no significant improvement was observed for higher iterations with or without ordering. Hence, the rest of the simulation results are provided with one iteration and random ordering of the antenna groups.

Figs 5.11, 5.12 and 5.13 present the BER performance of the presented receiver structures for single user, half-load and full-load scenarios respectively, where the receiver has perfect knowledge of the channel state information. In the single user case, MMSE-MUD and STF-MMSE have almost the same performance and MSIC performs

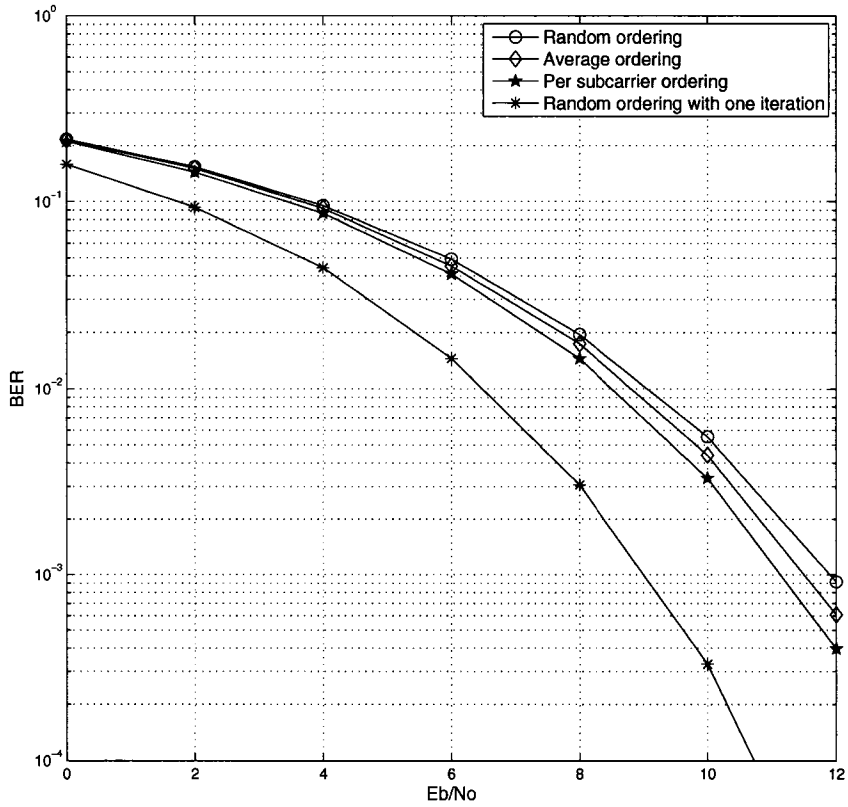


**Fig. 5.10** BER performance of the proposed scheme with random, average and per subcarrier ordering for a single user system.

worse (approximately 1dB at BER of $10^{-3}$). As the number of users increases, the degradation in performance in MMSE-MUD is noticeable, such that it performs worse than MSIC for a half-load system at high SNRs and performs significantly worse in a full-load scenario. The degradation of performance in STF-MMSE and MSIC on the other hand is very small. At a BER of $10^{-3}$ the STF-MMSE scheme requires 8.2, 8.8 and 9.9 dBs for single user, half-load and full-load scenarios respectively. Similarly, for MSIC these figures are 9, 9.8 and 10.6 dBs. Hence, the degradation of both systems is

almost the same and the 1dB difference between their performances is preserved in all cases. It should be noted, however, that 1dB better performance of the STF-MMSE structure comes at an extremely high price in terms of the complexity of the receiver structure.

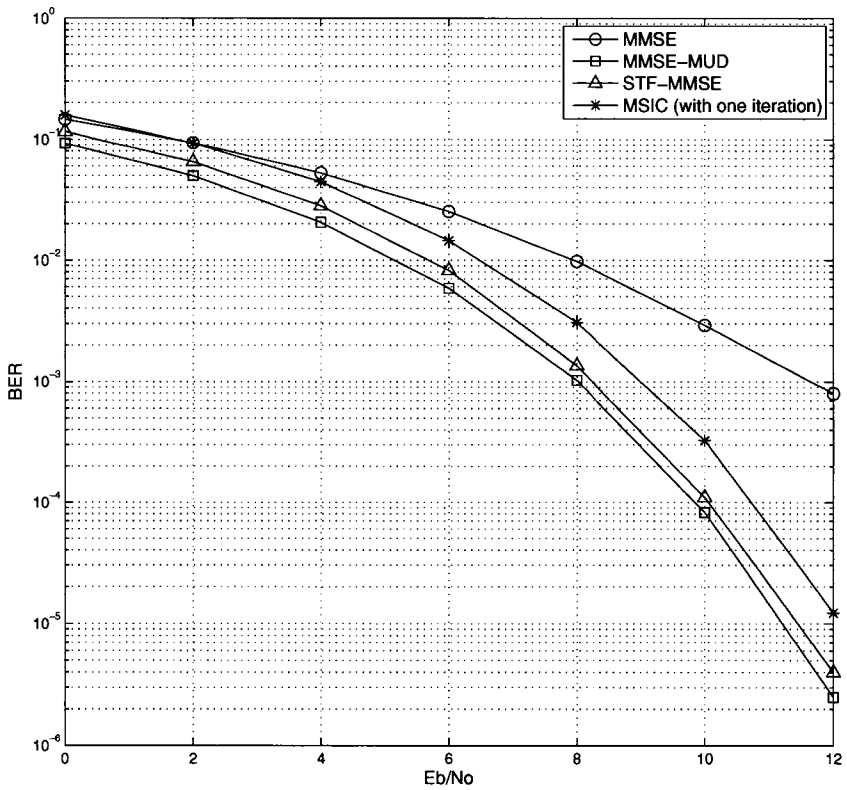


**Fig. 5.11** BER performance comparison of the proposed structure in a single user system with perfect channel state information at the receiver (CSIR) ($K = 1$).

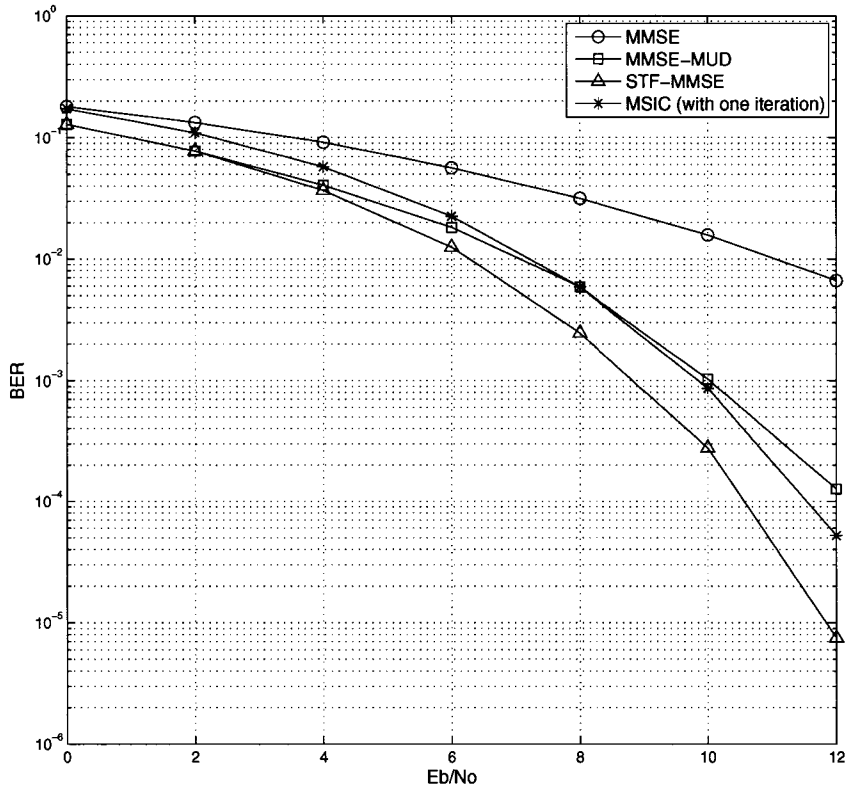


**Fig. 5.12** BER performance comparison of the proposed structure in a half-load system with perfect CSIR ($K = 4$).

### 5.3.3 b) Proposed scheme and comparisons (imperfect CSIR)

The BER curves of the MIMO structures with 30% channel estimation error at the receiver are provided in Figs 5.14, 5.15 and 5.16 for single user, half and full-load systems respectively. The perfect channel estimation performance of the corresponding systems are also provided (see the solid lines - For clarity of the figures the performance of the perfect channel estimated MMSE receiver has been omitted). Following

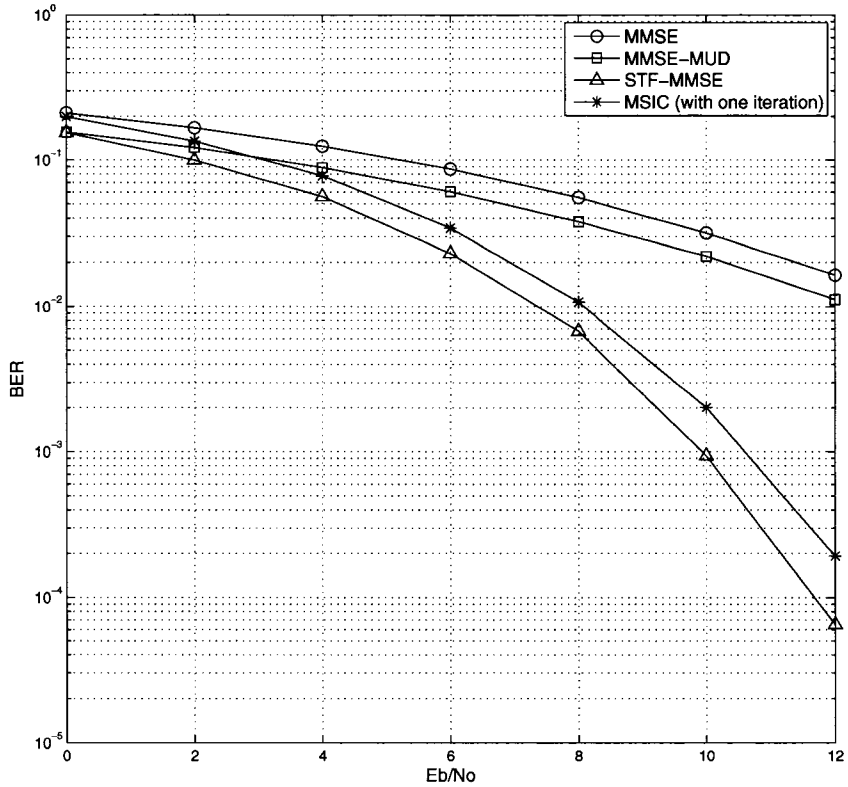


**Fig. 5.13** BER performance comparison of the proposed structure in a full-load system with perfect CSIR ($K = 8$).

[38], imperfect channel estimation is modeled as:

$$\hat{H}^u_{nm} = \sqrt{1-\epsilon^2} H^u_{nm} + \epsilon \omega^u_{nm} \tag{5.1}$$

where $\hat{H}^u_{mn}$ represents the channel coefficients used by the receiver for detection and $\{\omega^u_{nm}\}$ are independent zero-mean Gaussian random variables with unit variance. In order to achieve a channel estimation error of 30%, $\epsilon$ is chosen such that $\frac{\epsilon^2}{1-\epsilon^2} = 0.3$.

Fig. 5.14, shows that in a single user system in order to achieve a BER of $10^{-3}$ an

additional 3.1dB for STF-MMSE and 1.15dB for MMSE-MUD is required (in comparison to the perfect CSIR scenario). The loss in the proposed system on the other hand is only 0.3dB. In the half-load system (Fig. 5.15) the required additional SNR at BER of $2 \times 10^{-2}$ are 5.7dB, 2.6dB and 0.55dB for STF-MMSE, MMSE-MUD and MSIC respectively. Fig. 5.16 shows that all of the full-load systems encounter error floors. MSIC and STF-MMSE have error floors of 0.00615 and 0.0551 respectively. The spatial multiplexing MMSE structures behave in a very peculiar manner, that from approximately 10dB the BER increases as the SNR grows. One possible explanation for such behavior is provided here:

Based on (5.1), the estimated channel matrix can be written as:

$$\hat{\mathbf{H}} = \sqrt{1-\epsilon^2}\mathbf{H} + \epsilon\boldsymbol{\Omega}$$

where $\boldsymbol{\Omega}$ is assumed to have independent random Gaussian elements with unit variance.

The MMSE-based receivers multiply the received signal $\mathbf{r}$ with a weighting matrix with a general form of:

$$\mathbf{W} = \left(\hat{\mathbf{H}}^H\hat{\mathbf{H}} + \frac{N_0}{2}\mathbf{I}\right)^{-1}\hat{\mathbf{H}}^H$$

and based on (2.27) the received signal can be written as:

$$\mathbf{r} = \mathbf{H}\mathbf{s} + \mathbf{n} \tag{5.2}$$

hence we have:

$$\mathbf{W}\mathbf{r} = \left(\hat{\mathbf{H}}^H\hat{\mathbf{H}} + \frac{N_0}{2}\mathbf{I}\right)^{-1}\hat{\mathbf{H}}^H(\mathbf{H}\mathbf{s} + \mathbf{n}) \tag{5.3}$$

When SNR is very large, the weighting vector tends to $\hat{\mathbf{H}}^{-1}$ (assuming that $\hat{\mathbf{H}}$ is

invertible) hence:

$$\begin{aligned}\mathbf{Wr} &\approx \left(\sqrt{1-\epsilon^2}\mathbf{H}+\epsilon\mathbf{\Omega}\right)^{-1}\mathbf{Hs}\\ &\approx \left(\sqrt{1-\epsilon^2}\mathbf{H}+\epsilon\mathbf{\Omega}\right)^{-1}\left(\mathbf{H}^{-1}\right)^{-1}\mathbf{s}\\ &\approx \left(\sqrt{1-\epsilon^2}\mathbf{H}^{-1}\mathbf{H}+\epsilon\mathbf{H}^{-1}\mathbf{\Omega}\right)^{-1}\mathbf{s}\\ &\approx \left(\sqrt{1-\epsilon^2}\mathbf{I}+\epsilon\mathbf{H}^{-1}\mathbf{\Omega}\right)^{-1}\mathbf{s}\end{aligned}$$

which using the matrix inversion lemma[1] can be simplified to:

$$\mathbf{Wr} \approx \frac{1}{\sqrt{1-\epsilon^2}}\left[\mathbf{I}-\overbrace{\frac{\epsilon}{\sqrt{1-\epsilon^2}}\left(\mathbf{H}+\frac{\epsilon}{\sqrt{1-\epsilon^2}}\mathbf{\Omega}\right)^{-1}\mathbf{\Omega}}^{\text{error}}\right]\mathbf{s}$$

which states that as the channel estimation error grows the BER performance can degrade significantly, as the error term becomes more dominant.

Furthermore, it is a well known classical result that when a reliable estimate of the channel is not available, it is better not to decorrelate the received signal rather than decorrelating with a highly unreliable weighting matrix (in our case with a channel estimation error of 30%). In Fig. 5.16 as the SNR grows, the MMSE-based receivers attempt to decorrelate the received signal. However, since the estimation error is fairly high and a full-load system is considered, decorrelation results in considerably high error floors (even higher than the BER achieved at lower SNRs). Fig. 5.17 shows the BER performance of MMSE and decorrelator receivers in a full-load system with 30% channel estimation error. As can be seen, the BER of the MMSE structure tends to the BER of the decorrelating receiver as SNR grows.

[1] $(\mathbf{A}+\mathbf{UCV})^{-1} = \mathbf{A}^{-1} - \mathbf{A}^{-1}\mathbf{U}\left(\mathbf{C}^{-1}+\mathbf{VA}^{-1}\mathbf{U}\right)^{-1}\mathbf{VA}^{-1}$

### 5.3.3 c) Proposed scheme and comparisons (correlated channel)

Figs 5.18 and 5.19 provide the simulation results for the single user and full-load systems in a low correlated MIMO environment. The correlation matrices of the base and mobile stations are provided in Table 5.2 which are taken from [31] and correspond to a picocell environment with low correlation between the antenna elements at both base and mobile stations. At a BER of $10^{-2}$, STF-MMSE, MMSE-MUD and MSIC require an additional 1.3dB, 2.9dB and 3dB respectively in the single user case and 2.3dB, 4.2dB and 3.3dB in a full-load system.

In Figs 5.20 and 5.21 the performance of the MIMO structures in an environment with high correlation between the transmitter antenna elements for single user and full-load systems are investigated respectively. The correlation matrices of the base and mobile stations are provided in Table 5.2 [31], which correspond to a correlated microcell environment. As can be seen in Figs. 5.20 and 5.21 the performance of the proposed scheme degrades significantly. This degradation is a result of the high correlation (a mean absolute value of 0.96) between the transmit antenna elements which causes a considerable loss in the diversity gain and the overall performance of the system. As can be seen in Fig. 5.21 performing iterative detection in the full-load system has degraded the BER performance which is due to the unreliable initial estimates provided by the first detection step. However, in the single user system where there are no interfering signals the iterative detection still performs better (see Fig. 5.20).

**Table 5.2** Transmit and receive antenna correlation matrices (Picocell Decorrelated)

$$\mathbf{R}_{BS} = \begin{pmatrix} 1 & -0.45+0.53i & 0.37-0.22i & 0.19+0.21i \\ -0.45-0.53i & 1 & -0.35-0.02i & 0.02-0.27i \\ 0.37+0.22i & -0.35+0.02i & 1 & -0.1+0.54i \\ 0.19-0.21i & 0.02+0.27i & -0.1-0.54i & 1 \end{pmatrix}$$

$$\mathbf{R}_{MS} = \begin{pmatrix} 1 & -0.13-0.62i & -0.49+0.23i & 0.15+0.28i \\ -0.13+0.62i & 1 & -0.13-0.52i & -0.38+0.12i \\ -0.49-0.23i & -0.13+0.52i & 1 & 0.02-0.61i \\ 0.15-0.28i & -0.38-0.12i & 0.02+0.61i & 1 \end{pmatrix}$$

**Table 5.3** Transmit and receive antenna correlation matrices (Microcell Correlated)

$$\mathbf{R}_{BS} = \begin{pmatrix} 1 & -0.61+0.77i & 0.14-0.94i & 0.24+0.89i \\ -0.61-0.77i & 1 & -0.85+0.5i & 0.57-0.78i \\ 0.14+0.94i & -0.85-0.5i & 1 & -0.91+0.4i \\ 0.24-0.89i & 0.57+0.78i & -0.91-0.4i & 1 \end{pmatrix}$$

$$\mathbf{R}_{MS} = \begin{pmatrix} 1 & -0.12-0.18i & 0.08+0.05i & -0.02-0.13i \\ -0.12+0.18i & 1 & -0.17-0.16i & 0.11+0.04i \\ 0.08-0.05i & -0.17+0.16i & 1 & -0.17-0.16i \\ -0.02+0.13i & 0.11-0.04i & -0.17+0.16i & 1 \end{pmatrix}$$

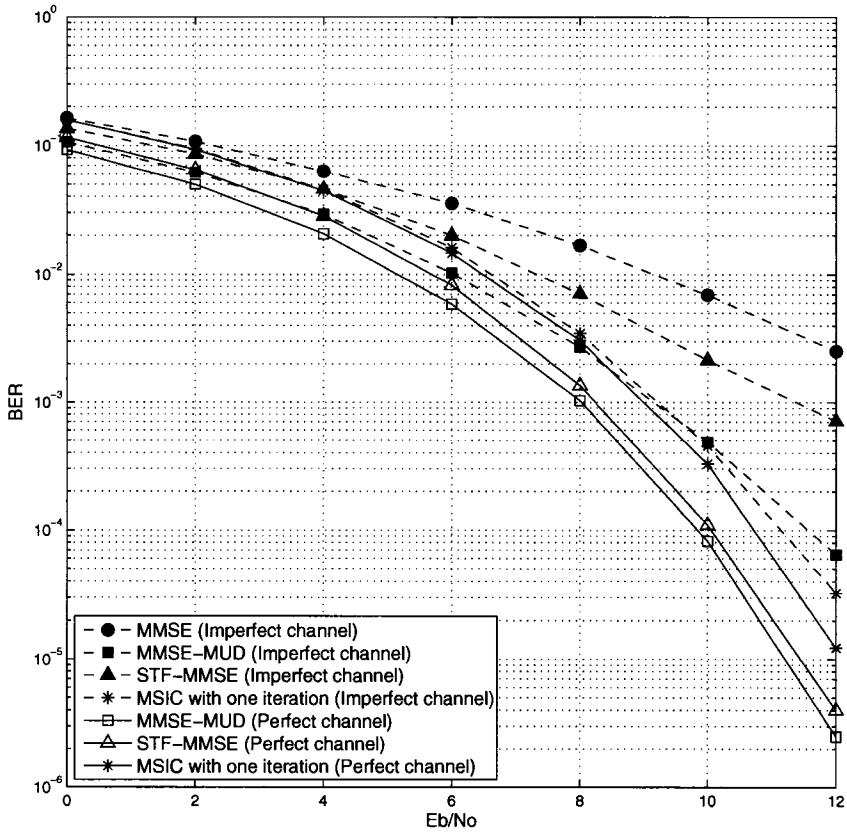


**Fig. 5.14** BER performance comparison of the proposed structure in a single user system with 30% channel estimation error ($K = 1$).

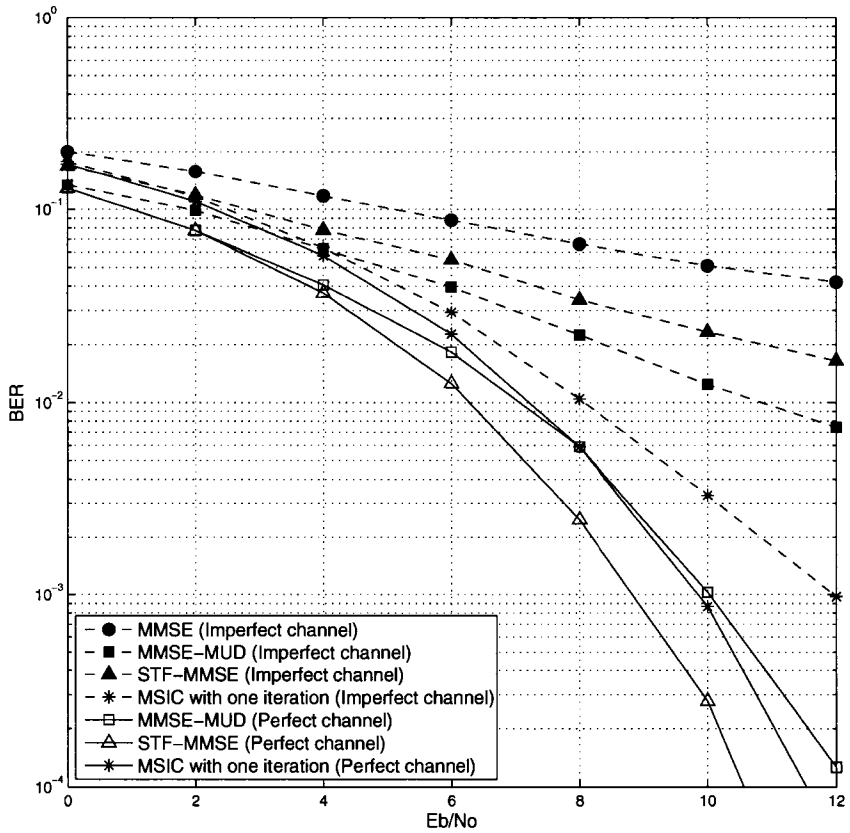


**Fig. 5.15** BER performance comparison of the proposed structure in a half-load system with 30% channel estimation error ($K = 4$).

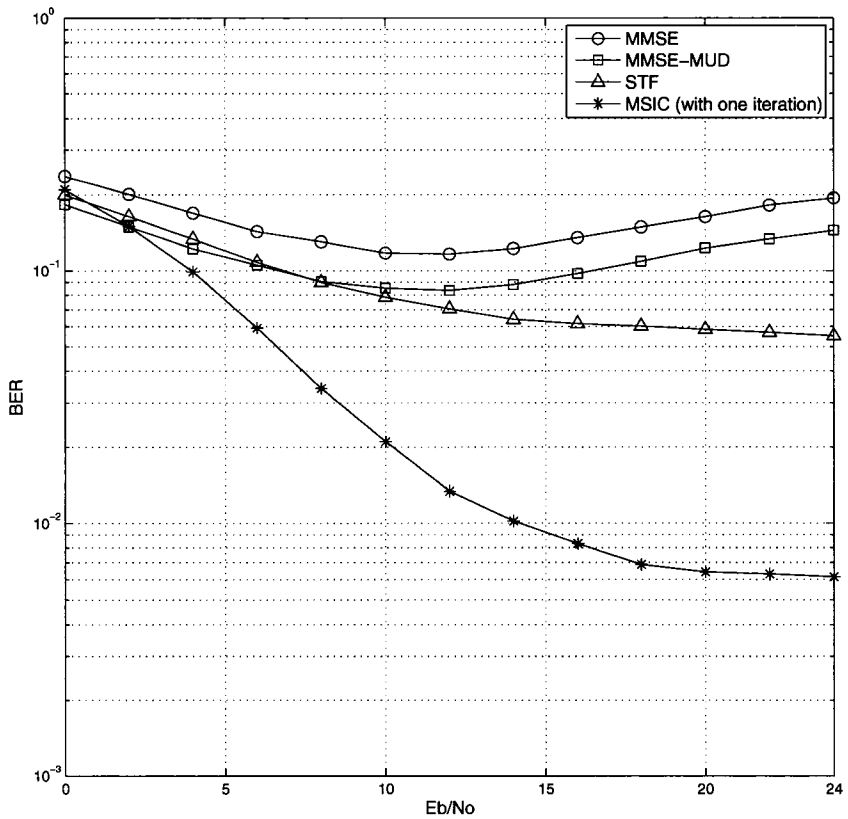


**Fig. 5.16** BER performance comparison of the proposed structure in a full-load system with 30% channel estimation error ($K = 8$).

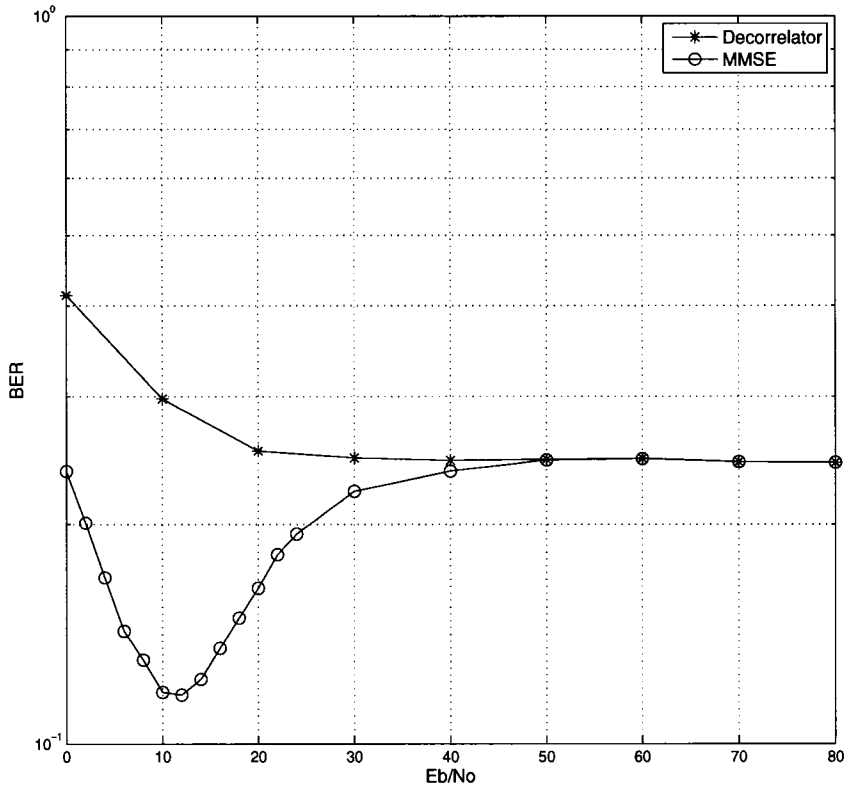


**Fig. 5.17** BER performance of the MMSE and decorrelator receivers in a full-load system with 30% channel estimation error ($K = 8$).

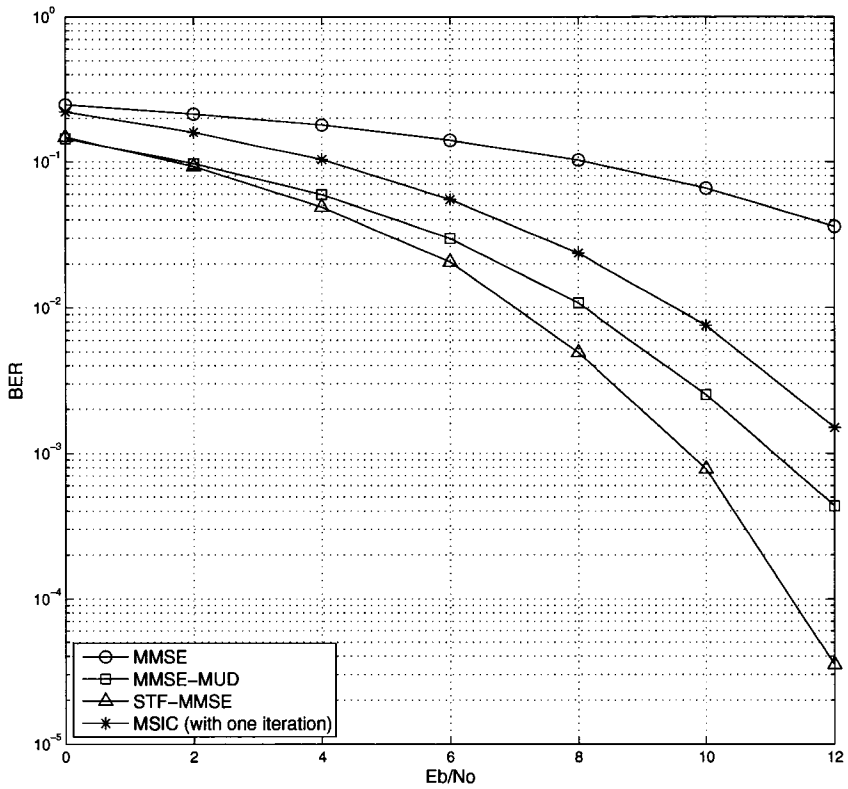


**Fig. 5.18** BER performance comparison of the single user proposed structure in a low correlated MIMO environment ($K = 1$).

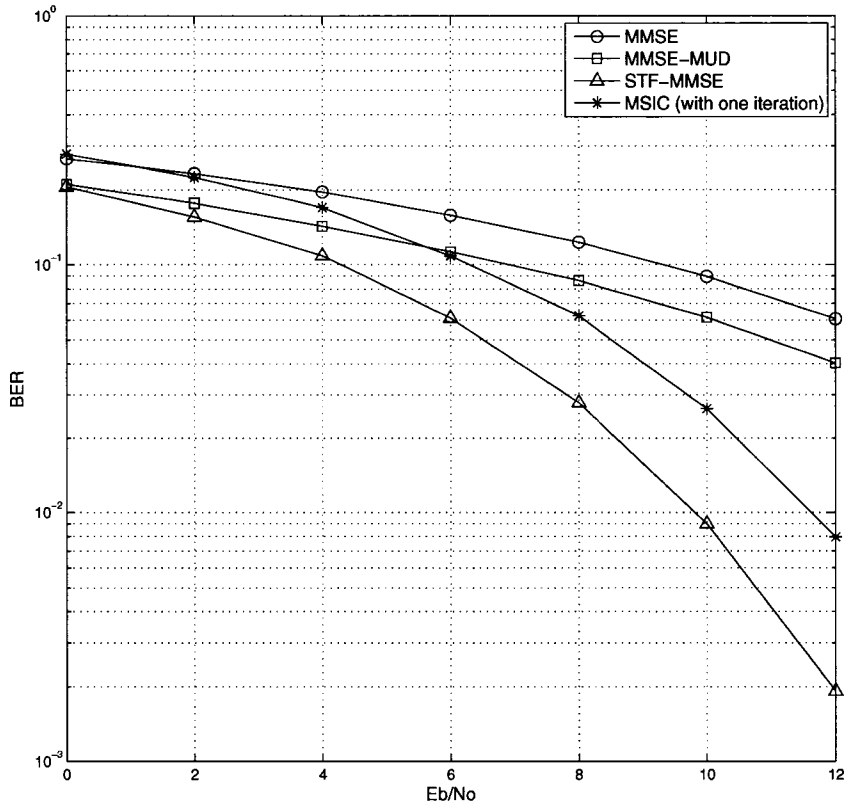


**Fig. 5.19** BER performance comparison of the full-load proposed structure in a low correlated MIMO environment ($K = 8$).

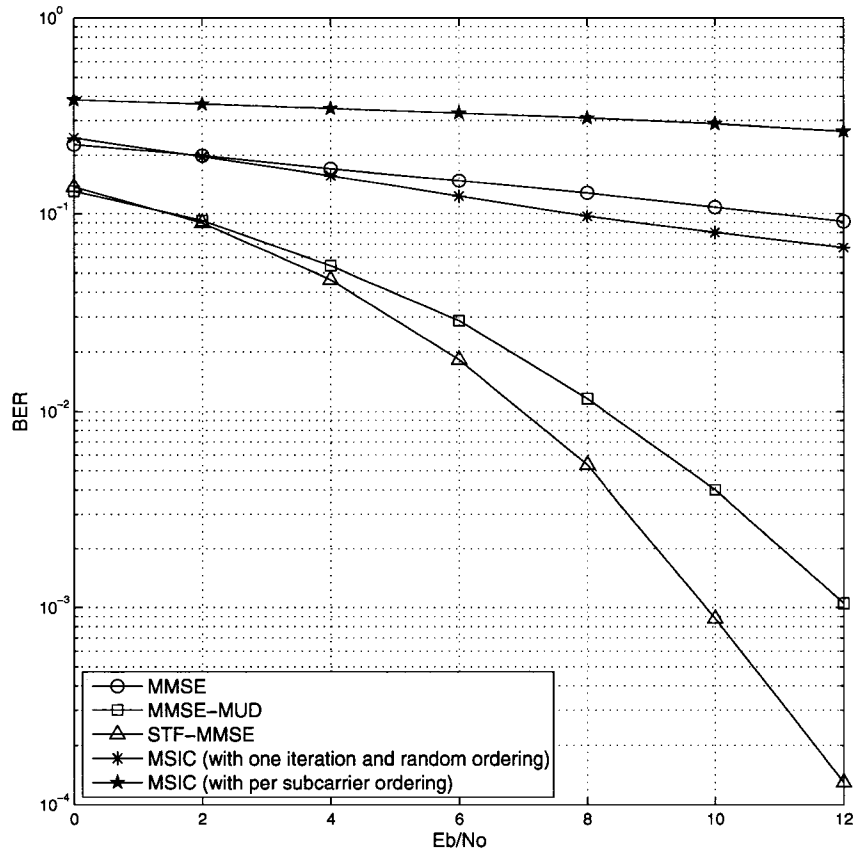


**Fig. 5.20** BER performance comparison of the single user proposed structure in a highly correlated MIMO environment ($K = 1$).

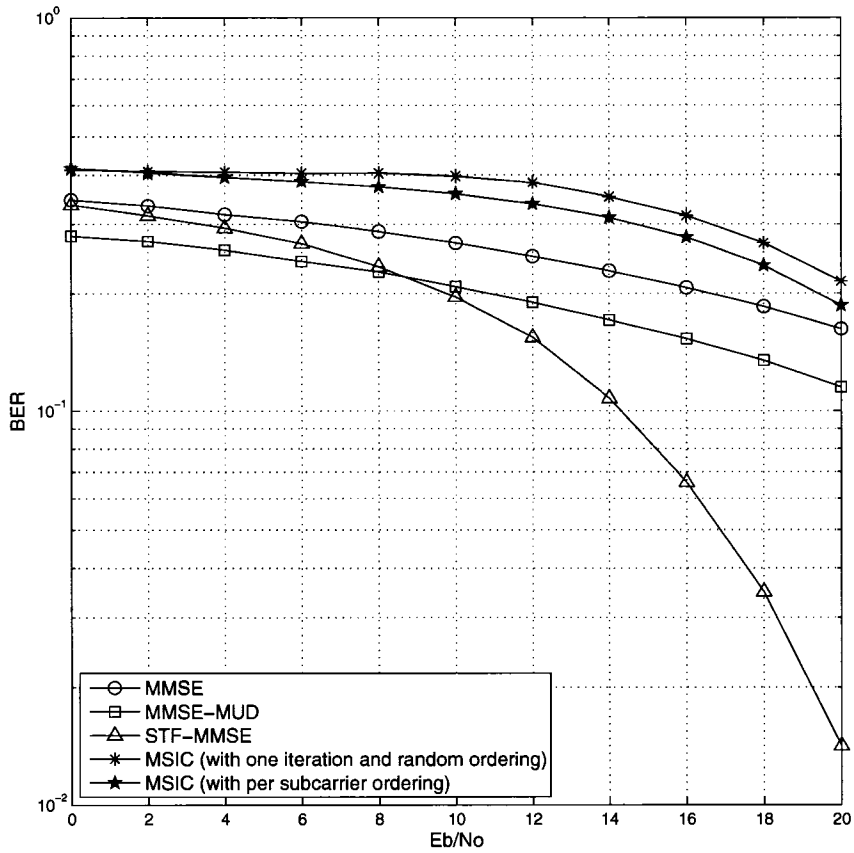


**Fig. 5.21** BER performance comparison of the full-load proposed structure in a highly correlated MIMO environment ($K = 8$).

# Chapter 6

# Conclusions

## 6.1 Summary

In this thesis we have proposed a new architecture for MC-CDMA systems to exploit the high spectral efficiencies of the spatial multiplexing systems and the diversity gain of the space-time coded structures simultaneously. Furthermore, a thorough analysis of the MC-CDMA systems has been carried out and analytical expressions for multi-user Single-Input Single-Output (SISO) and Alamouti space-time coded MC-CDMA systems in correlated frequency selective fading channels have been derived.

As a first step in the design of a suitable receiver, a thorough study of available MIMO structures, with two different goals (either increasing the diversity gain or the overall data rate of the system), and their extensions to MC-CDMA systems were studied. The primary studies revealed that MMSE is the best linear detection technique for both SISO and Alamouti space-time coded systems. The MIMO-MMSE structure with single-user detection (the simplest spatial multiplexing MIMO structure considered), however, performs quite poorly particularly when the receiver does not have perfect knowledge of the channel state information. The VBLAST structures

in MC-CDMA systems were discussed and it was shown that the VBLAST scheme cannot improve the performance of the MC-CDMA system on its own[1]. The MMSE-MUD receiver architecture was studied and the results show that the architecture is quite complex and performs poorly under imperfect channel estimation conditions and in MIMO correlated channels. Consequently, spatial multiplexing and space-time coding were combined. A quite complex architecture known as the STF-MMSE detector was analyzed and a new scheme was proposed. The complexity of the proposed method and three other MIMO structures were evaluated and compared. The results show that the proposed system achieves a desired BER performance with significantly less complexity. The bit error performances of the MIMO architectures under perfect and imperfect channel knowledge of the receiver were compared. The results in section 5.3.3 reveal that the proposed system is very robust against channel estimation errors, regardless of the number of active users. Subsequently, the performance of the proposed scheme was studied in spatially correlated MIMO channels. It was observed that in highly correlated channels the performance of the MSIC scheme degrades significantly, which is due to the minimal achievable diversity gain in the channel. A frequency multiplexing technique was proposed in the structure and it was shown that when the number of active users is not very high, a desired BER (with same data rate) can be achieved with much less complexity.

Furthermore, this thesis investigated the bit error analysis of MC-CDMA systems. The concept of independent equivalent paths in a frequency selective fading channel was developed and an analytical expression for the BER of the multi-user MC-CDMA system was derived. The BER analysis of Alamouti space-time coded system was addressed; the probability density function of a frequency selective channel in a MIMO

[1]This result is quite counter-intuitive since this is not the case in the single carrier systems [11] or even in OFDM structures [39].

environment with two transmit and one receive antenna elements was calculated and the BER expression of the space-time coded MC-CDMA system was derived.

## 6.2 Future Work

- Comparison of the proposed MIMO system with other narrowband MIMO structures in terms of performance, complexity and spectral efficiencies can be investigated.

- In this work, the system is designed under the assumption that the channel conditions for two consecutive symbol intervals are the same. By modifying the Alamouti space-time coding blocks, the scheme can be enhanced to become robust to time variations of the channel within two consecutive intervals. The STF-MMSE architecture proposed in [32] is one such receiver which is robust to channel variations over two consecutive intervals, but as was shown in this thesis the structure is very complex.

- In this thesis, a MIMO structure with 4 transmit and receive antennas has been considered and due to practicality issues higher numbers of antennas at either end have not been addressed. The trade-off between spatial multiplexing and diversity gains has been thoroughly studied in [13] and further developed in [14]. The application of the ideas presented in these works and deriving an optimal grouping of the transmit antennas for an arbitrary number of antennas in MC-CDMA systems is a potential area of research.

- The BER analysis of the space-time coded MC-CDMA system was carried out for a MIMO structure with two transmitters and one receiver. A generalization of the formulas for an arbitrary number of transmit/receive antennas and ulti-

mately for the layered space-time coded MC-CDMA systems is an interesting topic to be further investigated.

- The analysis has been carried out for Walsh-Hadamard codes. A study of the BER analysis for different spreading codes (Gold codes, Kasami codes, Complex codes, ...) is a possible extension of the work.

- The structure proposed in this thesis, exploits space-time coding and frequency coding at the same time but independently. The structures with 3-dimensional codes, jointly exploiting space, time and frequency are extremely interesting and have a very high potential [40].

# Appendix A

# Singular value decomposition (SVD) and orthonormal basis for null space of matrix A

**Theorem (Singular Value Decomposition).** *If $\boldsymbol{A}$ is a $N \times M$ matrix, then there exist orthogonal (or unitary) matrices*

$$\mathbf{U} = [\mathbf{u}_1, \cdots, \mathbf{u}_N] \in \mathbb{C}^{N \times N} \quad \text{and} \quad \mathbf{V} = [\mathbf{v}_1, \cdots, \mathbf{v}_M] \in \mathbb{C}^{M \times M}$$

*such that*

$$\mathbf{U}^H \mathbf{A} \mathbf{V} = \mathbf{W} (= diag(w_1, \cdots, w_p)) \in \mathbb{R}^{N \times M} \quad , \quad p = \min(M, N)$$

*or*

$$\mathbf{A} = \mathbf{U} \mathbf{W} \mathbf{V}^H$$

The rank of the matrix $\mathbf{A}$ can be determined from its SVD decomposition. If $w_1 \geq w_2 \geq \cdots \geq w_r = \cdots = w_p = 0$, then $\text{rank}(\mathbf{A}) = r$.

Assuming $N \geq M$, the SVD decomposition of $\mathbf{A}$ can be written as:

$$\mathbf{A} = \overbrace{\begin{pmatrix} u_{11} & \cdots & u_{1M} & \cdots & u_{1N} \\ u_{21} & \cdots & u_{2M} & \cdots & u_{2N} \\ \vdots & \ddots & \vdots & \ddots & \vdots \\ u_{N1} & \cdots & u_{NM} & \cdots & u_{NN} \end{pmatrix}_{N\times N}}^{\mathbf{U}} \overbrace{\begin{pmatrix} w_1 & 0 & \cdots & 0 \\ 0 & w_2 & \ddots & 0 \\ \vdots & \vdots & \ddots & \vdots \\ 0 & 0 & \cdots & w_M \\ --- & --- & --- & --- \\ & \mathbf{0}_{(N-M)\times N} & & \end{pmatrix}_{N\times M}}^{\mathbf{W}} \mathbf{V}^H_{M\times M}$$

Multiplying $\mathbf{U}$ and $\mathbf{W}$ gives:

$$\bar{\mathbf{H}}^u_g = \begin{pmatrix} w_1u_{11} & \cdots & w_bu_{1M} \\ w_1u_{21} & \cdots & w_bu_{2M} \\ \vdots & \ddots & \vdots \\ w_1u_{N1} & \cdots & w_bu_{NM} \end{pmatrix}_{N\times M} \mathbf{V}^H_{M\times M}$$

Since the columns of $\mathbf{U}$ are orthogonal we have $\mathbf{u}_i^H\mathbf{u}_j = 0$ for all $i \neq j$ ($\mathbf{u}_i$ is the $i^{th}$ column of $\mathbf{U}$). Hence in order to find the null space of $\mathbf{A}$ such that $\mathbf{NA} = \mathbf{0}$ we choose $\mathbf{N}$ as:

$$\mathbf{N} = \left\{ \begin{pmatrix} u_{1\,M+1} & \cdots & u_{1N} \\ u_{2\,M+1} & \cdots & u_{2N} \\ \vdots & \ddots & \vdots \\ u_{N\,M+1} & \cdots & u_{NN} \end{pmatrix}_{N\times(N-M)} \right\}^H$$

since:

$$\begin{pmatrix} u_{1\,M+1}^* & u_{2\,M+1}^* & \cdots & u_{N\,M+1}^* \\ u_{1\,M+2}^* & u_{2\,M+2}^* & \cdots & u_{N\,M+2}^* \\ \vdots & \ddots & \ddots & \vdots \\ u_{1N}^* & u_{2N}^* & \cdots & u_{NN}^* \end{pmatrix}_{(N-M)\times N} \begin{pmatrix} w_1u_{11} & \cdots & w_bu_{1M} \\ w_1u_{21} & \cdots & w_bu_{2M} \\ \vdots & \ddots & \vdots \\ w_1u_{N1} & \cdots & w_bu_{NM} \end{pmatrix}_{N\times M} = \mathbf{0}$$

which is due to the fact that the columns of $\mathbf{U}$ are orthogonal.

Based on the above, in order to obtain an orthogonal set of vectors for the null space of matrix $\mathbf{A}$, the calculation of $\mathbf{U}$ is required. Table A.1 provides the number of floating point operations (flops[1]) for calculating $\mathbf{U}, \mathbf{V}$ or $\mathbf{W}$ using either the Golub-Reinsch decomposition or the R-SVD algorithm.

For our purpose, where the order of the matrices are not very high the Golub-Reinsch SVD algorithm with $4N^2M + 8NM^2$ flops is less complex, and this method is considered for the complexity assessment.

**Table A.1** Number of flops required for calculating $\mathbf{U}, \mathbf{V}$ or $\mathbf{W}$

| Required | Golub-Reinsch SVD | Riemannian-SVD (R-SVD) |
|---|---|---|
| $\mathbf{W}$ | $4NM^2 - 4M^3/3$ | $2NM^2 + 2M^3$ |
| $\mathbf{W}, \mathbf{V}$ | $4NM^2 + 8M^3$ | $2NM^2 + 11M^3$ |
| $\mathbf{W}, \mathbf{U}$ | $4N^2M + 8NM^2$ | $4N^2M + 13M^3$ |
| $\mathbf{W}, \mathbf{U}, \mathbf{V}$ | $4N^2M + 8NM^2 + 9M^3$ | $4N^2M + 22M^3$ |

[1]Following [29], we define a flop as one addition or one multiplication.

# Appendix B

# Complexity Analysis

In this appendix a thorough analysis of the complexity of the proposed method is provided. The complexity of the MSIC algorithm can be categorized into two main sections: Nulling operation using SVD decomposition and the matrix multiplications/additions. The latter is further divided into the steps of detection, namely, Nulling, Alamouti detection, despreading of the users' data and interference cancellation. It should be noted that throughout this analysis all the antenna groups are assumed to have two antenna elements ($m_g = 2$ for $g = 1, \cdots, G$) and the complexity of each section is given in terms of the number of flops required for each operation [29].

## B.1 Nulling matrix calculation

In order to detect the signals transmitted from the $g^{th}$ group of the transmitter structure, the receiver has to cancel the effect of the interferers from the other antenna groups which have not yet been detected. This task is proposed to be done by performing SVD decomposition on the channel matrix corresponding to the not yet de-

tected transmit antenna groups ($\bar{\mathbf{H}}_g^u$), which is a $N \times (M - \sum_{i=1}^{g} m_i)$[1] matrix (see appendix A).

The SVD decomposition has to be performed on $\bar{\mathbf{H}}_g^u$ and carried out for all groups except for the last. Hence the number of flops for the nulling operation will be[2]:

$$\sum_{l=1}^{G-1}\left[4N^2\left(M-\sum_{i=1}^{l}m_i\right)+8N\left(M-\sum_{i=1}^{l}m_i\right)^2\right]$$

$$=\sum_{l=1}^{G-1}\left[4N^2\left(M-2l\right)+8N\left(M-2l\right)^2\right] \quad \text{assuming that } m_g=2 \text{ for all } g=1,\ldots,G$$

$$=4N^2\sum_{l=1}^{G-1}(M-2l)+8N\sum_{l=1}^{G-1}\left[M^2-4lM+4l^2\right]$$

$$=\left[4N^2M+8NM^2\right](G-1)+\left[-8N^2-32NM\right]\left(\sum_{l=1}^{G-1}l\right)+32N\left(\sum_{l=1}^{G-1}l^2\right)$$

$$=\left(4N^2M+8NM^2\right)(G-1)-\left(8N^2+32NM\right)\left[\frac{(G-1)G}{2}\right]$$

$$+32N\frac{(G-1)G(2(G-1)+1)}{6}$$

$$=(G-1)\left[4N^2M+8NM^2-(4N^2+16NM)G+\frac{16}{3}NG(2G-1)\right]$$

$$=\left(\frac{M}{2}-1\right)\left[4N^2M+8NM^2-2N^2M-8NM^2+\frac{16}{3}N\frac{M}{2}(M-1)\right]$$

$$=\left(\frac{M}{2}-1\right)\left[2N^2M+\frac{8}{3}NM^2-\frac{8}{3}NM\right]$$

$$=\frac{M}{2}\left[2N^2M+\frac{8}{3}NM^2-\frac{8}{3}NM\right]-\left[2N^2M+\frac{8}{3}NM^2-\frac{8}{3}NM\right]$$

$$=N^2M^2+\frac{4}{3}NM^3-4NM^2-2N^2M+\frac{8}{3}NM$$

[1] See (3.17).

[2] The following identities have been used:

$$\sum_{k=0}^{n}k=\frac{n(n+1)}{2} \quad , \quad \sum_{k=0}^{n}k^2=\frac{n(n+1)(2n+1)}{6} \quad , \quad \sum_{k=0}^{n}k^3=\left[\frac{n(n+1)}{2}\right]^2$$

and the total number of flops for all subcarriers can be written as:

$$UN^2M^2 + \frac{4}{3}UNM^3 - 4UNM^2 - 2UN^2M + \frac{8}{3}UNM$$

## B.2 Matrix Multiplications and Additions

In this section the number of flops required for the rest of the calculations in the proposed method is calculated. In each iteration of detection the following four steps should be carried out:

### 1) Nulling ($\mathbf{N}_g^u \mathbf{r}_g^u$)

In order to remove the interference from the not yet detected antenna groups the received signal in the $g^{th}$ stage ($\mathbf{r}_g^u$) is multiplied by the nulling matrix ($\mathbf{N}_g^u$).

$\mathbf{N}_g^u$ and $\mathbf{r}_g^u$ are $(N - M + \sum_{i=1}^{g} m_i) \times N$ and $N \times T$ matrices respectively. Assuming that $T = 2$ and $m_g = 2$ for $g = 1, \ldots, G$, the total number of flops required for the multiplication can be written as[3]:

$$2\left(N - M + \sum_{i=1}^{g} m_i\right) NT = 4N^2 - 4MN + 8gN$$

which has to be done for all the groups except for the last one and all subcarriers:

$$U\left[\sum_{g=1}^{G-1}\left(4N^2 - 4MN + 8gN\right)\right] = 2UMN^2 - UM^2N + 2UMN - 4UN^2 \qquad \text{(B.1)}$$

### 2) Alamouti detection

After deriving the equivalent channel for each group the data transmitted over each group is detected by simple Alamouti detection (see (3.19)). The received signal in

[3]The number of flops for the multiplication of two matrices of sizes $a \times b$ and $b \times c$ is $2abc$.

the equivalent system is:

$$\mathbf{r}^u_{eq,g} = \mathbf{H}^u_{eq,g}.\mathbf{S}^u_g + \mathbf{n}^u_{eq,g}$$

which can be rewritten as:

$$\mathbf{r}_{2N_{\text{eq}}\times 1} = \mathbf{H}_{2N_{\text{eq}}\times m_g}\mathbf{s}_{m_g\times 1} + \mathbf{n}$$

where $\mathbf{r} = \left[r^u_{eq,11}, r^{u*}_{eq,12}, r^u_{eq,21}, r^{u*}_{22}, \cdots, r^u_{eq,N_{eq}1}, r^{u*}_{eq,N_{eq}2}\right]^T$ is the rearranged form of $\mathbf{r}^u_{eq,g}$ and $N_{\text{eq}} = N - M + \sum_{i=1}^{g} m_i$. The detection is carried out by multiplying the received signal ($\mathbf{r}$) by $\mathbf{G}_{\text{MMSE}}$ which is defined as:

$$\mathbf{G}_{\text{MMSE}} = \frac{1}{\sum_{n=1}^{N_{eq}}\left(\left|H^u_{eq,n1}\right|^2 + \left|H^u_{eq,n2}\right|^2\right) + \frac{N_0}{2}} \cdot \begin{pmatrix} H^{u*}_{eq,11} & H^u_{eq,12} & \cdot\cdot & H^{u*}_{eq,N_{eq}1} & H^u_{eq,N_{eq}2} \\ H^{u*}_{eq,12} & -H^u_{eq,11} & \cdot\cdot & H^{u*}_{eq,N_{eq}2} & -H^u_{eq,N_{eq}1} \end{pmatrix}$$

Hence the total number of flops for multiplication can be written as:

$$2 \times 2N_{\text{eq}}m_g + (N_{\text{eq}}m_g + 3)^{\S} = 10(N - M + 2g) + 3$$

which is performed for all the groups and all subcarriers:

$$U\left[\sum_{g=1}^{G}(10(N - M + 2g) + 3)\right] = 5UMN + 5UM - \frac{5}{2}UM^2 + \frac{3}{2}UM \qquad \text{(B.2)}$$

### 3) Despreading of the users' data

Despreading of the users' data: The estimate of the signals transmitted from the $g^{th}$ antenna group over all subcarriers obtained in Step 2, can be stacked in one matrix

§Number of flops required for calculating $\frac{1}{\alpha + \frac{N_0}{2}}$.

($X_{m_g \times U}$) and by multiplying it with the coding matrix of the users' spreading codes ($\mathbf{C}_{U \times K}$) the information of each user can be derived (see (3.20)). Hence the number of flops required for this operation will be:

$$2Um_gK \quad (\text{for } g^{th} \text{ group}) \qquad \longrightarrow \qquad \sum_{g=1}^{G} 2Um_gK = 2UMK \quad (\text{for all the groups}) \tag{B.3}$$

### 4) Interference cancellation

The estimates calculated in Step 2 are removed from the received signal for the detection of subsequent groups (see (3.14)). First, the estimates of data transmitted from the $g^{th}$ group ($\tilde{\mathbf{S}}_g^u$), which is a $m_g \times 1$ column vector is multiplied by its corresponding channel matrix ($\mathbf{H}_g^u$), which has an order of $N \times m_g$. Subsequently, the result is removed from the received signal in the $g^{th}$ stage ($r_g^u$). Hence the total number of flops for all the groups except the last and all the subcarrier can be calculated as:

$$\sum_{g=1}^{G-1}(2Nm_g + N)U = \sum_{g=1}^{G-1} 5NU = \frac{5}{2}UMN - 5UN \tag{B.4}$$

The number of flops required for the total number of multiplications in this method (without iteration) can be obtained by summing the number of flops in each stage in equations (B.1)-(B.4):

$$2UKM + 2UMN^2 - UM^2N + \frac{19}{2}UMN - 4UN^2 - \frac{5}{2}UM^2 + \frac{13}{2}UM - 5UN \tag{B.5}$$

### 5) Additional flops for subsequent iterations

In subsequent iterations, the data transmitted from the $g^{th}$ group is detected by canceling the interference from the other groups using the estimates from the previous

iteration and thus, no nulling matrix calculation is required. In this case, the interference cancellation process for subsequent iterations can be written as:

$$\mathbf{r}_g^u = \mathbf{r}^u - \tilde{\mathbf{H}}_{g\,N\times(M-m_g)}^u \bar{\mathbf{s}}_{g\,(M-m_g)\times 1}^u$$

which requires

$$U\sum_{g=1}^{G}(2N(M-m_g)+N) = UM^2N - \frac{3}{2}UMN$$

flops. Subsequently, an Alamouti space-time coded system with $m_g$ transmit and $N$ receive antennas will be decoded with a total number of flops:

$$U\sum_{g=1}^{G}(2\times 2Nm_g + Nm_g + 3) = 5UMN + \frac{3}{2}UM$$

Hence the total number of flops for the additional operations is:

$$UM^2N + \frac{7}{2}UMN + \frac{3}{2}UM \tag{B.6}$$

Thus the total number of flops for multiplication/addition after $i^{th}$ iteration is the sum of the flops in (B.5) and (B.6):

$$\begin{aligned} 2UKM + 2UMN^2 - UM^2N + \frac{19}{2}UMN - 4UN^2 - \frac{5}{2}UM^2 + \frac{13}{2}UM - 5UN \\ + i(UM^2N + \frac{7}{2}UMN + \frac{3}{2}UM) \end{aligned}$$

# Appendix C

# Walsh-Hadamard spreading codes:

## $\mathbf{E}[c_{ku}c_{ku'}|c_{1u}c_{1u'}] = -\frac{c_{1u}c_{1u'}}{U-1}\ (k \neq 1)$

The Hadamard codes are obtained from the Hadamard matrix with the following structure:

$$\mathbf{H}_{2^{n+1}} = \begin{pmatrix} \mathbf{H}_{2^n} & \mathbf{H}_{2^n} \\ \mathbf{H}_{2^n} & -\mathbf{H}_{2^n} \end{pmatrix} \quad \text{for} \quad n = 1, 2, \cdots$$

where:

$$\mathbf{H}_2 = \begin{pmatrix} 1 & 1 \\ 1 & -1 \end{pmatrix}$$

Clearly this matrix is Hermitian and considering each two columns or rows of the matrix the inner product will be zero. Without loss of generality, we assume that the rows of the matrix correspond to the users' spreading codes and take the first user as the desired user. Due to the orthogonality of the rows and columns of the matrix:

$$\sum_{k \neq 1} c_{ku}c_{ku'} = -c_{1u}c_{1u'} \quad \text{for all } u \neq u' \tag{C.1}$$

Defining the random variable $X$ as $c_{ku}c_{ku'}$ when $(u \neq u')$, the expected value of the random variable can be written as:

$$\mathrm{E}[X] = \sum_{\text{all x}} xp\left(X = x\right) = \sum_{\text{all l}} x_l p\left(l\right) = \frac{1}{U-1}(-c_{1u}c_{1u'}) \quad , \quad \begin{cases} k \neq 1 \\ u \neq u' \end{cases}$$

where $p(l)$ denotes the probability of choosing the $l^{th}$ row of the Hadamard matrix as the spreading code.

The last expression is due to (C.1) and the fact that the interferer $k$ chooses the spreading code from the $U-1$ available codes at random and with equal probability.

# Appendix D

# Confidence Interval

In order to obtain an estimate of the true bit error rate of a communication system, Monte Carlo simulations are carried out. The simulations are performed over a large number of symbols and the bit error rate is approximated as $\hat{p} = \frac{n}{N}$, where $n$ is the total number of errors over $N$ number of observed symbols. In order to quantify the reliability of the estimated bit error probability the concept of confidence intervals is introduced. The simulation is said to have a reliability of $1 - \alpha$ percent when the following equation is satisfied [41]:

$$\Pr[h_1 \leq p \leq h_2] = 1 - \alpha$$

where $p$ is the true bit error probability and $[h_1, h_2]$ is the confidence interval for a given reliability.

Since $\hat{p}$ is binomially distributed, the values for $h_1$ and $h_2$ can be derived as:

$$\sum_{k=0}^{N} \binom{N}{k} h_1^k (1 - h_1)^{N-k} = 1 - F(h_1; n, N - n - 1) = \frac{\alpha}{2}$$

$$\sum_{k=0}^{N} \binom{N}{k} h_2^k (1-h_2)^{N-k} = 1 - F(h_2; n, N-n-1) = \frac{\alpha}{2}$$

where $F(x;\alpha,\beta)$ is the cumulative beta distribution given by:

$$F(x;\alpha,\beta) = \frac{(\alpha+\beta+1)!}{\alpha!\beta!} \int_0^x t^\alpha (1-t)^\beta dt$$

For scenarios of interest, the normal approximation of the binomial distribution applies, and the confidence interval can be derived as:

$$\Pr\left\{ \frac{N}{N+d_\alpha^2} \left[ \hat{p} + \frac{d_\alpha^2}{2N} - d_\alpha \sqrt{\frac{\hat{p}(1-\hat{p})}{N} + \left(\frac{d_\alpha}{2N}\right)^2} \right] \le p \right.$$
$$\left. \le \frac{N}{N+d_\alpha^2} \left[ \hat{p} + \frac{d_\alpha^2}{2N} + d_\alpha \sqrt{\frac{\hat{p}(1-\hat{p})}{N} + \left(\frac{d_\alpha}{2N}\right)^2} \right] \right\} \qquad \text{(D.1)}$$

where $d_\alpha$ is chosen to satisfy:

$$\frac{1}{\sqrt{2\pi}} \int_{-d_\alpha}^{d_\alpha} e^{-\frac{t^2}{2}} dt = 1 - \alpha$$

which for a reliability of 95% is caculated to be 1.96.

Almost for all scenarios of interest we can assume $\frac{N}{N+d_\alpha^2} \approx 1$ and $\hat{p}(1-\hat{p}) \approx \hat{p}$, hence (D.1) is simplified as:

$$\Pr\left\{ \hat{p}\left[1 + \frac{d_\alpha^2}{2\eta}\left(1 - \sqrt{\frac{4\eta}{d_\alpha^2}+1}\right)\right] \le p \le \hat{p}\left[1 + \frac{d_\alpha^2}{2\eta}\left(1 + \sqrt{\frac{4\eta}{d_\alpha^2}+1}\right)\right] \right\}$$

where $\eta = N\hat{p}$. So $\left[\hat{p}\left\{1 + \frac{d_\alpha^2}{2\eta}\left(1 - \sqrt{\frac{4\eta}{d_\alpha^2}+1}\right)\right\}, \hat{p}\left\{1 + \frac{d_\alpha^2}{2\eta}\left(1 + \sqrt{\frac{4\eta}{d_\alpha^2}+1}\right)\right\}\right]$ represents the confidence interval for $p$ and is indicated for example by the error bars in Fig. 5.1.

# References

[1] L. Hanzo, M. Münster, B. J. Choi, and T. Keller, *OFDM and MC-CDMA for Broadband Multi-User Communications, WLANs and Broadcasting.* John Wiley & Sons, 2003.

[2] S. Hara and R. Prasad, "Overview of Multicarrier CDMA," *IEEE Communications Magazine*, vol. 35, pp. 126–133, Sept. 1997.

[3] N. Yee and J. P. Linnartz, *Multi-Carrier CDMA in an Indoor Wireless Radio Channel.* University of California, Berkeley: Technical Memorandum UCB/ERL M94/6, 1994.

[4] I. E. Telatar, "Capacity of multi-antenna Gaussian channels," *European Trans. Telecommunications*, vol. 10, pp. 585–595, nov-dec 1999.

[5] G. Foschini, "On limits of wireless communications in a fading environment when using multiple antennas," *in Wireless Pers. Commun.: Kluwer*, vol. 6, pp. 311–335, 1998.

[6] S. Alamouti, "A simple transmit diversity technique for wireless communications," *IEEE Journal on Selected Areas in Communications*, vol. 16, pp. 1451–1458, Oct. 1998.

[7] V. Tarokh, H. Jafarkhani, and A. Calderbank, "Space-time block codes from orthogonal designs," *IEEE Trans. Inform. Theory*, vol. 45, pp. 1456–1467, July 1999.

[8] V. Tarokh, N. Seshadri, and A. R. Calderbank, "Space-time codes for high data rate wireless communication: Performance criterion and code construction," *IEEE Trans. Inform. Theory*, vol. 44, pp. 744–765, Mar. 1998.

[9] H. J. Su and E. Geraniotis, "Space-time turbo codes with full antenna diversity," *IEEE Trans. Communications*, vol. 49, pp. 47–57, Jan. 2001.

[10] G. Foschini, "Layered space-time architecture for wireless communication in a fading environment when using multi-element antennas," *Bell System Technical Journal*, vol. 1, pp. 41–59, Aug. 1996.

[11] G. Foschini, G. Golden, R. Valenzuela, and P. Wolniansky, "Simplified processing for high spectral efficiency wireless communication employing multi-element

arrays," *IEEE Journal on Selected Areas in Communications*, vol. 17, pp. 1841–1852, Nov. 1999.

[12] G. J. Foschini, D. Chizhik, M. J. Gans, C. Papadias, and R. A. Valenzuela, "Analysis and Performance of Some Basic SpaceTime Architectures," *IEEE Journal on Selected Areas in Communications*, vol. 21, pp. 303–320, Apr. 2003.

[13] L. Zheng and D. N. C. Tse, "Diversity and multiplexing: a fundamental tradeoff in multiple-antenna channels," *IEEE Trans. Inform. Theory*, vol. 49, pp. 1073–1096, May 2003.

[14] K. Azarian and H. E. Gamal, "The ThroughputReliability Tradeoff in Block-Fading MIMO Channels," *IEEE Trans. Inform. Theory*, vol. 53, pp. 488–501, Feb. 2007.

[15] M. Tao and R. S. Cheng, "Generalized layered space-time codes for high data rate wireless communications," *IEEE Trans. on Wireless Communications*, vol. 3, pp. 1067–1075, July 2004.

[16] C. E. Shannon, "Communication in the presence of noise," *Proc. IRE*, vol. 37, pp. 10–21, Jan. 1949.

[17] R. Prasad, *CDMA for Wireless Personal Communications.* Boston London: Artech House, 1996.

[18] N. Yee, J. P. Linnartz, and G. Fettweis, "Multi-carrier CDMA in indoor wireless radio networks," *IEEE PIMRC International Conference*, pp. 109–113, 1993.

[19] T. Rappaport, *Wireless Communications: Principles & Practice.* NJ: Prentice Hall, 2002.

[20] L. Hanzo and T. Keller, *OFDM and MC-CDMA: A Primer.* John Wiley & Sons, 2006.

[21] W. H. Press, B. P. Flannery, S. A. Teukolsky, and W. T. Vetterling, *Numerical Recipes in C.* NY: Cambridge University Press, 1988.

[22] J. Proakis, *Digital communications.* New York: McGraw-Hill, 2000.

[23] A. Chouly, A. Brajal, and S. Jourdan, "Orthogonal multicarrier techniques applied to direct sequence spread spectrum CDMA systems," in *Proc. of IEEE GLOBECOM*, (Houston, USA), pp. 1723–1728, Nov. 1993.

[24] V. M. DaSilva and E. S. Sousa, "Performance of Orthogonal CDMA Codes for Quasi-Synchronous Communication Systems," in *Proc. of IEEE ICUPC*, (Ottawa, Canada), pp. 995–999, Oct. 1993.

[25] S. Kondo and L. B. Milstein, "Performance of Multicarrier DS-CDMA Systems," *IEEE Trans. Communications*, vol. 44, pp. 238–246, Feb. 1996.

[26] L. Vandendorpe, "Multitone Direct Sequence CDMA System in an Indoor wireless environment," *Proc. of IEEE First Symposium of Communications and Vehicular Technology in the Benelux, Delft, The Netherlands*, Oct. 1993.

[27] D. Gesbert, M. Shafi, D. S. Shiu, P. J. Smith, and A. Naguib, "From theory to practice: an overview of MIMO space-time coded wireless systems," *IEEE Journal on Selected Areas in Communications*, vol. 21, pp. 281–302, Apr. 2003.

[28] S. Verdu, *Multiuser detection.* Cambridge University Press, 1998.

[29] G. H. Golub and C. F. V. Loan, *Matrix computations.* Baltimore and London: The Johns Hopkins University Press, 1996.

[30] H. Jafarkhani, *Space-Time Coding: Theory and Practice.* NY: Cambridge University Press, 2005.

[31] J. Kermoal, L. Schumacher, K. Pedersen, P. Mogensen, and F. Frederiksen, "A stochastic MIMO radio channel model with experimental validation," *IEEE Journal on Selected Areas in Communications*, vol. 20, pp. 1211–1226, Aug. 2002.

[32] L. Zexian and M. Latva-aho, "Nonblind and semiblind space-time-frequency multiuser detection for space-time block-coded MC-CDMA," *IEEE Trans. on Wireless Communications*, vol. 4, pp. 1311–1318, July 2005.

[33] V. Tarokh, A. Naguib, N. Seshadri, and A. Calderbank, "Combined array processing and space-time coding," *IEEE Trans. Inform. Theory*, vol. 45, pp. 1121–1128, May 1999.

[34] X. Gui and T. S. Ng, "Performance of asynchronous orthogonal Multicarrier CDMA system in frequency selective fading channel," *IEEE Trans. Communications*, vol. 47, pp. 1084–1091, July 1999.

[35] S. Hara and R. Prasad, "Design and performance of multicarrier CDMA system in frequency-selective Rayleigh fading channels," *IEEE Trans. Vehicular Technology*, vol. 48, pp. 1584–1595, Sept. 1999.

[36] Q. Shi and M. Latva-aho, "Exact bit error rate calculations for synchronous MC-CDMA over a Rayleigh fading channel," *IEEE Communications Letters*, vol. 6, pp. 276–278, July 2002.

[37] X. Hu and Y. H. Chew, "On the performance and capacity of an asynchronous space-time block-coded MC-CDMA system in the presence of carrier frequency offset," *IEEE Trans. Vehicular Technology*, vol. 53, pp. 1327–1340, Sept. 2004.

[38] X. Zhang and B. Ottersten, "Performance analysis of V-BLAST structure with channel estimation errors," *4th IEEE Workshop on Signal Processing Advances in Wireless Commun., 2003. SPAWC 2003.*, pp. 487–491, June 2003.

[39] H. Bölcskei, D. Gesbert, and A. J. Paulraj, "On the Capacity of OFDM-Based Spatial Multiplexing Systems," *IEEE Trans. Communications*, vol. 50, pp. 225–234, Feb. 2002.

[40] Z. Liu, Y. Xin, and G. B. Giannakis, "Space-Time-Frequency Coded OFDM Over Frequency-Selective Fading Channels," *IEEE Trans. Signal Processing*, vol. 50, pp. 2465–2476, Oct. 2002.

[41] M. C. Jeruchim, "Techniques for Estimating the Bit Error Rate in the Simulation of Digital Communication Systems," *IEEE Journal on Selected Areas in Communications*, vol. 2, pp. 152–170, Jan. 1984.